CRITICAL SURVEY OF MECHANICAL PROPERTY TEST – METHODS FOR BRITTLE MATERIALS

TECHNICAL DOCUMENTARY REPORT NO. ASD–TDR–63–491

July 1963

JUN 1 5 1964

AF Materials Laboratory
Aeronautical Systems Division
Air Force Systems Command
Wright–Patterson Air Force Base, Ohio

Project No. 7381, Task No. 738105

NOTICES

When Government drawings, specifications, or other data are used for any purpose other than in connection with a definitely related Government procurement operation, the United States Government thereby incurs no responsibility nor any obligation whatsoever; and the fact that the Government may have formulated, furnished, or in any way supplied the said drawings, specifications, or other data, is not to be regarded by implication or otherwise as in any manner licensing the holder or any other person or corporation, or conveying any rights or permission to manufacture, use, or sell any patented invention that may in any way be related thereto.

Qualified requesters may obtain copies of this report from the Defense Documentation Center (DDC), (formerly ASTIA), Arlington Hall Station, Arlington 12, Virginia.

This report has been released to the Office of Technical Services, U.S. Department of Commerce, Washington 25, D.C., for sale to the general public.

Copies of this report should not be returned to the Aeronautical Systems Division unless return is required by security considerations, contractual obligations, or notice on a specific document.

FOREWORD

This report was prepared by the Engineering Experiment Station, The Ohio State University, under USAF Contract No. AF 33(657)-8064. This contract was initiated under Project No. 7381, "Materials Application," Task No. 738105, Ceramic and Graphite Technical Evaluation. The work was administered under the direction of the Directorate of Materials and Processes, Aeronautical Systems Division, with Mr. B. R. Emrich acting as project engineer.

This report covers work conducted from 15 March 1962 to 14 March 1963.

The author wishes to acknowledge the many contributors who have added significantly to this survey. This applies particularly to more than one-hundred hosts who provided the opportunity for personal inspection of their laboratories and discussed with the author the current practices, limitations, and needs in furthering brittle material developments. Dr. Francis Niedenfuhr and Mr. Allen Wallskog of the Engineering Mechanics Department, The Ohio State University, provided assistance in formulating the theoretical bases of the tests.

Special thanks are also due to Miss Rose Marie Castellarin for her continuing assistance in organizing and arranging the travel and the resulting notes of observations, and her faithful typing of the manuscript.

ABSTRACT

A critical survey of the state-of-the-art of mechanical property tests of brittle materials are presented. The format utilized in presenting the information is based on property categories, since no significant breakdown for specific materials is justified. The common characteristics of the materials included in the survey permit general testing procedures to be discussed, with special adaptations developed for certain materials being applicable to all.

The capabilities in programming test performance variables have exceeded the ability to define materials and performance requirements. Large gaps still remain in the statistical interpretation of strength and other material parameters, particularily under conditions of complex stress-state and with previous exposure to testing conditions. Certain probabilistic descriptors have shown promising indications, but much remains to be explored in this area.

This technical documentary report has been reviewed and is approved.

D. A. SHINN
Chief, Materials Information Branch
Applications Division
AF Materials Laboratory

TABLE OF CONTENTS

TABLE OF CONTENTS (Cont'd.)

TABLE OF CONTENTS (Cont'd.)

vii

TABLE OF CONTENTS (Cont'd.)

Page

LIST OF ILLUSTRATIONS

I. INTRODUCTION

1.1 Purpose of Report

It has long been recognized that the available data on the mechanical properties of brittle materials are far from adequate for most critical design purposes. The current emphasis on new materials development, and consequent evolution of promising materials for modern technology, have focused attention on the general area of mechanical evaluation.

This study was undertaken for the purpose of setting forth the present state-of-the-art regarding mechanical property determinations with brittle materials. The report is intended to be useful to individuals engaged in the actual testing, evaluation of test results, designing research and development programs, and applying engineering information in design of components.

1.2 Scope and Organization

The scope of the work encompasses present practices in the evaluation of oxides; glass and/or glass ceramics; intermetallics, such as the silicides, beryllides, etc.; borides; carbides; nitrides; sulfides; graphites; ceramic compositions which are adaptable to generalized tests; vitrified ceramics; and cermets. It is considered of primary importance to make the context readily available through cross-indexing and through organization of the text. The information is therefore presented on the basis of property or behavior categories, with information pertinent to all materials of consideration appearing within each category.

The behavior peculiar to brittle materials is basic to the testing procedures and evaluation philosophies for all properties of interest. To prevent unnecessary repetition in the cross-referencing it is therefore felt necessary to introduce the subject of testing procedures through a general discussion of brittle behavior. As there are a number of excellent references on the subject this section is by no means intended to portray a comprehensive treatment of brittle behavior, or the statistics of brittle materials.

1.3 General References Pertaining to Brittle Behavior

ASD Technical Report 61-628, "Studies of the Brittle Behavior of Ceramic Materials", is the most recent publication in the general field of brittle behavior which permits a broad concept of the present state of knowledge. The research program, under the overall direction of N. A. Weil, is described in the foreword of that document as consisting of the following tasks:

Manuscript released by author May 1963 for publication as an ASD Technical Documentary Report.

1.3

Task 1   S. A. Bortz, Armour Research Foundation
          Effect of Structural Size; "The Zero Strength"

Task 2   H. R. Nelson, Armour Research Foundation
          Effect of Strain Rate

Task 3   N. A. Weil, I. M. Daniel, Armour Research Foundation
          Effect of Non-Uniform Stress Fields

Task 4   P. R. V. Evans, Armour Research Foundation
          Effect of Microstructure

Task 5   P. D. Southgate, Armour Research Foundation
          Internal Friction and Lattice Defects

Task 6   N. J. Petch, University of Durham, England
          Effect of Surface Energy in Brittle Fracture

Task 7   E. Orowan, Massachusetts Institute of Technology
          Fracture Mechanisms

Task 8   I. B. Cutler, University of Utah
          Impurity Influences

Task 9   R. J. Charles, General Electric Company
          Static Fatigue; Delayed Fracture

Task 10   R. J. Stokes, Minneapolis-Honeywell Research Laboratories
          Effect of Thermal-Mechanical History

Task 11   G. T. Murray, Materials Research Corporation
          Surface Active Environments

A further publication dealing more specifically with the bases of statistical design concepts is in preparation.

Barnett, R. L., Armour Research Foundation
Design of Brittle Components Under Static Loading.

Earlier work in the area of mechanical property evaluation and statistical failure concepts for brittle materials is reported in the series of publications by Battelle Memorial Institute, as follows:

2

Duckworth, W. H., Schwope, A.D., Salmassy, O.K., Carlson, R.L., Schofield, H.Z., WADC Technical Report No. 52-67
Mechanical Property Tests on Ceramic Bodies

Salmassy, O.K., Duckworth, W.H., and Schwope, A.D., WADC Technical Report No. 53-50
Mechanical Property Tests on Ceramic Bodies

Salmassy, O.K., Bodine, E.G., Duckworth, W.H., and Manning, G.K., WADC Technical Report No. 53-50, Part 2
The Behavior of Brittle-State Materials.

Books that include a wide diversity of interests are as follows:

Kriegel, W.W., and Palmour, H., (Editors)
The Mechanical Properties of Engineering Ceramics
Interscience Publishers, New York (1961)

Dorn, J., (Editor)
Mechanical Behavior of Materials at Elevated Temperatures
McGraw-Hill Book Company, New York (1961)

Westbrook, J.H., (Editor)
Mechanical Properties of Intermetallic Compounds
J. H. Wiley and Sons, Incorporated, New York (1960)

Walton, W.H.
Mechanical Properties of Non-Metallic Brittle Materials
Interscience Publishers, New York (1958)

Kingery, W.D.
Property Measurements at High Temperatures
J. H. Wiley and Sons, Incorporated, New York (1959)

II. DEFINITION OF THE PROBLEM

2.1 Elastic Behavior

Brittleness is a characteristic which denotes a degree of inability for plastic deformation. This behavior may be best illustrated by reference to a stress-strain diagram for a material, and noting the degree of linearity exhibited by such a curve prior to failure. A perfectly elastic material will recover its original shape upon removal of the load, although in some cases this recovery may be time-sensitive. If the conditions of the test are such that a linear stress-strain diagram results, the material is said to follow Hooke's law and the constant of proportionality is the modulus of elasticity.

2.2 Brittleness

With this brief description of elastic behavior, it is possible to define a range of brittleness which depends upon the departure from linear stress-strain behavior. An extremely brittle material would be one that exhibits no deviations before complete failure occurs. A less brittle behavior may be shown by a uniform curvature beyond an initial linear range in the curve, brittleness being roughly inverse to the degree of curvature. This behavior is usually strongly dependent upon time. Other degrees of brittleness may be illustrated by a constant modulus of elasticity close to the failure stress, followed by some limited amount of strain with little or no additional stress application before failure.

2.3 Consequence of Brittleness

A spectrum of brittleness has been illustrated, defining brittle behavior as sudden fracture with little or no plastic deformation. Materials may be caused to exhibit brittle or plastic behavior dependent upon the conditions of the test, such as time, temperature and other environmental control, stress-state, and previous specimen history. The influence of the degree of brittle behavior is pronounced in determining the strength of a brittle material, since this restricts any deformation about local regions of high stress. Any crack which promotes stress-concentration will remain active as long as no plastic yielding can occur, and if the local stress exceeds the ultimate strength of the material, the crack will propagate from that source. If a small amount of yielding can take place in the highest stress field, the degree of stress-concentration will be reduced by blunting of the sharp crack front. It is then very clear that the consequence of brittleness is a severe reduction in the useful strength of a material.

2.4 Strength of Glass

Griffith (Ref. 1) proposed the existence of microcracks in glass as an explanation for the large discrepancy between theoretical strength and observed strength. He reasoned that the condition for growth of such a crack must be an equality between the strain-energy released by the crack extension and the energy of the new surfaces so formed. Measurements of the surface tensions of glass at various temperatures were extrapolated to room temperatures, and his calculations predicted that the critical crack size was in the order of 10^{-3} cm.

2.5 Strength of Crystalline Ceramics

Extensions of Griffith's work have been carried on by Orowan (Ref. 2). To account for the much higher energy required for crack propagation in crystalline materials, he proposed an additional consideration for the plastic deformation energy. On the basis of normally observed reductions in theoretical strength, the deduced minimum crack lengths become about one micron. From considerations of the stress theoretically necessary to overcome the attractive force between the atoms in a crystal, the ratio of failure stress to theoretical stress depends approximately on the ratio of interatomic spacing, a, to half the crack length as $\sqrt{a/c}$.

2.6 Surface Importance

It should be pointed out that a surface crack of length c is theoretically equivalent to an interior crack of length 2c, since the freshly-formed surface on crack extension is only one half as great at the material surface.

It is virtually impossible to maintain a surface completely free of micron or submicron size cracks, as the slightest contact with any other hard object, or the abrading action of light contact with hard grains, will result in the formation of such microcracks. Further difficulties are encountered with the formation of microcracks due to chemical attack by the environment, particularly in areas of high local strain. Other atmospheric effects are thought to be due to the reactivity of adsorbed gases or liquids on newly formed surfaces, thus changing the surface energy factor important in determining the critical stress by the Griffith-Orowan theory.

III. STATISTICAL DESCRIPTION OF BRITTLE FAILURE

3.1 Probabilistic Failure Description

Since the observed strength of materials exhibiting brittle behavior is so profoundly dependent upon the occurrence of flaws, it follows that the scatter of results in mechanical tests of these materials will be dependent in some fashion upon the volume and surface area of the material under stress, as well as on the surface treatment, environment, and other manufacturing history of the specimen which may in some way influence the severity and concentration of the flaws. On the basis of this probabilistic nature of the failure of brittle materials, Weibull (Ref. 3) has defined a distribution function of general nature which finds wide application in describing the behavior of brittle materials under load. This function is of the form

$$S = 1 - \exp. \quad -V \left(\frac{\sigma - \sigma_u}{\sigma_0} \right)^m \tag{1}$$

where

S = probability of fracture

σ_0 = strength of a flawless specimen

σ_u = lower limit of stress below which fracture cannot propagate (zero strength)

V = the volume of the component subjected to tensile stress

m = flaw density

3.2 Effect of Volume

Using this form of distribution, Weibull showed that the effect of volume on the observed mean failure strength of geometrically similar specimens of volumes V_1 and V_2, for $\sigma_u = 0$:

$$\frac{\sigma_1}{\sigma_2} = \left(\frac{V_2}{V_1} \right)^{1/m} \tag{2}$$

He also showed that with identical fracture probabilities in pure bending and in tension, the ratio of the mean bending failure stress to the mean tensile failure stress would be according to the following equation:

$$\frac{\sigma_{bending}}{\sigma_{tension}} = (2m + 2)^{1/m} \tag{3}$$

The above limiting statement of identical fracture probabilities infers identical volumes of material under near critical stress levels. The effective volume of the bend specimen can be shown through the application of Weibull's reasoning to be as follows:

$$V_{eff.} = \frac{V}{2(m+1)} \tag{4a}$$

In case the "zero strength" σ_u is not equal to zero, an additional term must be included in this expression, as follows:

$$V_{eff.} = \frac{V}{2(m+1)} \quad 1 - \frac{\sigma_u}{\sigma_o} \tag{4b}$$

In a study of the effect of non-uniform stress fields, Daniels and Weil (Ref. 4) have chosen to define the effective volume of a bend specimen as that volume of material which is subjected to at least 95 per cent of the peak tensile stress, since the above definitions of effective volume apply only to the limited case of pure bending in a beam of rectangular cross section, and $V_{eff.}$ for more complicated stress distribution factors are not well-defined.

3.3 Evaluation of Weibull Parameters

If it can be shown that the Weibull parameter σ_u, (the stress at which the probability of the failure is equal to zero), is in fact zero psi, then the flaw density parameter m may be evaluated directly from tests of identical material involving different volumes in the region of high stress. Bortz (Ref. 5) has shown that the Weibull parameters σ_u and m are not truly material constants but are sensitive to prior specimen history. For instance, annealing of specimens can cause the σ_u value to drop to zero, while m increases. For "as received" specimens of the same material, σ_u was shown to have a finite value. This reference develops plotting methods which permit the evaluation of the Weibull parameters from test data, as summarized below.

3.3.1 Uniaxial stress

For the uniaxial stress state, equation 1 may be rewritten as

$$\log \log \frac{1}{1-S} = m \log (\sigma - \sigma_u) - m \log \sigma_o + \log V + \log \log e \tag{5}$$

7

3.3

A plot of the distribution function will be linear with log log 1/1-S plotted as a function of log $(\sigma - \sigma_u)$. The slope of the distribution function will determine the parameter $\underline{m}$, while the intercept on the vertical axis will yield σ_0. If the "zero strength" is truly equal to zero, and is so used in plotting the data, the function will be linear. If this assumption for zero strength is invalid, the resulting graph will exhibit a curvature. If the curvature is concave upward, there is no single value of o_u which adequately describes the data (Ref. 4), indicating the presence of more than one failure probability distribution. An iterative procedure may be used for successive approximations to the value of σ_u, since excessively large values for σ_u will cause an upward convex curvature to reverse, and the best value of σ_u will produce a linear plot.

3.3.2 Pure bending stress

In the case of a rectangular beam subjected to pure bending, the expression is as follows (Ref. 5):

$$\log \log \frac{1}{1 - S} = (m + 1) \log (\sigma - \sigma_u) - \log \sigma + \log \frac{V}{2(m+1)\sigma_0^m} \qquad (6)$$

The values m, σ_u, and σ_0 are obtained graphically by plotting

$$\log \log \frac{1}{1 - S} + \log \sigma \quad \text{versus} \quad \log(\sigma - \sigma_u)$$

The value of σ_u which yields a straight line plot is again determined by trial and error; the quantity $(m + 1)$ defines the slope of the straight line, and σ_0 is determined from the intercept of this line on the vertical axis. The ordinate in the above expressions may be easily determined from the relationship

$$S = \frac{n}{N + 1} \qquad (7a)$$

where
N = total number of samples tested
n = rank of the specimen when listed in increasing order of fracture stresses from 1 to N

which yields the equality

$$\log \log \frac{1}{1 - S} = \log \log \frac{N + 1}{N + 1 - n} \qquad (7b)$$

A specific example of the iterative procedure as described above for flexural test specimens is shown in Figure 1.

8
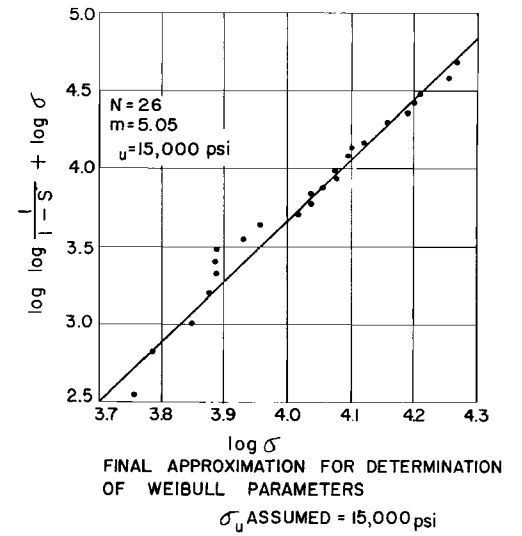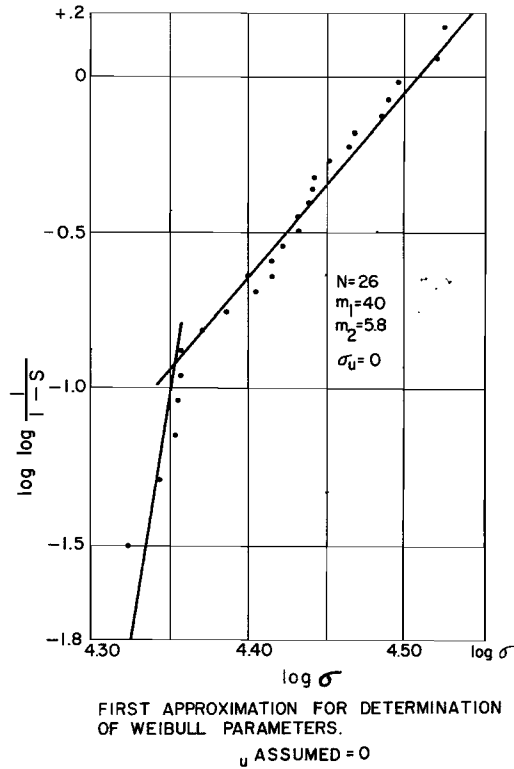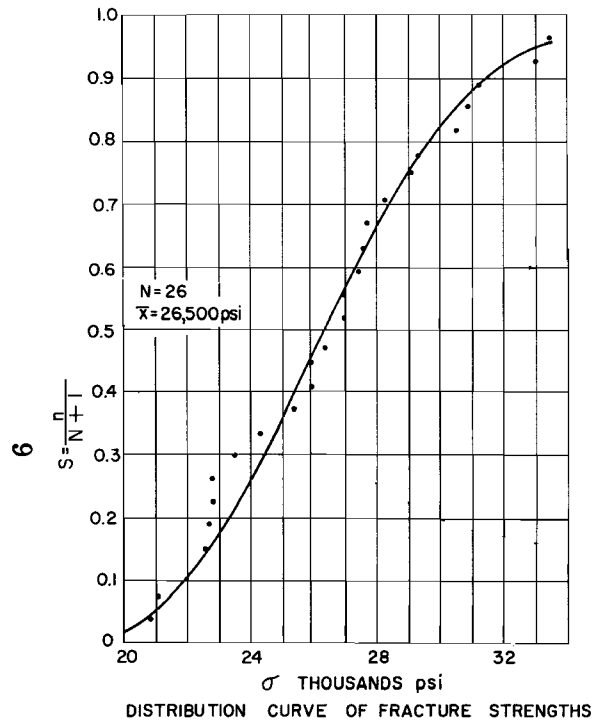
Figure 1: Illustration of Graphical Technique for Determination of Composite Weibull Parameters.

3.4 Stress Distribution Factors

The analysis which leads to the form of the failure probability expression in equation 6 is complicated by the inclusion of the zero strength lower bound. With the simplifying assumption that stress distribution factors based on a lower bound of zero (σ_u equals zero) may be applied as an approximation, Gregory and Spruill (Ref. 6) have used the form of equation 5 with stress distribution factor described by a term K. The expression in terms of natural logarithms then becomes

$$\ln \ln \frac{1}{1 - S} = m \ln (\sigma - \sigma_u) - m \ln \sigma_0 + \ln (K \, V) \tag{8}$$

Log plots of this function can be performed as described previously in the case of a uniaxial tension case, for which the value of K is equal to unity. The slope of the straight line (for the correct assumption of σ_u) will yield the value of $\underline{m}$, while the σ_0 may be calculated from the vertical intercept. However, with this less complex form of the equation for all bending stress distributions, the value of σ_0 may be read directly on the graph. It is seen that for the case where $(\sigma - \sigma_u)$ is equal to σ_0, equation 8 reduces to

$$\ln \ln \frac{1}{1 - S} = \ln (K \, V) \tag{8a}$$
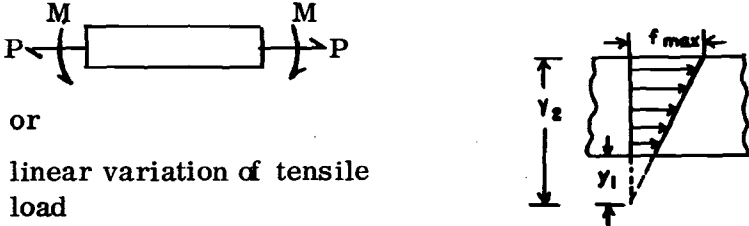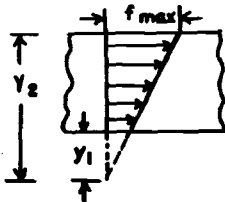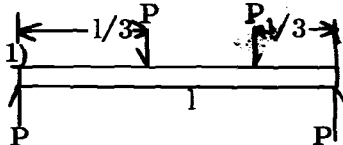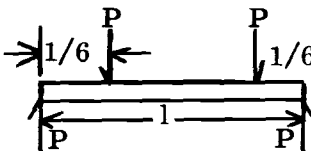
The value of the term (K V) may be calculated from the test configuration, and according to equation 8a the graph may be entered at the probability value according to ln (K V), thus determining the corresponding value of ln $(\sigma - \sigma_u)$. The anti-log of this value is therefore σ_0.

The profound advantage of the simplification is in the calculation of the K factor describing the particular loading under consideration. The disadvantage may be the oversimplification of the inherent assumption, leading to unknown consequences in the error of the determination. The K factors and their definitions in terms of geometrical descriptors, and stress distributions are shown in Table 1 for beams of rectangular cross section. This presentation is useful in the analysis of a complicated loading problem which may be reduced to a series of simpler problems. The resulting probabilities of failure for the simple cases may be multiplied to arrive at the overall probability of failure for the complicated shape. The values of K factors for a variety of stress distributions, and of beam loading situations for both rectangular and circular cross section are shown in Figures 2, 3, and 4.

TABLE 1. STRESS-DISTRIBUTION FACTORS FOR VARIOUS CONFIGURATIONS FOR
USE IN THE WEIBULL DISTRIBUTION FUNCTION.

"K" Factor	Type of Loading	Stress or Load Diagram	Typical Use in Analysis
1			Any configuration may be reduced to units small enough to consider uniform stress level. Failure probability may be calculated as the product of all unit probabilities.
$\frac{1}{2}(m+1)$			Rectangular beam of constant section. The value for use with this factor is the volume of the entire beam. It may also be used with beams that combine bending with axial loading for the case where the combined loading results in compressive stress. This may be affected by using an effective beam with same volume under tensile load. In this case the total volume of the effective beam should be used.
$1/(m+1)$	general case		Rectangular beam of constant cross section. This case may be used for any linear stress distribution that has a point of zero stress. As the compressive stress does not contribute to failure, this expression must be used with the actual volume of material under tensile stress. It is possible to use this for the case where the tensile load never reached zero by computing probability of success for the fictitious beam with zero stress (see h_{eff} in sketch) and dividing that probability by the probability of success of the fictitious portion.

11

TABLE 1 . (Contd.)

"K" Factor	Type of Loading	Stress or Load Diagram	Typical Use in Analysis
$\dfrac{y_2 - y_1}{y_2}{}^m /(m+1)$	Bending plus axial loading Tensile stresses present only or linear variation of tensile load		Rectangular beam, constant cross section. The quantities y_1 and y_2 are measured from the point where tensile stresses would be zero (see sketch). v used is that of actual volume under load. If $y_1/y_2 > .9$, it is recommended that an average uniform stress be assumed and Case 1 be used.
Same as above			Same as above
$\dfrac{1}{2(m+1)^2}$	Beam bending, midpoint loading		This distribution is of primary interest in the reduction of test data.
$(\dfrac{2}{m+1} + 1)/6(m+1)$	Beam bending, one-third point loading		This distribution is of primary interest in the reduction of test data
$(\dfrac{1}{m+1} + 2)/6(m+1)$	Beam bending, one-sixth point loading		This distribution is of primary interest in the reduction of test data

12
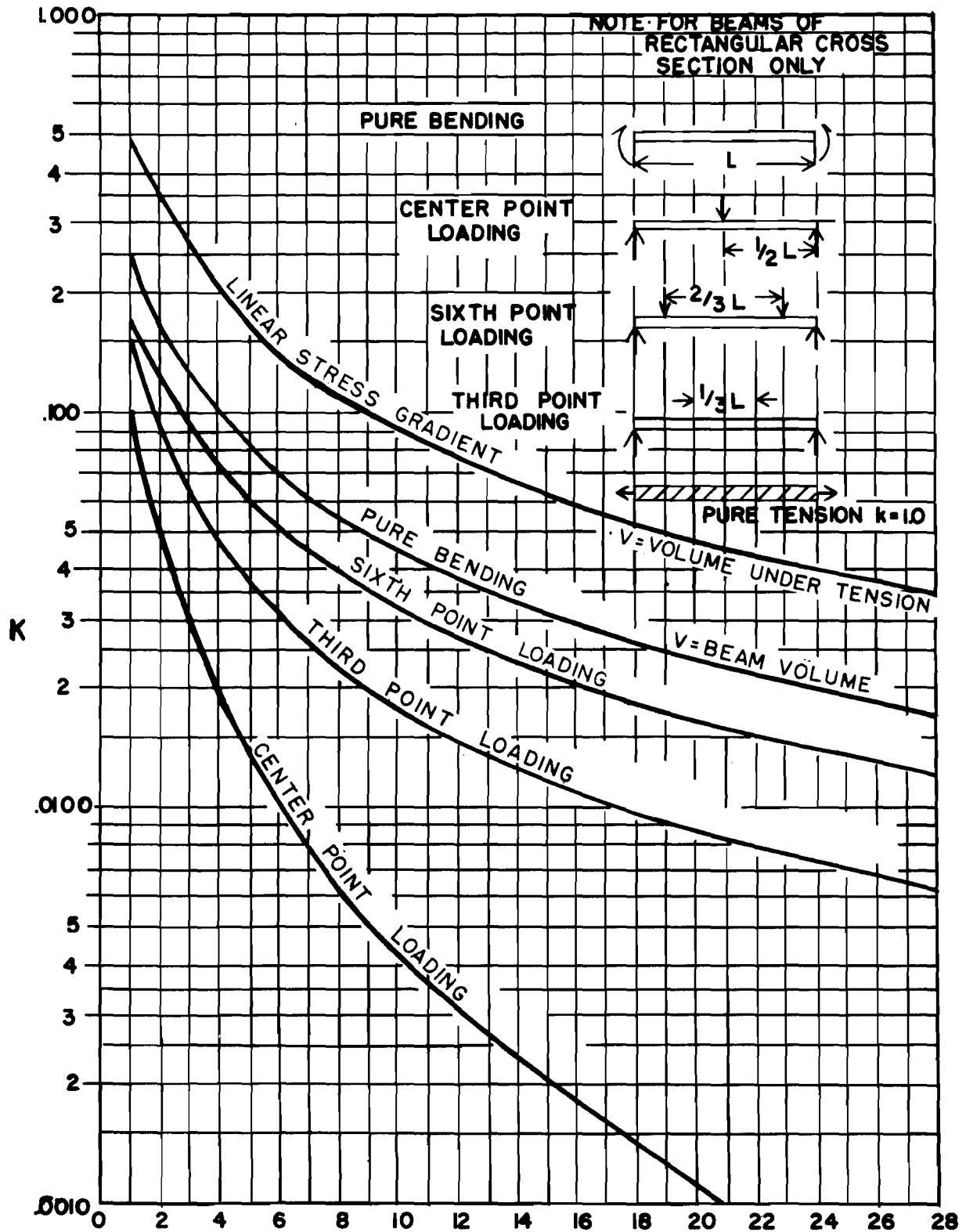
FIGURE 2: LOADING K FACTOR; VS. WEIBULL "m" FACTOR BEAM BENDING

13
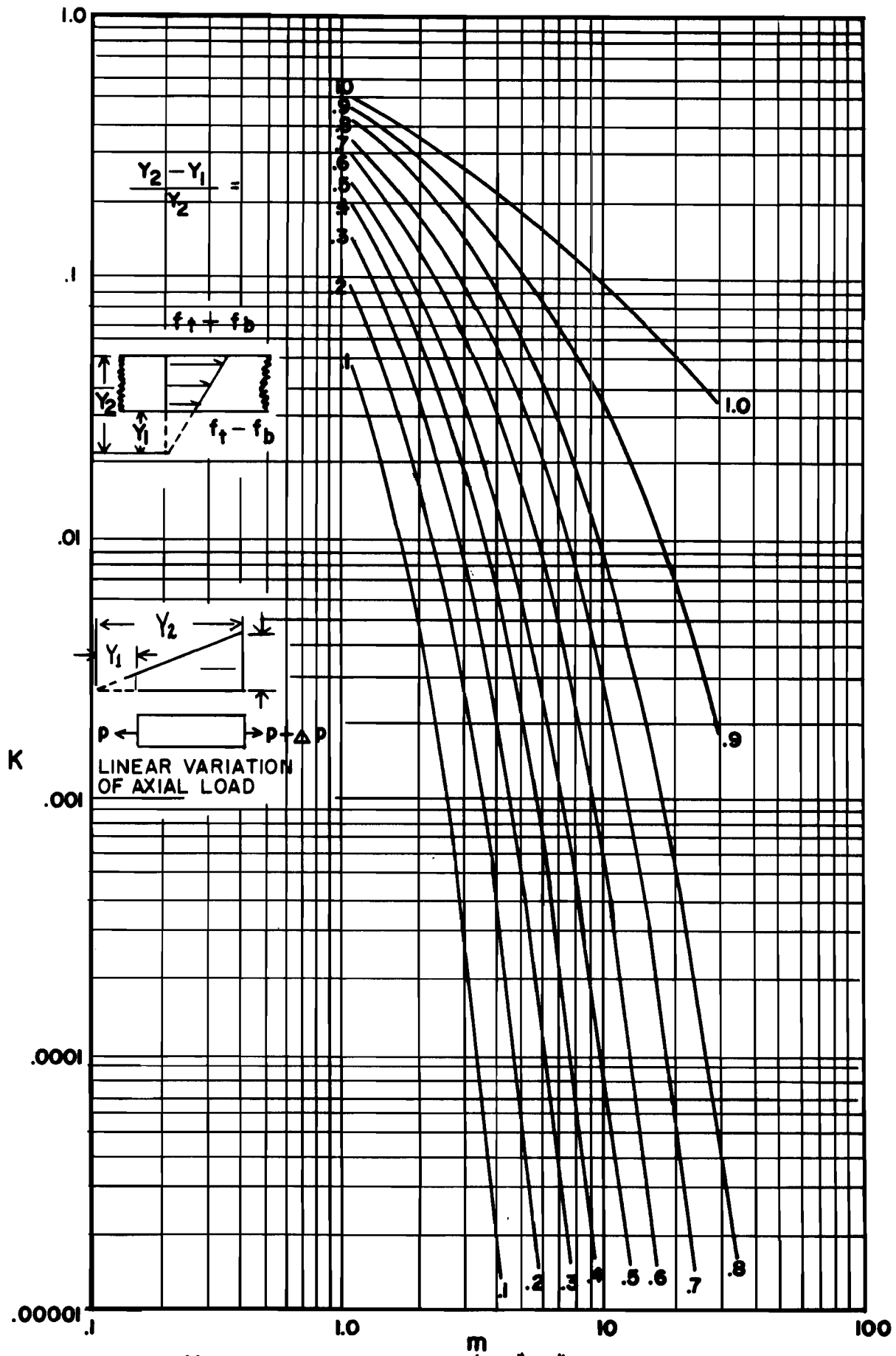
FIGURE 4 : LOADING K FACTOR VS. WEIBULL'S "m" FACTOR BEAM BENDING PLUS AXIAL LOAD

14

3.5 Comparison of Methods for Determining Weibull Parameters

Reference 6 also describes other methods of analysis for determination of the Weibull parameters. Two methods based on moments of the statistical sample are McClintock's method and the Rowley method. A least-mean-square approximation has been developed at Vought Astronautics for a computer program analysis of the best value of σ_u to permit a straight line plot. The methods have been compared on the basis of several types of data appearing in the literature, with the result that the Rowley method is not recommended due to the inherent assumption of $\sigma_u = 0$. The McClintock and least-mean-square give consistent results that are less dependent upon the personal judgment of the investigator. The log plot approach to the analyses of these types of data remains the most simple approximation method for the determination of Weibull parameters. It is believed that effective use of these statistical tools may be accomplished by combining the log plot determination of Weibull descriptors with the extensive K value information provided in the accompanying graphs, even though this remains in need of more exploration.

3.6 Number of Specimens Required

Gregory and Spruill (Ref. 6) have also performed an experiment with a controlled sample population in which the Weibull parameters were built-in at known values to the statistical distribution. This general study method holds great potential for evaluation of methodology, as was suggested independently by several interests during the survey. With this model they have tested the McClintock and least-mean-square method of analyses as a function of number of specimens randomly selected from the population. The results are shown in Figure 5. This illustrates clearly the need for larger sample sizes than are presently being used for the evaluation of ceramic materials, if the generated data is to be successfully used in minimum-weight, high-reliability design procedures.

3.7 Reliability versus Variability

The influence of the material value $\underline{m}$ in determining the safety factor is illustrated in Figure 6, with two different levels of confidence shown. Examination of the high dependence of safety factor on $\underline{m}$ emphasizes the need for accurate information on the Weibull distribution parameters, and on the degree of variation that may be anticipated in the value $\underline{m}$ in the routine production of a material. As indicated previously, it has been demonstrated that the characteristics $\underline{m}$, σ_0, σ_u are not necessarily material constants but are varied by the influence of thermal and mechanical history.

DATA EVALUATED BY C.B. SHIELDS
OF VOUGHT ASTRONAUTICS DIVISION

NOTES 1. CURVES SHOWN ARE APPROXIMATE
ENVELOPE OF PARAMETERS DERIVED

2. M^{c}CLINTOCK METHOD IS DEFINITELY SUPERIOR
AT INTERMEDIATE SAMPLE SIZES

3. LEAST MEAN SQUARES METHOD SEEMS TO
GIVE SLIGHTLY BETTER RESULTS AT VERY
LARGE SAMPLE SIZES

——————— LEAST MEAN SQUARES METHOD

— — — — — — M^{c}CLINTOCK METHOD

NUMBER OF SPECIMENS IN SAMPLE

FIGURE 5: WEIBULL PARAMETERS DERIVED FROM VARYING SAMPLE SIZES

16

FIGURE 6: VARIATION OF MATERIAL SAFETY FACTOR WITH MATERIAL CONSTANT "m"
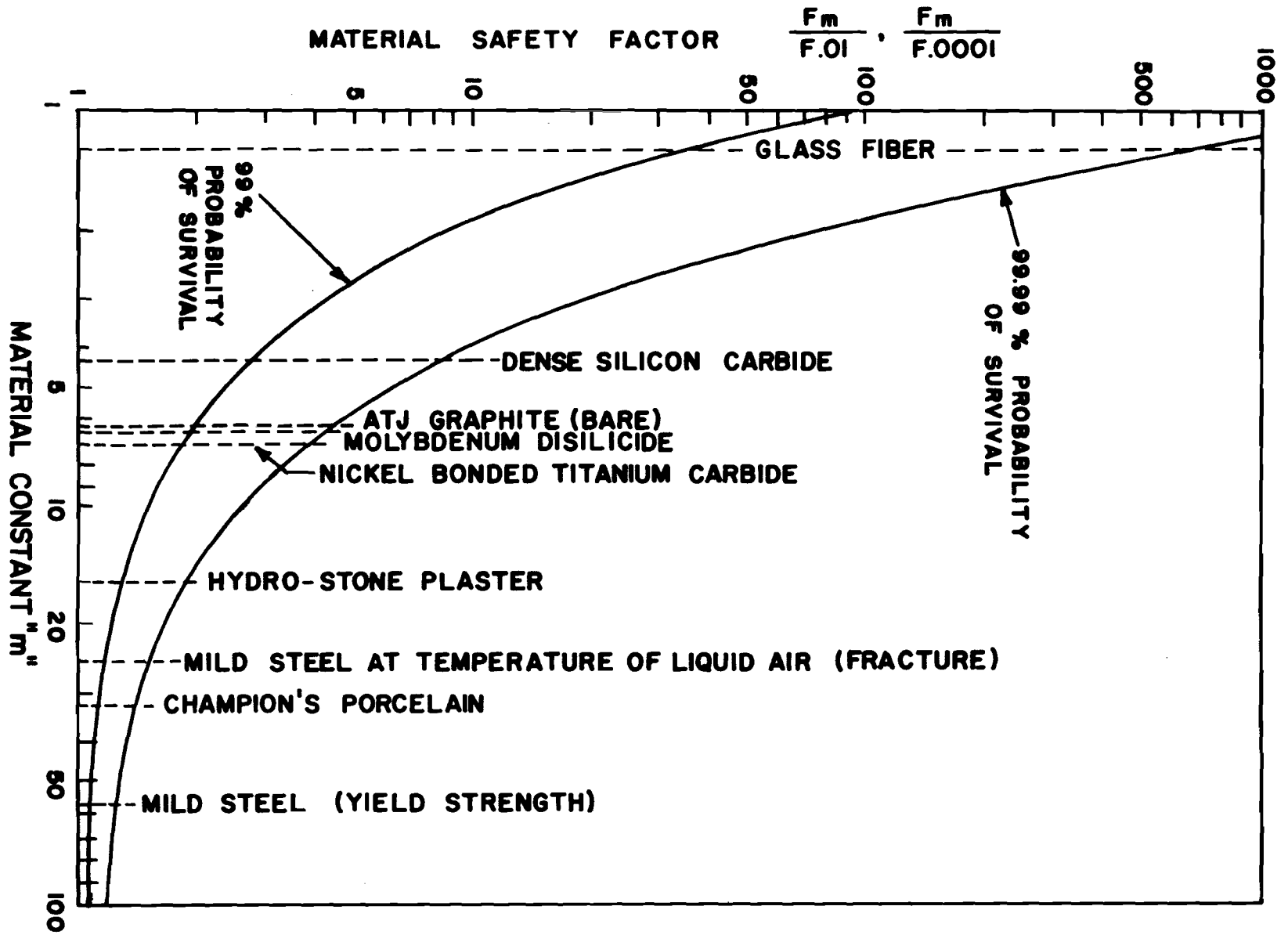
3.8

3.8 Current Limitations

The purpose of this presentation has been to illustrate the need for much more detailed information than is presently available for brittle materials. In addition to the needs on the basis of design information, the use of Weibull's statistics in analyzing test data has also been found to be an extremely powerful tool in providing insight in materials development programs. Although the emphasis has been placed on a Weibull description, it should be recognized that this approach is not completely satisfactory. A "weakest link" basis of failure probability certainly contains limited applicability for varying degrees of brittle behavior, since any local yielding will obviate the strict interpretation of a chain model. Considerable difficulty in application to biaxial stress-states has been illustrated (Ref. 7) and any useful design information must include a spectrum of stress variation. Further, if the descriptors are shown to be highly dependent on thermal-mechanical history and sensitive to surface treatment, the problems become more formidable.

IV. TESTING PROCEDURES

A. INTRODUCTION

4.1 Design of Testing Program

Any testing procedure must be based on a combination of concessions to the ideal situation. The previous section has dealt with the statistical interpretation of data for purposes of high reliability design, and concludes that large numbers of carefully controlled and representative specimens are required for the complete description of a material. If a testing program is designed for use with a routine production item which is consistently available in a proper configuration for test, then the realization of sufficient numbers of specimens may be possible. In such a case it would be desirable as a sensitive quality control technique, to define the variation of Weibull parameters as production proceeds from day to day, or as processing variables are introduced in the manufacturing spectrum of activities. On the other hand, in the case of laboratory investigations involving material resources of an expensive nature in short supply, or forming techniques of complicated, time consuming, or otherwise expensive nature, a testing program of the indicated magnitude becomes highly impracticable.

The testing program associated with a specific material is generally designed to yield information for a particular purpose. Such objectives may range from relatively simple comparative needs, commonly applied as production control techniques, to extremely sophisticated research attempts to define underlying behavior mechanisms. The selection or design of a testing procedure therefore represents an engineering judgment attempting to optimize a program on a need versus cost basis. Often this task is avoided by the dictates of standard acceptance procedures, such as outlined in various federal, state or industrial specifications, utilizing recognized standard of performance qualifications which have evolved through mutual consent or supply and demand. There is also the ever-present need for a supplier to provide some kind of test data which purports to describe his products. This type of information very often is available only in the form of a single number associated with a material property, with minimal or no accompanying information regarding the conditions of the test, the size of the specimen, the caliber of the machine, or the many other qualifying boundary conditions that can be significant in the selection of a material for a particular purpose. In many cases, it is possible to obtain more detailed information on direct question so that better informed judgments can be made. However, it is clearly established that very few materials in commercial supply are yet described to the degree ultimately necessary in structural applications demanding high reliability and minimum weight.

4.2

4.2 Correlative Value of Data

It is also true, but to a lesser degree, that a large amount of the data appearing in technical literature is of limited usefulness because of inadequate description. There is generally more concern for detailed description of specimen size, considerable recognition of the importance of surface preparation, specific statements regarding ambient conditions only when they are controlled, generally acceptable statistical treatment of mean values and standard deviations, but often a complete departure from the procedures utilized by another investigator. This situation attests to the inventiveness and ingenuity of materials researchers, and also points to the inadequacy of standard testing procedures. Attempts are underway to compile all published mechanical property data pertaining to certain ceramic materials of modern interest in an effort to arrive at a comparative property evaluation of "most likely" engineering values. This is proving to be a difficult, if not impossible, task. In addition to the above-mentioned short-comings, there is often insufficient chemical and physical description of the material to permit quantitative comparison. This is traceable in some cases to a gap between analytical techniques and requirements, such as the precise determination of free carbon in carbides, included nitrogen or other gas phases, and description of the grain boundaries where bulk impurities can concentrate.

It is obvious that comparative information in the literature would be valuable. At the same time, it is doubtful that our present technology is capable of completely defining standards in a way that would permit the necessary degree of freedom to encourage progress in materials development and understanding.

If future research in the field of brittle behavior can quantitatively define the basic mechanisms governing crack nucleation and propagation, and the relative importance of all of the significant extraneous influences, and can do so with realistic demands regarding sample sizes, then we may eventually look forward to the comparative capability that is ultimately going to be a necessity.

B. PROPERTY MEASUREMENT

The following descriptions of evaluative methods for brittle materials are evolved from selective observation, correspondence, and literature review of pertinent studies. Each category within the scope of this survey is treated in turn regarding the theoretical basis of the test, the practical limitations to the ideal performance of the test, and the present practice which illustrates the state-of-the-art.

4.3 Tensile Strength

4.3.1 Theoretical basis of the test

The determination of tensile strength involves placing some portion of the specimen in a state of uniform tensile stress. The stress at fracture is defined as the tensile strength, as given by the equation

$$\sigma = \frac{P}{A} \tag{9}$$

where
σ = stress, pounds per square inch
P = load, pounds
A = cross-sectional area at the fracture, square inches

The load is increased until fracture occurs within the rate-limitations of the load-applying machine so that the precise load at the instant of failure can be easily recorded. The load is applied at a sufficient distance from the gage section so that inadvertent stress concentrations due to gripping may be dissipated.

4.3.2 Practical limitations

A tensile test of a brittle material is undoubtedly the least used property evaluation technique. The reason for this is the extreme care that is essential to insure that maximum stresses of a pure tensile nature occur within the region of the gage length.

4.3.2.1 Grip alignment: Regardless of the type of grips utilized for exerting the tensile pull on each end of the specimen, and regardless of the specimen shape, there is the possibility, indeed the likelihood, of unsymmetrical displacements in the contact zones between specimen ends and grips. This problem of gripping eccentricity is perhaps the most important barrier to achieving uniform stress fields. Additionally there is the problem that surface damage at the point of the grips can easily result in significant stress concentration effects with subsequent failure of the specimen in the grips rather than in the gage length of the testing configuration. Also the problem of unsymmetrical grip dimensions and un-symmetrical specimen dimensions can contribute to the eccentric loading of the specimen. The magnitude of stresses arising from uncontrolled eccentricity can be a large portion of the anticipated tensile strength of the material. For instance, the per cent increase in stress on the surface of the specimen will be a function of the eccentricity:width ratio. In the case of a square rod the stress increase is eight times the ratio, and for a round rod will be six times the ratio (Ref. 4).

4.3

It has been found that photoelastic studies performed with plastic birefringent materials are not sufficiently sensitive to predict the eccentricity problems arising in tests with brittle materials in grip designs which rely on a seating of shouldered specimens into the grip (Ref. 5). Strain gage analysis of brittle specimens mounted in apparently acceptable fashion has shown bending strains amounting to as high as 60 per cent of the tensile components. Great care has been taken to overcome these difficulties through highly refined precision machining of brittle specimens combined with studies of potting compounds for accurate seating and of soft metal shims at the contact areas.

4.3.2.2 Bearing friction: Friction in the pins or bearings associated with grip attachments can also contribute significantly to the problem, although probably more success has been achieved in overcoming this latter factor than any other part of the general problem of tensile tests (Ref. 8).

4.3.2.3 Alignment aids: Even with the aid of strain gages in insuring proper seating of the specimen grips and specimen, and precision machining of specimens, the fact remains that most experimental data have shown between 25 and 75 per cent of the samples breaking apparently due to stress concentrations at places other than in the gage length or have indicated failure patterns which clearly illustrate the presence of bending strain. At temperatures beyond the capabilities of strain gage use the problem becomes more severe. However, at very high temperatures there is the possibility for local yielding and plastic behavior to relieve the eccentricity problem, so that test data in these regions of temperature are perhaps more meaningful. A fairly successful method of determining the tensile properties of refractory materials utilized this behavior in subjecting the specimens to very high temperatures under a sustained axial load and subsequently carrying the load to failure at some lower temperatures (Ref. 9).

4.3.3 Present practice

4.3.3.1 Bearing design: A very active tensile test facility at the present utilizes a gas bearing support system with a hemispherical upper bearing and a flat lower bearing. The degree of refinement in this facility is such that near perfect frictionless conditions prevail in the bearings which support the specimen holder. The improvement is significant as shown by the consistently higher tensile strength data achieved in this configuration when compared with tensile tests performed on identical materials at other facilities. However, it is believed that the associated problems of gripping and perfect alignment are not completely overcome with this degree of refinement. More usual bearing configurations are of the universal joint type, involving two hinged joints at right-angles. Cable or wire attachments between the grips and the testing machine have also been used to eliminate moment development at the bearings.

22

4.3.3.2 Direct tensile specimens: Dogbone specimens are the most popular configuration for pull tests. One type is illustrated in Figure 7. The main feature is a reduced section for the gage-length with increased section at the ends. The ends may be rounded or wedged for seating in the grips, or they may be threaded, grooved, centrally pinned, or otherwise prepared to mate with gripping fixtures. The cross section in the gage length may be circular or rectangular, with the enlarged ends usually formed with a corresponding similar geometry. An outstanding exception is the square-ended cylindrical bar, the enlarged gripping ends having greater dimensions across flats than the diameter of the gage length. Such shapes have been used in combined axial, bending, and torsional loading configurations.

Straight bars with constant cross section through the full length are unsatisfactory. Stress-concentrations acting at the grips prevent full strength development in the remaining length of specimen.

4.3.3.3 Indirect tensile specimens: Recognition of the major problem in direct tensile pulling configurations has led to the development of numerous ingenious specimens which may be loaded compressively and because of the specimen design give rise to significant gage lengths of uniaxial tension.

4.3.3.3.1 Theta specimen: Noteworthy of this class of specimen design is the so-called theta geometry (Ref. 4). shown in Figure 8. This has been shown to be relatively sensitive to size effects, and requires considerable machining precision of difficult materials. The sensitivity of size is described in Figure 9, where failure stress in the uniformly stressed central bar may be calculated as

$$\sigma = \frac{K P}{d t} \qquad (10)$$

where

σ = stress , pounds per square inch
P = applied load , pounds
D = diameter, inches
t = thickness of the specimen , inches

The value K may be read directly from Figure 9, corresponding to the particular geometry described by the parameter 30 times bar width divided by overall diameter.

4.3.3.3.2 Two-hole disk: Other specimens of interest giving rise to fairly uniform tensile stress fields are the class of disks which may be diametrically loaded and contain two holes separated centrally by a narrow strip of material. Photoelastic studies show that a uniform tensile stress area exists under the diametral load between the two holes.
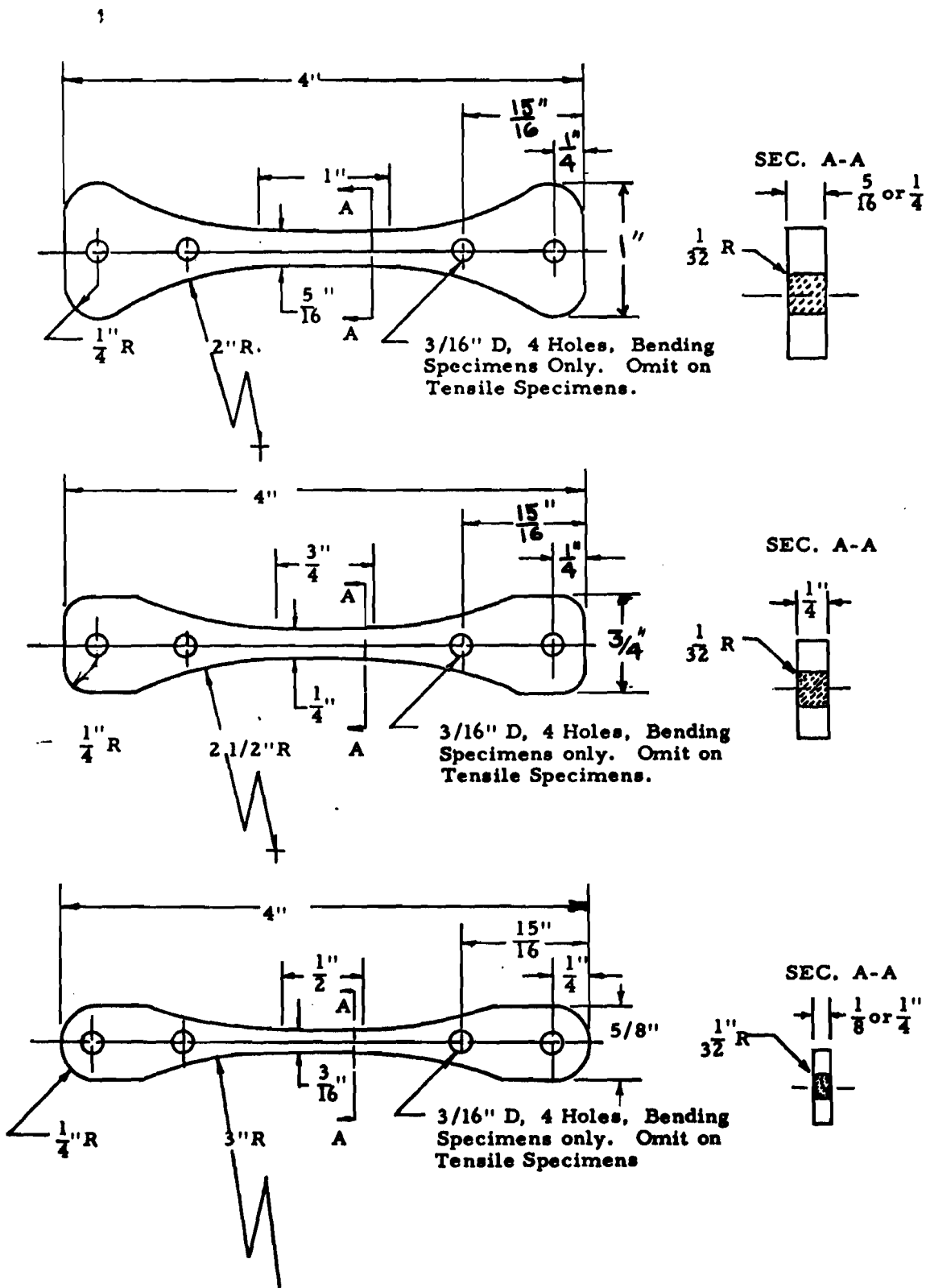
Fig. 7 DETAILS OF MULTICRYSTALLINE DOGBONE SPECIMENS
FOR TENSION AND BENDING

Minimum Thickness
to Avoid Buckling
will depend on
Modulus of Elasticity
(About .250)

1.047

0.750

0.625

0.312R

0.750R

0.887

0.125R

0.250

0.100

0.050

1.775

1.250

1.500

2.095

3.000 D
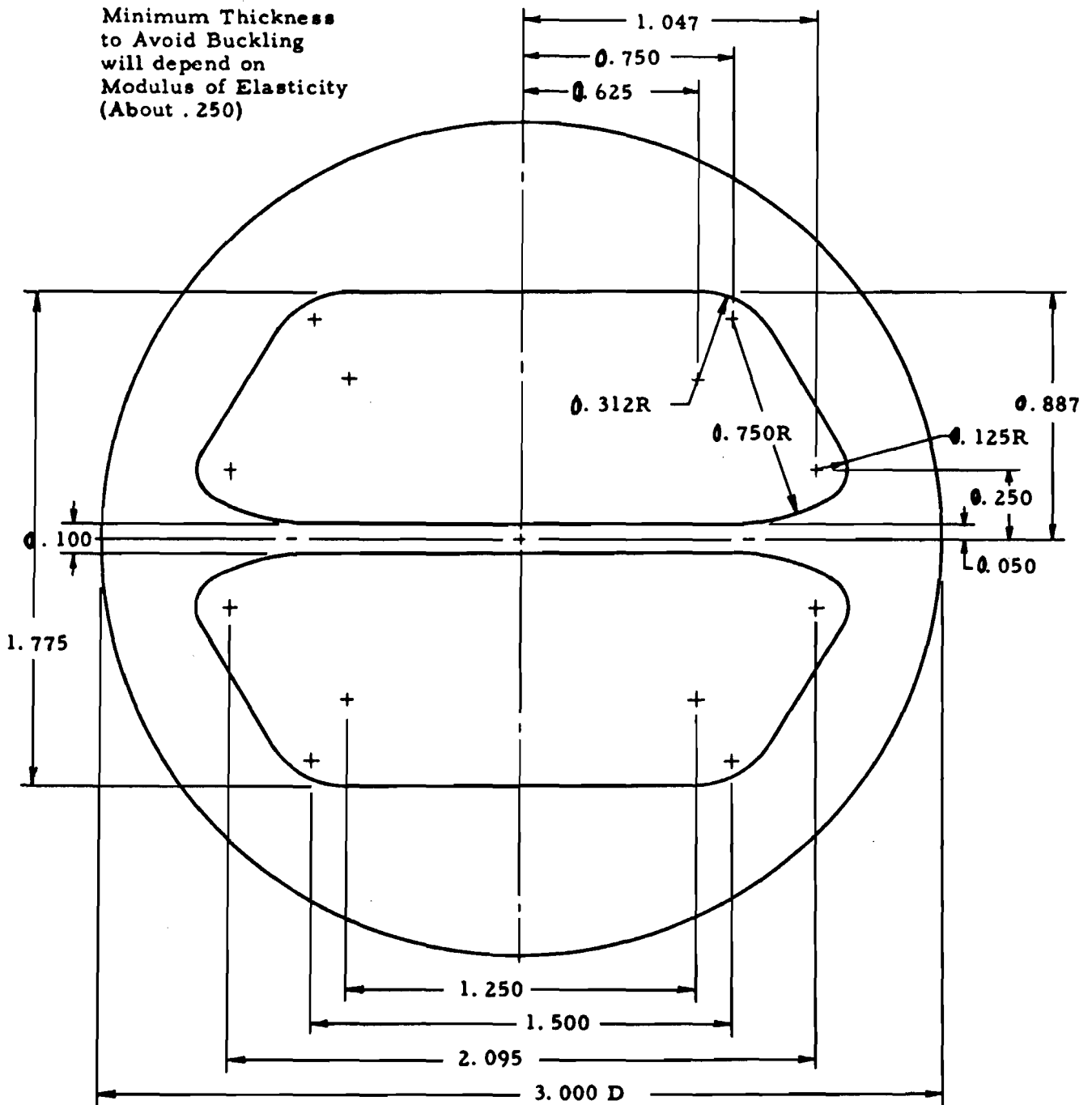
Fig. 8   THETA SPECIMEN GEOMETRY

(When a compressive load is applied perpendicularly
to the bar direction, the bar will be subjected to uni-
form tension.   Dimensions can be scaled linearly.)

25
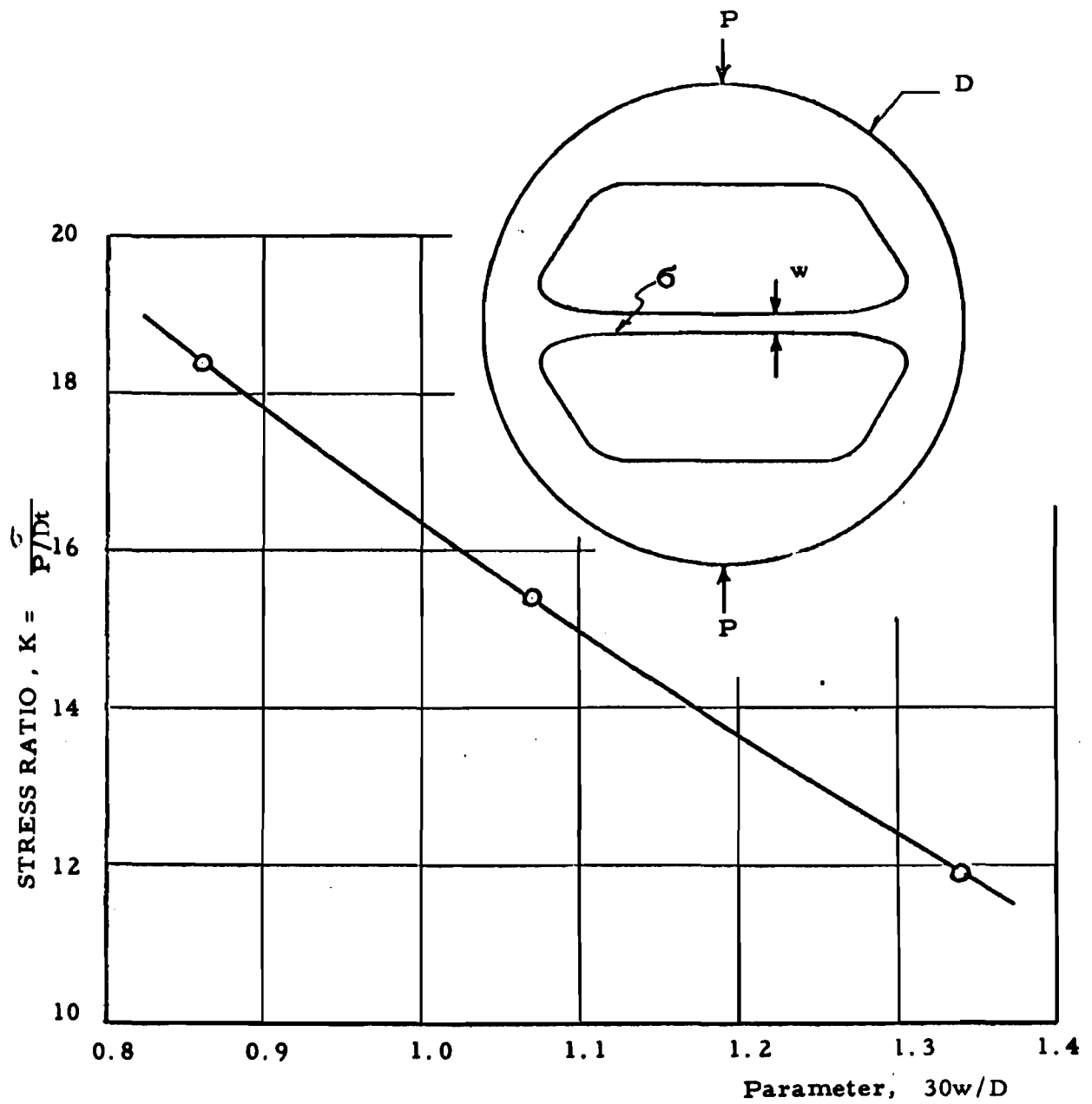
Fig. 9   STRESS-LOAD RELATION FOR GEOMETRIC
VARIATIONS IN THE THETA SPECIMEN

26

4.3.3.3.3 Trussed beam: The most recent development in attempts to achieve simple load configurations resulting in uniform stress regions is the trussed beam specimen pictured in Figure 10 (Ref. 10). Conventional center-point flexural loading on a specimen of this configuration results in a bending stress across the heavier upper beam segment and a uniform tensile field throughout most of the length of the lower segment. Studies are continuing in the development of this specimen in regard to its size sensitivity, but at present it appears to be the most promising of the flexural loading techniques for achieving a tensile field.

4.3.3.3.4 The Brazilian Test or Diametral Compression Test: This has received a great deal of attention in recent studies (Ref. 11) (Ref. 12), principally because of the ability to produce maximum tensile stresses within the body of a material, rather than at the surface. This then becomes an extremely important tool in evaluating material in the absence of surface effects. Figure 11 describes the test configuration. The length of loaded diameter which is placed under uniform tensile stress is highly dependent upon the distribution of the loads at the contact points, so that the elastic properties of specimen and loading surfaces are very important. Photoelastic studies of stress distribution in such tests have shown widely different results because of the different elasticity of various photoelastic materials (Ref. 13). The stress distribution is independent of length if uniformly loaded. The cylinder faces will be stressed in tension along the loaded diameter unless the diameter of these end faces is reduced. There are reservations in introducing the Brazilian Test at this point, but because it is often referred to as a tension test, it will be discussed in this section with future reference under the discussion of biaxial stress testing.

The simple theory describing the stress distribution under a diametral load on a disk shaped specimen would indicate that a uniform tensile stress field is developed at the geometrical center of the disk shape. The magnitude of this stress is calculated as

$$\sigma_t = \frac{2P}{\pi Dt} \tag{11}$$

where
  P = applied load, pounds
  D = diameter of the disk, inches
  t = thickness of the disk, inches
In the vertical direction, the axis of loading, the stress field in the transverse direction is highly dependent on the width of load application. The stress becomes highly compressive in both directions under the loads. The stress distribution along the loaded diameter is described in the accompanying graphs of Figure 11 (Ref. 11).
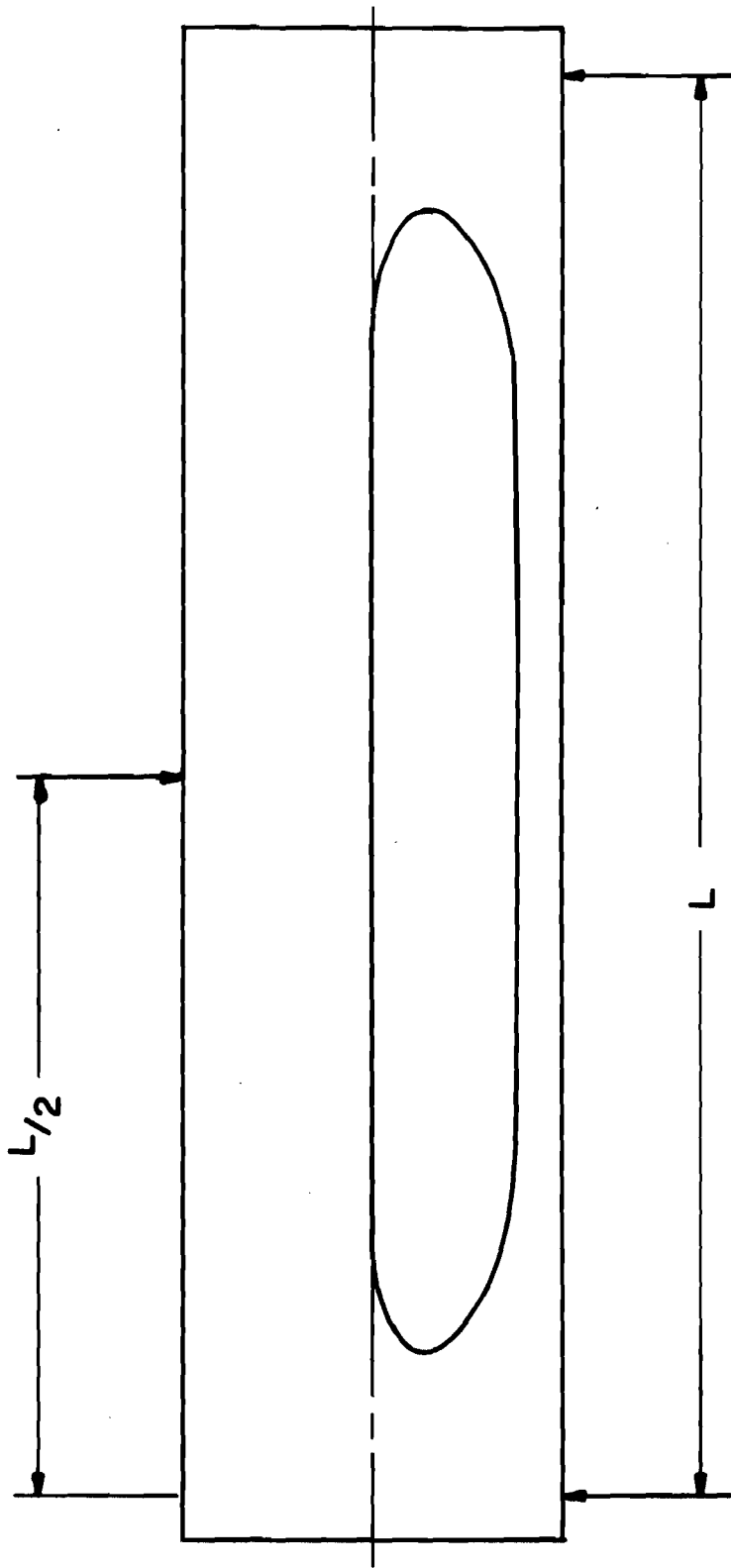
FIGURE 10: TRUSSED BEAM SPECIMEN

$$K = \frac{2P}{\pi D t}$$
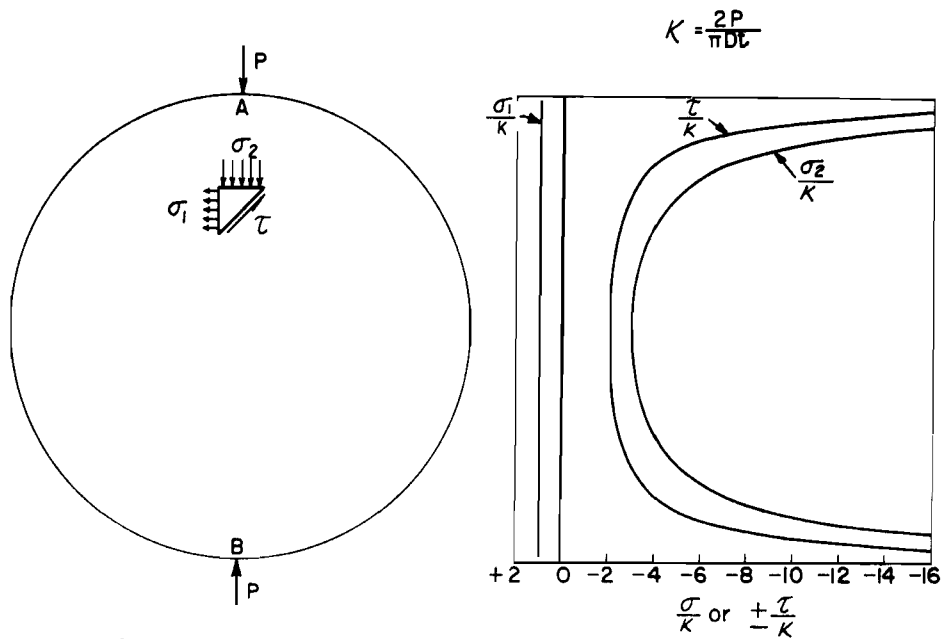
A. STRESS DISTRIBUTION ACROSS LOADED DIAMETER FOR
A CYLINDER COMPRESSED BETWEEN TWO LINE LOADS

$$k = \frac{2P}{\pi D t}$$
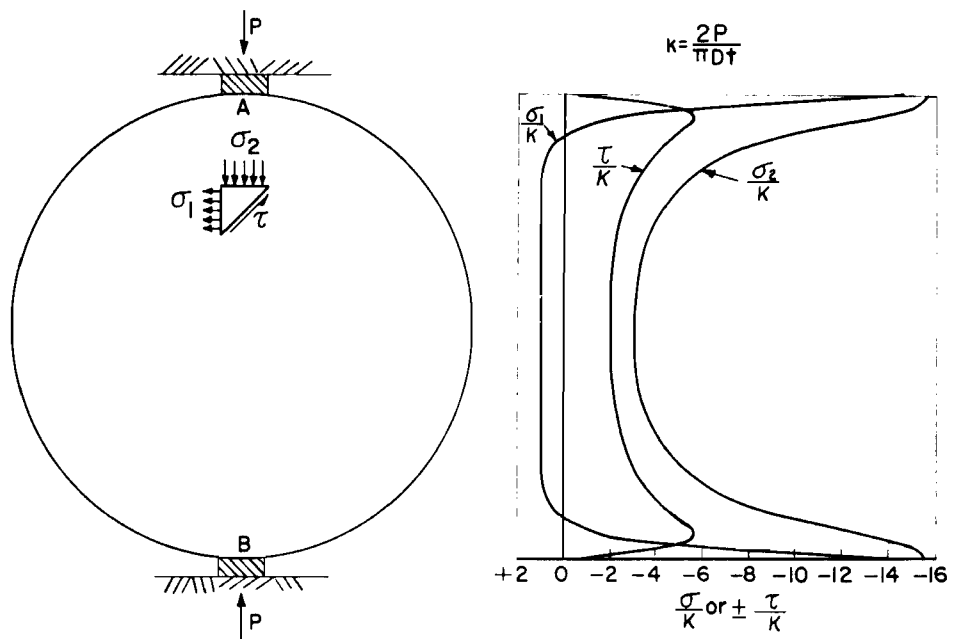
B. STRESS DISTRIBUTION ACROSS LOADED DIAMETER FOR
A CYLINDER COMPRESSED BETWEEN TWO FLAT PLATES

Figure 11. Loading Configuration for Diametral Compression Test

29

4.3

Moore (Ref. 12) has investigated the potential of this type of specimen in examining the stress characteristics of a porcelain body with attempts to eliminate profound surface influences. It is recognized that the stress distribution which is described above exists ideally throughout the thickness of a specimen of this type, so that each face of the specimen would exhibit a biaxial stress field, maximum at the geometrical center. However, in the formation of test cylinders for this work, a slight reduction in diameter at the faces of the disk has been seen to occur as a natural consequence of the shrinkage behavior during drying and firing. This permits a load distribution on the generators of the cylinder which is maximum at the center of the thickness, and tapers to a very low value or zero near the ends of the thickness. The biaxial stress state therefore no longer obtains to the same degree on the faces. This has the advantage of almost completely eliminating surface effects in evaluating the tensile strength of the brittle material.

It has been found necessary to provide a slight cushioning at the points of load application in order to minimize the important effects of slight surface or curvature irregularities. The use of blotting paper for this purpose has been successful. Analysis of the influence of such loading strips on the volume of material placed under stress shows that the wider loading region has the effect of reducing the area under tensile stress in the diametrical plane. For example, when the width of a loading strip equals 1/12 the diameter of the specimen, it is shown that approximately 5/6 of the diametrical plane is under tensile stress. The effective volume of material under test is therefore reduced by the spreading of the load.

Interpretation of results in terms of "volume under tensile stress" is not yet clearly defined, as steep stress-gradients can exist with various elastic parameters.

Modification of the diametral loading techniques involving a centrally located hole results in the so-called "brittle ring" test. Because this is essentially a bend test, discussion of the features of this specimen configuration will be presented under the topic of flexural testing (4.5.3.3).

4.3.3.3.5 Thin-walled ring: Cylindrical test specimens of short length and thin walls are used in a method for tensile testing of brittle materials developed by Sedlacek and Holden (Ref. 14). The specimen is carefully machined to dimensions of close tolerance on thickness of the ring. The prepared specimen is then contained in a testing jig which exerts a uniform internal pressure through the action of an expanding balloon contained within the internal dimensions of the cylinder. The failure stress is calculated according to the following formula

$$\sigma = \frac{P\,d}{2\,t} \tag{12}$$

where

d   = average diameter in inches

t   = wall thickness in inches

30

This expression has been accepted as adequate for cases where the radius: wall thickness ratio is ten or greater. The experimental results reported indicated no dependence of a critical nature on the precise wall thickness within the reasonable range investigated. The outstanding feature demonstrated by the reported data is the very small standard deviation associated with tensile testing. These deviations were noted to fall within the range of calculated measurement errors regarding the accuracy of wall thickness determination and pressure at failure.

The hydrostatic ring test appears to offer a significant advance in determination of the tensile strength of a brittle material. It has been pointed out that the method is easily expanded through the use of strain-gage instrumentation to the simultaneous determination of tensile strength, Young's modulus, and Poisson's ratio. It is also readily adaptable to fatigue and stress-corrosion studies, which are reported to be part of the present modifications.

4.4 Compressive Strength

4.4.1 Theoretical basis of the test

The determination of compressive strength involves placing some portion of the specimen in a state of uniform compressive stress. The stress at fracture is defined as the compressive strength given by the relationship

$$\sigma = \frac{P}{A} \tag{13}$$

where
σ = compressive strength, pounds per square inch
P = applied load, pounds
A = cross sectional area transverse to the load, square inches
The load is increased at a controlled rate until fracture occurs.

4.4.2 Practical limitations

4.4.2.1 Mode of compressive failure: The performance of a compression test at first glance would appear to be a straight-forward testing technique, even for a brittle material. There are several features of such a test which prevent this. First, the mode of failure in a compressive test is the same for a brittle material as in most other fracture cases; that is, a tensile failure. The compression test therefore becomes an exercise in applying a compressive load for the ultimate purpose of causing separation of the component parts of the material through tensile failure. This is achieved in any compressive test configuration (other than a hydrostatic case) through the influence of material expansion transverse to the direction of load, the Poisson ratio effect. As the load is applied and the material under test

31

expands in the transverse directions, continuity of the specimen demands that the segments expand in a circumferential direction by an amount that is proportional to the distance from the geometrical center of the test specimen. This means that the elemental volumes located around the outer circumference of a compression test specimen are required to exhibit more expansion in the circumferential direction than is allowed by the simple Poisson effect, so that a stretch must occur in this direction under the influence of tensile stresses. It is seen that this again results in a surface sensitive behavior, since it would be anticipated that the maximum tensile stresses would be developed at those fibers which are located at the maximum distance from the geometrical center. Since other fibers located between the center and the extreme are undergoing varying degrees of circumferential stress, the influence of flaws would be expected to appear also in compressive strength data. The triaxial stress state resulting from the applied compressive stress and the resulting circumferential tensile stress (with little development of radial stresses in the unrestrained direction) may be expected to influence the size and orientation sensitivity of flaw occurrence.

4.4.2.2 Uniformity of stress distribution: Other difficulties are inherent in the performance of compressive tests in the sense of achieving throughout the specimen a uniform compressive stress field. In compressing the specimen between the plane surfaces of a testing machine, it is not normal to find the compressive force uniformly distributed over the cross section. This is partially a reflection of the critical need for near-perfect surface contact to avoid local stresses, and is also due to friction between the contact surfaces of the specimen and the machine. The lateral expansion both radially and circumferentially is prevented at the contact surface, so that compressive stresses are developed also in the directions transverse to the load application at the contact surfaces. The result of this end-restraint is commonly seen in the conical type of fracture occurring in compressive tests of brittle materials. This is a clear illustration of the lack of lateral restraint at the midlength of the test specimen.

4.4.3 Present practice

4.4.3.1 Specimen size: The performance of compressive strength tests in the ceramic industry is quite common, in spite of a complicated problem of interpretation. Specimens sizes are usually kept fairly small, covering the range 1/4-inch diameter x 1/2-inch height to 4 1/2 x 4 1/2-inch cross section for materials commonly used in straight compressive application. Some degree of standardization in sample size is found within various organizations and product types. However, there is probably less concern for defining a standard specimen size in this test than in most others.

4.4.3.2 Uniformity of loading: There is ample recognition of the need for careful alignment of the specimen and the platens of the testing machine. This is accomplished in many cases by suitable potting compounds on the two compressed surfaces, and additionally through performance of tests on one hemispherical bearing plate to permit self-alignment under load. Surface irregularities are virtually eliminated with smooth end-caps of plaster or other suitable material.

4.4.3.3 Friction at loading area: The influence of head friction may be over-come in several ways, the most common procedure being to provide a dummy test specimen above and below the test piece and in contact with the head of a testing machine. Lateral restraint will occur between the dummy specimen and the head, but if the Poisson's ratio effect is permitted to occur at the interface at each end of the test specimen, restraint will not occur. Another possibility (not used) is to shape the heads of the testing machine so that the included angle of the cone in contact with the specimen is 180 -2 ϕ where ϕ is the angle of friction. Thus the effect of friction is compensated for by the wedging action, and results in uniform compression. These measures result in failure under compressive load which is essentially a subdivision into plates parallel to one of the lateral sides.

Another possibility would be the forming of a double cone test specimen con-taining a gage length between the narrower ends of the cones. If the cone angle approaches that of the same material exhibiting typical conical fracture, the shape would permit development of uniform compressive stress across the area of the gage section.

In compressive strength determinations of very hard dense ceramics, it has been found that the strength magnitude is severely influenced by the hardness of the loading faces. The use of mild steel plates between the platens of a testing machine and the ends of a hard specimen were thought to aid significantly through the ability of the material to seat into the loading member and thereby avoid un-desirable concentration of load. However, with careful preparation of the surface to be loaded, replacing the mild steel backup pieces with ceramic of similar qualities of that being tested results in much higher compressive strength values.

No example of conically ground seating plates for the avoidance of frictional forces between the specimen and the platen was found in use for brittle materials.

4.5 Flexural Strength

4.5.1 Theoretical basis of the test

The determination of flexural strength involves placing some portion of the specimen in a state of pure bending. The maximum stress at fracture is defined as the flexural strength, often called the modulus of rupture. The maximum stress is given by the equation

4.5

$$\sigma = \frac{Mc}{I} \tag{14}$$

where
σ = extreme fiber stress, pounds per square inch
c = distance from the neutral axis of the beam to the extreme fiber, inches
M = bending moment at the point of rupture, inch-pounds
I = moment of inertia of the cross section about the neutral axis, inches^4

4.5.1.1 Assumptions in the stress equation: The basic assumptions inherent in the development of the equation are that the original transverse plane of the beam at the location of moment calculations remains strictly as a plane after bending occurs and is normal to all longitudinal fibers after the bending; and that the homogeneous material follows Hooke's law of linearity with strain and stress so that the stress distribution is linear across the bent beam and is directly proportional to the distance from the neutral axis. It is further assumed that bending is occurring in a plane of symmetry of the beam. The equation presented above was qualified as being applied to the case of pure bending, which means the absence of shearing stresses. This situation holds in the case of moments acting on the ends of a specimen, or within the central region between two concentrated loads symmetrically placed between the supports, such as third-point or quarter-point loading. It can be shown that in the presence of a shearing stress gradient the assumption of remaining planes after bending is no longer valid; however, so long as the shearing force remains constant along the beam the warping across all cross sections is the same so that the stretching or shrinking produced by the bending moment in the longitudinal fibers is unaffected by shear. Because of this fact the above equation remains adequately valid in its applications to such cases as a cantilever which is bending in the presence of a constant shearing stress. The warping of cross sections due to the shear from a uniformily distributed load on the beam does not substantially affect the strain in longitudinal fibers, and therefore the equation still remains sufficiently valid.

4.5.1.2 Wedging correction: For center point loading the stress distribution is much more complicated in the vicinity of the point of load application. This perturbation in stress distribution is of localized character and is of importance only in the close vicinity of the load. If the cross section of the beam is considered at a distance greater than 1/2 the depth of the beam, the stress distribution in that cross section is approximately that given by the simple beam formula. However, there is a wedging action (Ref. 15) associated with the concentrated central load application which can become important depending upon the ratio of beam depth to span. This wedging action beneath a concentrated load results in the development of a bending moment reverse to the beam bending moment used in the simple formula, as well as a tensile stress distribution through the depth of the beam beneath the load. The combined effects of this action reduce the bending stresses calculated by the beam formula according to the following equations:

$$\sigma_{max} = \frac{Mc}{I} \left(1 - \frac{4}{3\pi} \frac{h}{L} \right) \qquad \text{(rectangular)} \qquad (15\ a)$$

$$\sigma_{max} = \frac{Mc}{I} \left(1 - \frac{3}{2\pi} \frac{d}{L} \right) \qquad \text{(circular)} \qquad (15\ b)$$

where

- h = depth of beam in direction of load, inches
- d = diameter, inches
- L = span, inches

It is possible that this behavior described as wedging action has contributed to the difficulty of interpretation in terms of Weibull's statistics for taking account of the influence of volume under high stress in the presence of center-point loading flexural testing, and also accounts in part for the observed influence of shorter span in yielding higher calculated stresses.

4.5.2 Practical limitations

4.5.2.1 Stress concentrations: So as to avoid stress concentrations there should be no abrupt changes in cross section in the vicinity of a reduced area. Also the loads should be supplied at sufficient distances from such a reduced area, such as four times a lateral dimension, to insure an even stress distribution. Since in flexure the maximum stress occurs at the outer surface, cracks and flaws at the surfaces are of primary importance. Localized stress-raising effects for gross disturbances in surface regularity are illustrated by the following example:
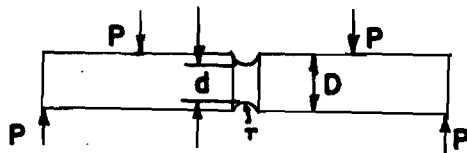
For r/D equal to 0.001 and d/D equal to 0.990, it is found that the stress-concentration factor is 5.8. For sharper crack radius (smaller r) this factor will increase rapidly.

4.5.2.2 Torsional stresses: Considerable care must be exercised to insure that the test specimen is free from torsional loading during the application of the test load. Torsion can occur as a result of bar warpage or other types of imperfect support alignment with the specimen. Several methods are proposed and are in use for eliminating the possibility of support nonalignment, such as the introduction of hemispherical or ball bearing pins or supports capable of rotary alignment in the transverse direction of the bar. Hemispherical heads are often used at the point of application of the concentrated loads. See section 4.6.1.2.

4.5.2.3 Elasticity in tension and compression: Duckworth (Ref. 16) has investigated the use of bending tests for precise determination of tensile failure stress in brittle materials. His evaluation leads to recommended specimen shapes for cross-bending tests in a reduced section with four-point loading outside the reduced section. The assumption that Young's modulus is the same in tension and compression is brought out in this analysis, with the more precise equation for tensile stress being dependent upon the outer fiber strains as:

$$\sigma_t = \frac{3 M (\epsilon_t + \epsilon_c)}{b d^2 \epsilon_t} \tag{16}$$

where

σ_t = maximum tensile stress due to bending, pounds per square inch
b = breadth of gauge section, inches
d = depth of gauge section , inches
ϵ_t = tensile bending strain of outer fiber, inches per inch
ϵ_c = compressive bending strain of outer fiber , inches per inch

4.5.2.4 Non-Hookeian behavior: In case the stress-strain diagram is not linear in either the compression or tension case the above equation is not valid. Non-linearity yields incorrect stress data. Baldwin (Ref. 17) has shown through more rigorous development of the equations that the load-deformation curve obtained either in flexure or torsion exhibits much less non-linearity than the stress-strain diagram of the material.

4.5.2.5 Strength comparisons: The size effects in comparison of results from geometrically similar flexural tests would be a strength lowering as predicted from the increased surface area and volume under high stress corresponding with the larger specimen or longer span of beam under uniform moment. In comparison with tensile specimens, it follows that the tensile specimen of similar size would fail at a lower nominal stress, due to the much greater probability of critical flaws occurring within the greater volume under high stress.

There are two underlying differences in comparing the results of flexural tests performed on rectangular cross section or circular cross section beams. In the former case it may be seen that the extreme fibers opposite the point of application are all theoretically in the field of maximum stress. Further, the effects of the edges of the bar give rise to stress concentration factors depending on their sharpness. In the case of round cross sections only the single extreme fiber in the farthest point from the load application is theoretically under the maximum stress and stress concentration factors due to abrupt changes in shape are absent. Comparison of results therefore should take into account the much higher probability for the occurrence of a critical flaw within the region of maximum stress in the case of the rectangular cross section. In general, the dispersion of test data in this case will be lower, as will the observed mean strength. For the circular cross section

there is less likelihood of critical flaw occurrence in the region of high stress, and therefore on the average the results will show greater strength. The philosophy of testing which dictates the shape of cross section to be used therefore depends on the type of data which is sought. It is generally accepted that the rectangular cross section yields more realistic results in terms of end usage, and perhaps lends itself somewhat better to statistical interpretation. Greater care must be exercised however, in preventing the above-mentioned torsional effects due to bar warpage or support misalignment.

4.5.2.6 Frictional Influences: An error introduced by frictional forces between the load points and specimen surface in four-point loading has been studied by several investigators (Refs. 5, 18). The frictional forces which are developed during the flexure of the specimen produce a bending moment which is opposing that being applied and measured during the test. Stresses as calculated from the beam equation neglecting these frictional effects are therefore in error, and should be reduced by the factor shown in the following equation (assuming μ is the same at each contact):

$$\sigma_f = \sigma \left(1 - \frac{\mu\, h}{a} \right) \tag{17}$$

where

σ_f = bending stress in the presence of friction, pounds per square inch

σ = calculated stress neglecting friction, pounds per square inch

μ = coefficient of friction between the fixture and the specimen, dimensionless

h = depth of specimen in direction of load, inches

a = distance from support to nearest load, inches

In the absence of frictional effects in a test on an identical specimen, the load at failure would be reduced by the ratio $(a - \mu h)/a$. The only known attempt at experimental verification of this phenomenon reports an opposite effect, thereby throwing the data into serious question. (Ref. 5)

With the assumption that the coefficient of friction existing between the ceramic and the loading members is in the order of 0.4, the correction terms can become very significant. Specifically, for quarter-point loading on a beam with span to depth ratio of 10, the reduction at maximum frictional force is 16 per cent. Third-point loading of the same beam predicts 12 per cent reduction.

Because frictional forces build to their maximum value and then reduce significantly in the presence of any sliding, the effect may be expected to be erratic and dependent to a large extent upon the surface finish. It is possible that these frictional effects are important in determining the degree of scatter normally obtained in flexural tests of brittle materials.

4.5

4.5.3 Present practice

Flexural tests are without any doubt the most popular procedures for evaluation of mechanical strength of ceramic materials. This is primarily due to the ease of physical setup, particularly with reference to strength determination at elevated temperatures, and the assumed simplicity of stress calculation.

4.5.3.1 Dogbone specimen: Dogbone specimens are generally described as bar shapes with enlarged ends, so as to permit loading and supporting attachments at the enlarged sections in the plane of the neutral axis of bending. This geometry has the advantage of eliminating the errors introduced by friction forces between the loading and supporting points and the surfaces of a normal bar specimen, as discussed above under the subject of practical limitations. The transition from the reduced section to be subjected to pure bending and the enlarged ends is made as smoothly as possible with a controlled radius of curvature. A central length of uniform depth is provided in the designed specimens, as shown in Figure 7. It has been shown that the design suggested here permits control of the stress concentration factors around the loading and supporting holes so that the maximum stress on bending does occur in the central region.

Frictional effects are often not considered, and dogbone shapes are loaded and supported on the surfaces.

Center-point loading is generally not practiced on dogbone specimens, except with a view toward analysis of the friction effects or comparison with other forms of loading.

4.5.3.2 Bar specimens: A wide variety of bar specimens is utilized in flexural strength measurements of ceramic materials. These range in size from micro specimens, one inch long by one-quarter inch diameter or one inch long by one-quarter inch wide by one-eighth inch deep (or even smaller on width and depth), to standard refractory brick sizes. The most satisfactory ratios of span to depth of specimen have been found to be in excess of ten to one as shown by Milligan (Ref. 19). It is further recommended that midpoint loading be avoided wherever possible, in favor of the practice of third-point or quarter-point loading. Midpoint loading is in common use, however.

Numerous designs have been generated for the application of bending loads to bar specimens at high temperatures. These may be classified as to whether the specimen is to be moved into position under the loading configuration at testing temperature, or the specimen is to remain as originally placed on the supporting configuration. The first type has the advantage of permitting large numbers of specimens to be easily tested during one test run, while the second insures more accurate positioning of the test bar on the support. Both methods are used extensively throughout the industry. A recent development especially

38

4.5

applicable to the micro specimens combines the advantage of both general types, allowing for a large number of specimens to be tested with one loading arrangement, while insuring precise positioning of the specimen. This involves a loading frame to support the individual specimens at the third point or quarter point, separate spaces being provided for each specimen and the specimens supported one above the other. The additional loading member then applies load at the ends of each specimen, either moving to the next specimen in turn while the supporting jig remains stationary, or accepting the ends of the bars as the supporting jig is moved into position. Such arrangements permit tests of up to 20 specimens to be performed before the necessity of reloading the jig.

4.5.3.3 Brittle ring test: The brittle ring test is performed by placing a diametral load on a thick-walled hollow cylinder. The brittle ring is a form of flexural specimen in the sense that a bending stress gradient exists under the applied load, resulting in the development of maximum tensile stresses at a surface. There are significant advantages to the use of a brittle ring, particularly at high temperatures. Alignment problems are avoided, since the specimen is loaded between two flat surfaces, and the bending moment depends on specimen size only. It should be emphasized however that a brittle ring test is more properly compared with a flexural situation than a tension test. The brittle ring will have in general very much less volume under maximum stress than the normal comparative flexural specimen in four point loading, so that somewhat higher strength results may be expected. The maximum stress at failure, occurring directly opposite the loading points on the inner periphery, is given by the equation

$$\sigma = \frac{P K}{\pi r_o} \qquad\qquad (18\ a)$$

where
P = load at failure, pounds
K = stress constant dependent on the ratio of the inside to outside diameter
r_o = the outside radius of the ring , inches

A discussion of the brittle ring test is offered in Reference 20. A distinct disadvantage to the method in its present stage of development is the degree of uncertainty regarding the correct stress concentration factor K to use in the above equation. The proper value of K for any particular material can be ascertained from a strain gage study in which the stress at failure is calculated from the product of Young's modulus of elasticity and measured strain, according to the following expression:

$$K = \frac{2 \sigma t (r_o - r_i)}{P} \tag{18 b}$$

where

σ = stress calculated from $E\epsilon$, pounds per square inch

t = thickness of the ring, inches

$r_o - r_i$ is the outside radius of the ring minus the inside radius, inches

P = load corresponding to stress, pounds

Figure 12 describes the variation of the stress concentration factor as a function of the ratio between inside and outside diameters of ring specimens, comparing the results of calculations for stress constants according to the above equation with values obtained from photoelastic studies and calculated theoretical values. It is seen that a ratio r_i/r_o of 0.15 to 0.3 will give the most constant results. It appears from the above that the stress concentration factor depends to some degree on the true linearity of the stress strain curve at or near the failure stress.

4.6 Torsional Strength

4.6.1 Theoretical basis of the test

The determination of torsional strength involves placing some portion of a round specimen in a state of pure shear. This is accomplished by the application of a twisting moment to a cylindrical specimen which is fixed on one end, or through the application of equal and opposite twisting moments. The maximum stress at fracture is defined as torsional strength, sometimes called modulus of rupture in torsion.

The maximum shearing stress in a circular cross section is given by the equation

$$\tau_{max} = \frac{16\ T}{\pi\ d^3} \tag{19}$$

where

T = twisting moment, inch-pounds

d = diameter of specimen, inches

4.6.1.1 Stress distribution: The distribution of shearing stress along a radius is linear, according to the following expression

P/A = NORMAL STRESS
S₄ = MAXIMUN TENSILE STESS

$K_4 = \dfrac{S}{P/A} = \dfrac{S(D-2r)t}{P}$

$\overline{K}_4 = \dfrac{S_u}{P/A}$

Sᵤ = ULTIMATE TENSILE STRESS
P' = BREAKING LOAD
D = OUTSIDE DIAMETER
2r = INSIDE DIAMETER
A = (D-2r)t

— — — K₄ THEORETICAL
O K₄ BAKELITE
◇ K₄ (SR-4) ACRYLIC
▲ $\overline{K}_4$ ACRYLIC TENSILE
        SPECIMENS
■ K₄ GRAPHITE (SR-4)
✕ K₄ CONCRETE (SR-4)
◆ K₄ PORCELAIN
□ ALUMINA
△ STEATITE
◇ CORDIERITE
▽ GYPSUM

FACTORS OF STRESS CONCENTRATION, K₄

RATIO 2r/D
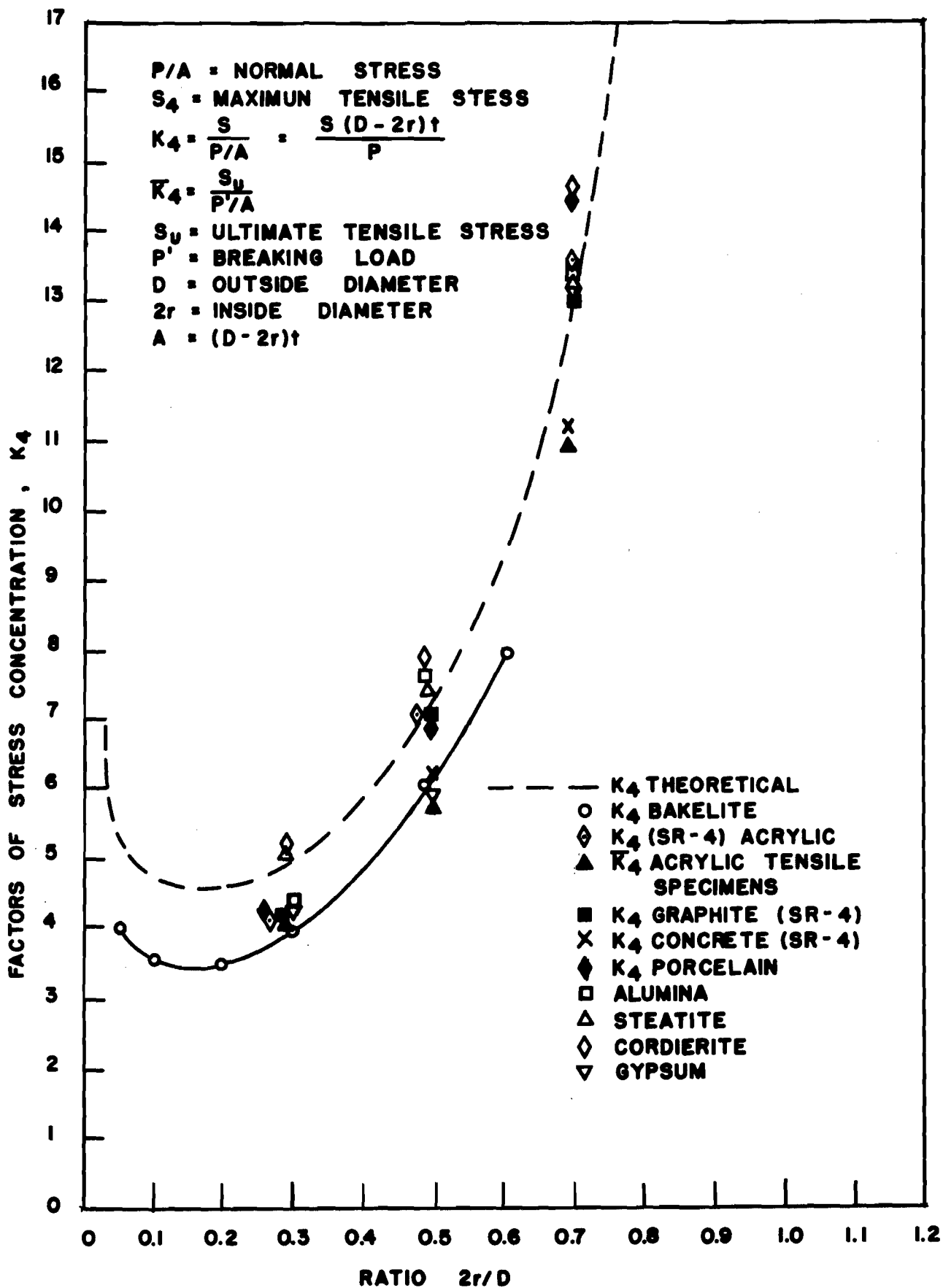
FIGURE 12 : RING STRESS FACTOR   (FROM REF. 20)

41

4.6

$$\tau = G r \theta \qquad (20)$$

where
  G = modulus of elasticity in shear, the rigidity modulus (4.9.1)
  r = radial distance from the geometrical center, inches
  θ = angle of twist per unit length of the shaft , radians per inch

The state of stress at the surface of a circular shaft subjected to torsion is described as pure shear, which is equivalent to a biaxial stress state of pure compression in one direction and pure tension of an equivalent magnitude in the transverse direction. The magnitude of shearing stress is precisely equal to the compressive stress or the tensile stress. The directions of shear stress at the surface of a twisted cylinder are parallel and transverse to the axis of the cylinder, or very nearly so. In fact, the small angular difference that exists is the definition of the shearing strain. Since the maximum tensile stress resulting from the shear occurs at an angle of 45° to this direction, tensile failure in such a specimen results in a helical fracture surface tilted at 45° from the axial direction.

For a material which is weaker in shear in the longitudinal direction than it is in the transverse direction, the first crack will be produced by shearing stresses acting in the axial sections and it will appear on the surface of the shaft in the longitudinal direction. If the material shows an isotropic shear strength which is weaker than the tensile strength, the cracks have an equal probability of occurring in the axial or transverse direction. For brittle materials which are generally much stronger in shear than in tension, the typical failure will be the helical cracking described above.

4.6.1.2 Assumptions in the equation: The assumptions made in the development of the equations for shearing stress and also the linear distribution of stress across a section are similar to those discussed previously for the bending stresses. It is assumed that circular boundaries of the cross section of the shaft remain undistorted and that the cross sections themselves remain plain and rotate as if absolutely rigid. This assumes that every diameter of the cross section remains straight and rotates through the same angle. Just as the equations for bending stresses assume the absence of torsional effects, the above equations for torsional stresses assume that no bending exists. Any bending transmitted through the shaft will result in additional stresses which may be calculated from the bending formulas and added by superposition to those resulting from torsion. The bending stresses are not oriented in the same direction as the tensile stresses resulting from shear, however, and it becomes necessary to add these vectorially as follows:

42

4.6

$$\sigma_{max} = \frac{16}{\pi d^3} (M + \sqrt{M^2 + T^2}) \tag{21}$$

where

σ_{max} = the tensile stress at the surface from the combined effects of bending and torsion, pounds per square inch

d = is the diameter of the rod, inches

M = bending moment , inch-pounds

T = twisting moment, inch-pounds

The direction in which the above maximum stress will act depends upon the relative magnitude of bending and shear stresses, and will result in failures greater than 45° but less than 90° from the axial direction.

4.6.2 Practical limitations

4.6.2.1 Stress concentrations: Since the maximum stress occurs at the outer surface in a torsional test, the condition of the surface as to cracks and other flaws is of primary importance, just as in a flexural specimen. In the torsional case, however, there are additional considerations which are of particular significance in many types of ceramic products that may be formed by extrusion processes, either in the sense of normal extruding or removed from a pressing die by extrusion from an end, or formed in a split die or mold which contains mating surfaces in the direction of the axial length. The stress concentration factor for a vanishing longitudinal groove is found to be two times the nominal stress. If the groove is oriented at 45° with the axis of the beam, this factor will approach three.

4.6.2.2 Bending stresses: The most outstanding limitation and difficulty in the performance of torsional tests of brittle materials is the complete elimination of undesirable bending moment. This limitation prescribes test specimens which are carefully machined to be truly straight, this becoming particularly important as the diameter increases. From this standpoint it is therefore desirable to work with samples of minimum length, but it is equally important to provide sufficient distance between the points of load application and the gage lengths so as to insure a true stress distribution.

The influence of bending stresses on the torsional test is described in section 4.5.2.2 and equation (21).

4.6.2.3 Strength comparisons: It is clear from the above discussion of stress distribution (4.6.1.1) within a torsional specimen that the statistical occurrence of flaws in the region of high stress would be very similar to that expected in a flexural specimen, except that the entire outer cylinder of material is under a high stress, rather than the small volume on one side of a flexural specimen. Comparisons on the basis of volume then would be intermediate between a tensile specimen and a flexural specimen.

43

4.6.2.4 Elastic properties: As will be discussed later under elastic property determination (4.9.1.1), torsional tests provide an excellent procedure for the determination of the modulus of elasticity in shear. Strain gage instrumentation can be accomplished so as to measure the strain, either as influenced by stray bending moments or completely apart from the effect of bending moment. This becomes a powerful tool for the measurement of Poisson's ratio within the temperature limit of such gages. Optical determination of twist may be performed to permit these same measurements at high temperatures.

4.6.3 Present practice

4.6.3.1 Specimen design: Because of the relative ease of applying the desired load, torsional tests have been more popular with brittle materials than have straight tensile tests. However, the numerous problems associated with perfect specimen alignment and elimination of bending moments do present some formidable demands upon the investigator. The most popular specimen shape is a machined cylinder with slightly enlarged ends, terminating in a gripping surface which is flattened to properly fit the chuck-type holder as described in Figure 13. The reduced section for the gage length of the specimen is generally centrally located with a gradual radius between the reduced section and the enlarged ends. In the case of elevated temperature studies, it is common practice to permit the specimen to extend from the ends of the furnace and subject the reduced section only to the test temperature. However, as pointed out in the above discussion on length limitation, this requires special attention to the problem of keeping the specimen truly straight. Some studies which have evolved more popular torsion testing techniques have permitted the specimen to remain a reasonable length and provide refractory shafts which can transmit the torque to the specimen in the interior of the furnace (Ref. 21).

4.6.3.2 Twist measurement: Torsion testing has been applied to the study of many refractory materials at elevated temperatures. The principal difficulty is in precise measurement of the twist in a furnace assembly. This has been accomplished at moderate temperatures through the use of extension rods attached to the gage length and protruding from the furnace for measurement, by optical lever, strain gage, differential transformers, or telescopic methods. The use of sapphire mirrors affixed to the specimen within the gage length permits an optical lever technique for precise measurement of the strain. For operation at very high temperatures this requires a powerful slit light source and an opal glass screen. Temperatures above 1350°C demand the use of modified light sources with suitable filters to separate the reflection from the general radiation within the furnace.
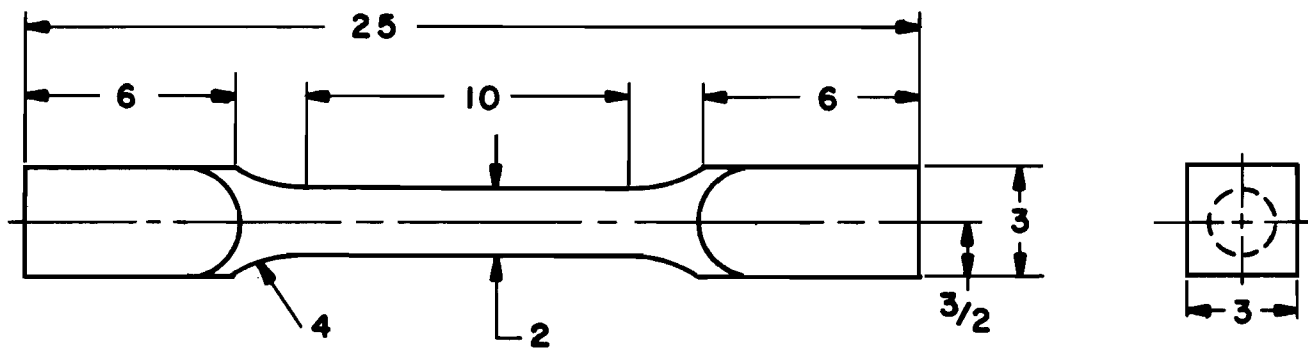
FIGURE 13   TYPICAL   TORSION   SPECIMEN   SHOWING
RELATIVE   DIMENSIONS

4.7

4.7 Impact Strength

4.7.1 Theoretical basis of the test

4.7.1.1 Energy measurement: Impact tests are most generally performed by rapidly loading either a cantilever or simply supported beam specimen. When applied to tough (or ductile) materials the impact test may be construed as a means for measuring the energy-absorbing qualities of the material. When the test is consistently applied to geometrically identical ductile specimens it gives an indication of the metallurgical condition of the specimen. The situation is quite different in regard to brittle materials, however, for they do not (by definition) absorb energy by plastic deformation to any marked degree. The energy recorded in an impact test is elastic energy, representing work done on the specimen. It is legitimate therefore to calculate the bending stress in a simply supported centrally loaded specimen by the formula derived from a bending energy statement, provided that the deflection curve of the loaded beam for use in this statement is in fact the curvature of the beam at failure. It is in this limitation that the theoretical basis of stress calculation from energy measurements has been limited. Neglecting the several assumptions necessary to the truth of the equality, the maximum bending stresses in a simply-supported, centrally-loaded beam specimen would be as follows:

$$\sigma^2 = 18 \; \frac{E\,u}{A\,L} \qquad \text{for a rectangular specimen} \qquad (22\ a)$$

$$\sigma^2 = 24 \; \frac{E\,u}{A\,L} \qquad \text{for a circular specimen} \qquad (22\ b)$$

where
σ = bending stress at rupture, pounds per square inch
E = Young's modulus of elasticity, pounds per square inch
A = cross sectional area, square inches
L = span, inches
$\underline{u}$ = energy absorbed by the specimen, inch-pounds

In the brittle material $\underline{u}$ is a small quantity which is likely to be overshadowed by the kinetic energy supplied to the specimen and to component parts of the testing machine.

4.7.1.2 Force measurement: In an effort to determine the failure stress more accurately during impact of brittle materials, a force measuring machine has been used in place of the conventional energy measurement machine. A mathematical analysis of the inertial forces necessary to accelerate the bar specimens into flexural behavior shows that the rate of application of bending stresses to a specimen in an impact test depends upon the geometry of the test specimen, and the Young's

46

modulus and density of the material, as well as on the approach velocity of the impacting hammer. The studies further showed that three general types of impact failure will be experienced as the testing velocity is increased. At low velocities corresponding to incremental types of testing, the impact is shown to be a series of blows of successively increasing intensity to the point of failure, often with a considerable time lag between the final peak loading and the previously achieved peak loading. A second general type of impact loading occurs at slightly higher approach velocities, characterized by the fact that the hammer is not in contact with the specimen at the time of failure. Sufficient inertia is imparted to the specimen during initial contact time to cause acceleration through the first flexural quarter wave, from which the specimen never recovers. The third general type of impact behavior was observed to be continually and uniformly increasing load to a peak achieved at time between 10 and 60 microseconds. The approach velocity in the later case exceeds the minimum required to accomplish characteristic loading rate defined by the relative hardness of the striker and tested material. The bending stress equation developed in this study is as follows: (Ref. 22)

$$\sigma_{max} = \frac{Mc}{I} (1 - K) \tag{23}$$

where

σ_{max}	=	bending stress at the extreme fiber at the opposite point of impact, pounds per square inch
M	=	bending moment computed from the applied force, inch-pounds
I/c	=	section modulus, inches^3
K	=	time dependent function determined from the graph of Figure 14 which applied to ratios of span to depth in excess of ten, dimensionless

4.7.1.3 Work to failure: In connection with the determination of work or energy to failure, a producer of mechanical carbon and graphite finds better correlation with experience by using the area under the stress strain curve obtained from the flexural testing of a 1/2 x 1/2 x 3 inch specimen. The appropriate dimensions are then used in the previous equation to yield the expression

$$I = \frac{0.0063 \, \sigma^2}{E} \tag{24}$$

where

I	=	impact strength, foot pounds
σ	=	flexural strength, pounds per square inch
E	=	Young's modulus, pounds per square inch

I - K

R = RADIUS OF GYRATION
L = SPAN
t = TIME TO FAILURE
E = YOUNG'S MODULUS
ρ = DENSITY AS SP. G.

$$\frac{R}{L} \frac{t}{\sqrt{\rho/E}} \times 10^3$$
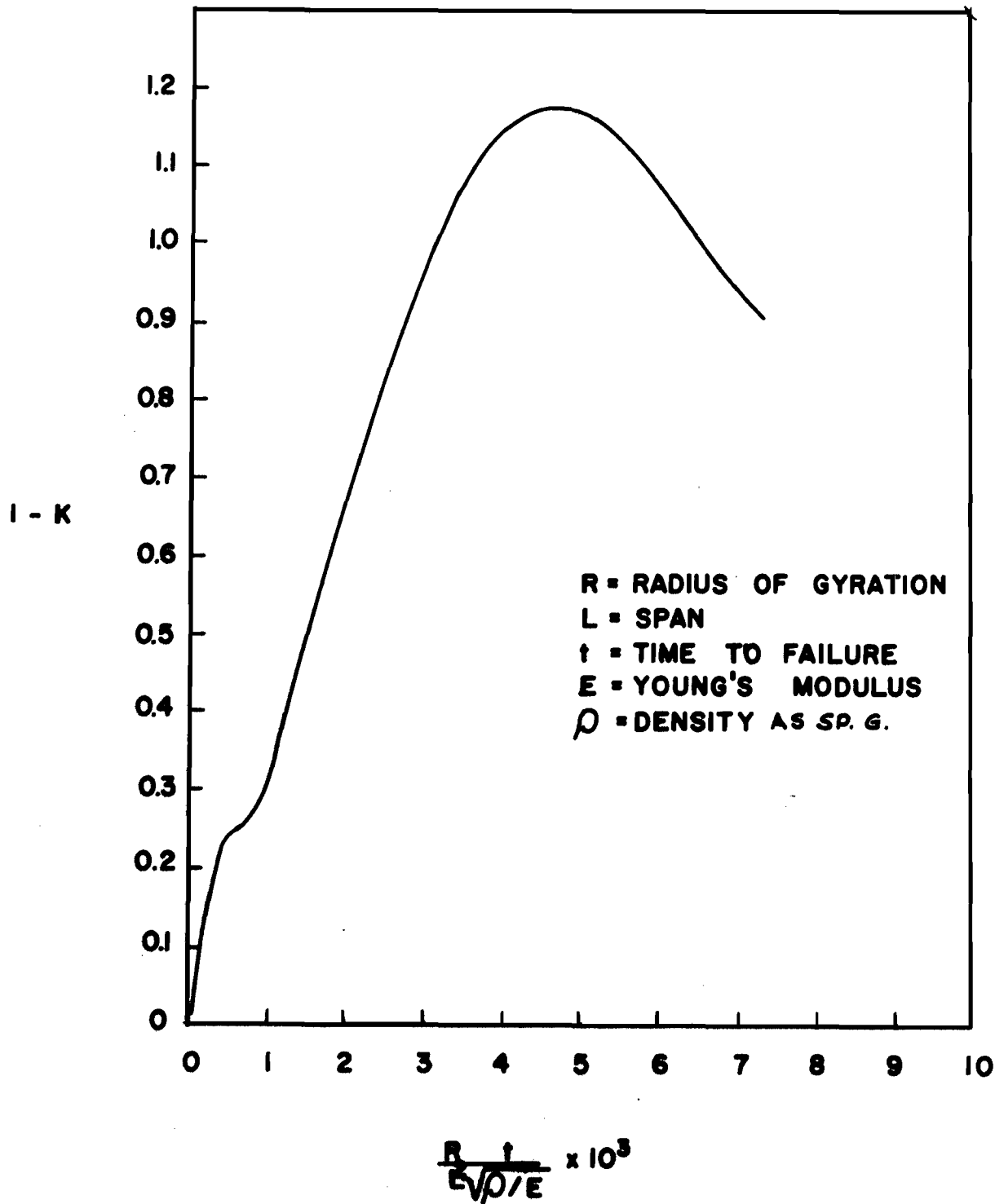
FIGURE 14 · STRESS MULTIPLIER (I-K) AS
INFLUENCED BY MATERIAL PROPERTIES

4.7.2 Practical limitations

4.7.2.1 Energy measurement: Many practical difficulties are attendant upon the use of bending energy derivations for calculation of impact stresses. Chief among these is the difficulty in sensing the energy absorbed by the specimen and differentiating this from the kinetic energy supplied to the specimen. One method involves subjecting the specimen to increasingly energetic blows until failure just occurs, so as to minimize the kinetic energy imparted to the specimen. As discovered in the force measuring machine described above, such treatment results in numerous repeated applications of force during the single devastating blow, so that the direct application of bending energy equality is seriously questioned.

4.7.2.2 Interpretation of results: In the case either of the force measuring machine or the energy measuring machine, the recorded data depend on the dynamic response of the specimen-machine system. Since measurements involved in an accurate impact test are complex and the calculation of failure stresses of the specimen viewed as the dynamic system are far from routine, great caution should be used in the evaluation and interpretation of impact tests on brittle materials. The state-of-the-art of brittle impact testing is not advanced and much more theoretical-experimental correlation will be required before impact testing can be used to predict the service behavior of brittle materials. Even where all the details of the dynamic loading problem for impact specimens are well understood, the difficulties of applying test information to impact design of manufactured parts would be formidable, for one would have to be able to calculate the dynamically generated stresses in the parts themselves to apply the test data.

4.7.2.3 Strength comparisons: Impact tests on brittle materials characteristically show a great deal of scatter, especially when different specimen size and shapes are considered. This is due in part to the statistical nature of the failure, but reflects in large measure the fact that the actual forces being applied are functions of the material, the particular specimen design, the particular machine design, as well as the specimen-machine interaction.

4.7.3 Present practice

4.7.3.1 Pendulum measurements: The various types of impact machine may generally be classified as energy-measuring or force-measuring. Since there are numerous types of energy-measuring machines, these will be described first. The most popular type of energy-measuring machine is the pendulum design, which is calibrated for various heights of swing of the pendulum and tup in inch pounds. Calibrated machines are usually corrected for the frictional effect at the pivot and wind resistance acting on the tup, and are so designed to strike the specimen at the center of percussion of the rotating pendulum assembly. The specimen is of the Izod or Charpy type, being respectively a cantilever beam held in the jaws of a vise or a

simply-supported, centrally-struck beam. The performance of the test can be of two types, either incremental loading of increasing intensity until failure occurs, or the single blow type in which more than ample energy is provided to break the specimens. In the incremental-blow type a record is made of the energy (height of the pendulum) which was necessary to just break the specimen, whereas the single blow type requires a calibrated measuring scale which records the maximum swing achieved by the pendulum after breaking the specimen. Various modifications have been employed in attempts to reduce or eliminate hidden energy losses from the systems. In some cases the pendulum is swung into a freely suspended specimen, so as to eliminate the grounding energy normally transmitted from the specimen through its rigid support. Another modification involves the inclusion of the specimen in the pendulum, causing the specimen to be swung into a rigid central knife edge. This represents an attempt to eliminate the so-called "toss energy", which is the kinetic energy imparted to the broken pieces during and after the failure. It is reasoned that the velocity of the broken pieces roughly approximates the velocity of the approaching specimen before failure, so that the kinetic energy terms before and after the impact cancel.

4.7.3.2 Dropping weights: Other machines employed for this work are of the dropping weight type, in which a freely falling body is released from a measured height so as to strike a specimen with known velocity and energy. The specimen again may be of the Charpy or Izod type.

4.7.3.3 Data reported: A standard method of reporting impact energy results is in terms of inch-pounds or inch-ounces. In recent years there has been increased use of the parameter inch-pounds per square inch of cross section. Numerous investigators have utilized a bending energy equality to permit expression of the bending stress in impact, as discussed above. The clear definition of specimen size and test configuration is essential.

4.7.3.4 Force measuring machine: The only force measuring machine known to exist and being used on brittle materials (Ref. 22) has combined the efforts of previous investigators in designing a pendulum-type of apparatus. The specimen is included with the pendulum on a controlled span, and swung into a freely hanging hammer. Although such elaborate precautions are entirely unnecessary for strict force-measuring performance, the purpose of this design is to permit precise energy-measuring techniques to be employed for direct comparative analysis of the methods. Unfortunately, this has not yet been accomplished. The stresses are calculated through the use of the graph in Figure 14 equation (23) (4.7.1.2).

4.7.3.5 Rotating beam: A rotating beam machine is particularly useful in studies encompassing higher velocity of impact than is normally achieved by pendulum machines. Such machines usually involve a rotating fly wheel which ejects a striking blade when the desired tangential velocity is reached. This blade strikes the center of a simply supported beam on its next rotation, or can strike the end of a cantilever beam supported from a vise. The energy extracted from the fly wheel by the performance of this work may be measured in the subsequent angular rotation of the assembly.

A rotating beam type of machine has been constructed for use with the same general force-measuring systems. In this machine the specimen is swung through the circumference of the rotating beam until the desired velocity is achieved, at which time a trip mechanism places the hammer directly in line for contact with the center of the specimen during the next rotation. The principle of measurement which has been employed in the force measuring machine involves a piezoelectric transducer in the anvil head, calibrated to yield an oscillograph for the force-time history.

4.7.3.6 Correlations between methods: No complete correlative attempt has been made in a study of impact measurements. As discussed above (4.7.2.2) the interpretation of these data is not sufficiently advanced for practical application to design problems. Normal practice involves comparison of energy absorption by identically-sized specimens tested on the same machine and under the same conditions. This is a questionable practice, since the specimen properties strongly influence the conditions of loading and subsequent energy distribution.

A complete description of the mathematical analysis and experimental procedures is offered in Reference 22.

4.8 Modulus of Elasticity

4.8.1 Theoretical basis of the test

By definition, the modulus of elasticity or Young's modulus (E) is the ratio of stress to strain. This material constant may be determined in a number of ways. The most usual of these methods are as follows:

4.8.1.1 Beam deflection: The deflection of an elementary beam may be measured under a known load. The modulus of elasticity can then be computed from a formula derived from the differential equation of beam flexure. For example:
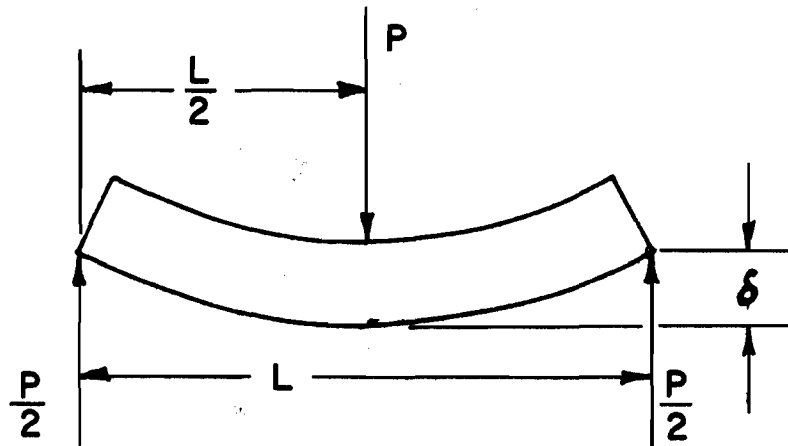
$$E = \frac{P L^3}{48 \delta I} \qquad (25)$$

where
δ = deflection, inches
P = applied load, pounds
L = span, inches
I = moment of inertia of the cross section about the neutral axis, inches^4

Or, to avoid errors from support deflection, we can take the difference between values. That is:

$$E = \frac{(P_2 - P_1) L^3}{48 (\delta_2 - \delta_1) I} \qquad (26)$$

where δ_1 is the deflection due to P_1 and δ_2 is the deflection due to P_2. Similar procedures are followed for other simple beam configurations, or other geometries adequately described by any strength of materials text.

4.8.1.2 Strain measurement: Several testing shapes are particularly well adapted to permit measurement of either or both tensile and compressive strains. The center-point loading described above is not recommended for tensile strain measurement, and does not permit compressive determination.

The most commonly used shape is a rectangular beam, loaded at the third-points or quarter-points. Gages may be mounted at the surfaces in compression and tension (4.5.2.3). Stress calculated for the point of strain measurement permits determination of Young's modulus, as follows:

$$E = \frac{\sigma}{\epsilon} \qquad (27)$$

where
   E = modulus of elasticity, pounds per square inch
   σ = calculated stress, pounds per square inch
   ϵ = measured strain, inches per inch

Similar procedures are followed with other test configurations. Ample data for elastic determination will usually be generated in alignment checks of tensile test specimens (4.3.2.3).

4.8.1.3 Resonant frequency: One determination of the modulus of elasticity involves the use of the natural resonant frequency of an elementary beam. The test beam is made to vibrate in one of its natural frequencies (usually the fundamental). From this resonant frequency the modulus of elasticity can be computed from an elementary formula. For example, consider a free-free beam in longitudinal vibration:
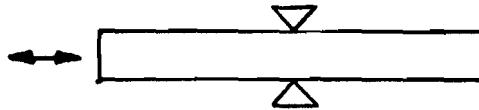
For the fundamental mode, the modulus of elasticity is calculated to be

$$E = \rho \left(\frac{\omega L}{\pi} \right)^2 \tag{28}$$

where
   ρ = mass density, pound-second^2 per inch^4
   ω = resonant frequency, cycles per second
   L = length, inches

We may also consider a free-free beam under transverse vibrations:
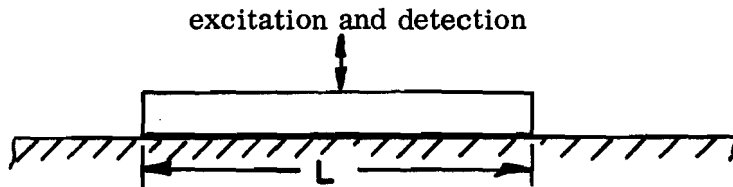
For the fundamental mode, we find for the modulus of elasticity of a thin, long cylinder

$$E = \frac{A \rho}{I} \left(\frac{\omega L^2}{22.37} \right)^2 \tag{29}$$

53

4.8

where
A = cross sectional area, square inches
ρ = mass density, pound-second^2 per inch^4
I = moment of inertia about the neutral axis, inch^4
ω = resonant frequency, cycles per second
L = length, inches

It is possible to support the beam and still have it vibrate as a free-free beam if the simple supports are at the node points of the fundamental mode shape.

Fundamental mode shape for transverse vibration:
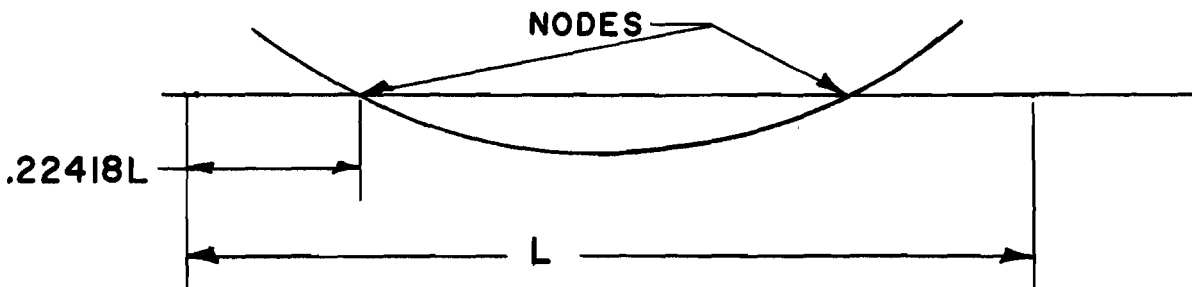
Note that care must be taken to be sure the beams are actually vibrating in their fundamental modes.

The equation for resonant flexural vibration has been investigated and modified for wider application to test specimen sizes. The influence of depth: span ratio in determining the relationship between resonant frequency and Young's modulus is expressed in a factor C_1 presented by Pickett (Ref. 23). The calculation of E is reduced to the simple statement

$$E = C_1 W \eta^2 \tag{30}$$

where
E = Young's modulus of elasticity, pounds per square inch
W = weight of the specimen, pounds
η = resonant frequency in fundamental mode of flexural vibration
The graphical solution for the factor C_1 (with Poisson's ratio assumed at 0.167) is shown in Figure 15.

4.8.1.4 Ultrasonic pulse techniques: The velocity of sound in a material is dependent upon its elastic constants, and therefore may be used to measure the elastic properties. The ultrasonic method of testing is the transmission of groups, or packets, of wave motion into the bulk of a material, and measurement of the time required for the packet to traverse a certain distance through the material. The

L/d, Length ÷ depth or diameter
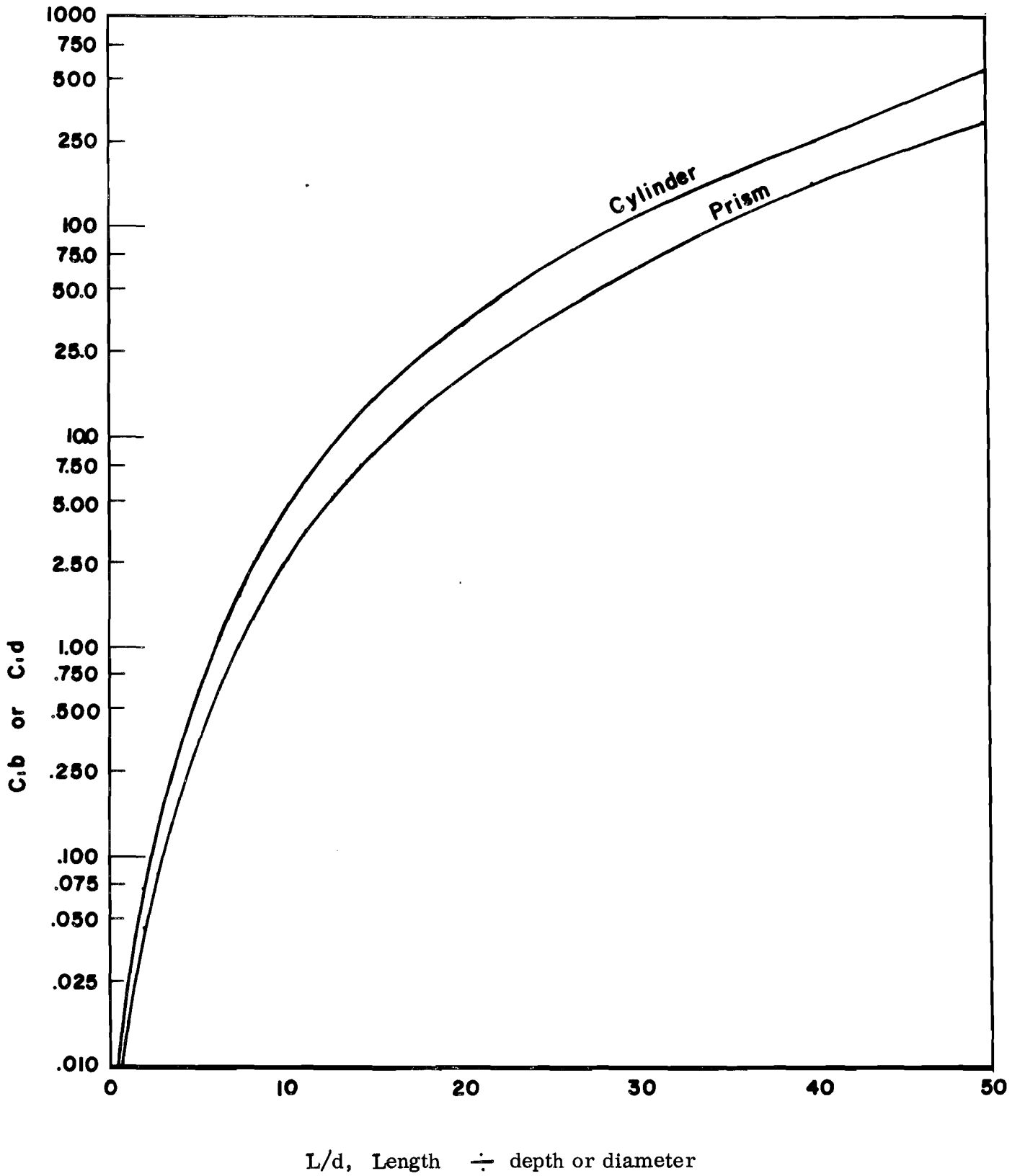
FIGURE 15 : Graphic Solution for Shape Factor

4.8

wave packets are generated in short bursts with idle time between. Detection of the arrival of a packet at a certain distance is accomplished with an electromechanical transducer, often the same unit which generated the packet.

The "group" velocity is independent of sample geometry, when the cross section is large compared to the beam area and the wavelength. For thin rods which do not qualify as above, the propagation velocity is not influenced by transverse effects, and is simply related to material properties as shown by the following equation:

$$V_0 = \sqrt{\frac{E}{\rho}} \tag{31}$$

where

V_0 = thin rod velocity, inches per second

E   = Young's modulus of elasticity, pounds per square inch

ρ = density, pound-second^2 per inch^4

The longitudinal propagation velocity in a body of large cross section is given by:

$$V_L = \sqrt{\frac{E}{\rho} \quad \frac{(1 - \mu)}{(1 + \mu)(1 - 2\mu)}} \tag{32}$$

where

V_L = velocity of longitudinal waves, inches per second

μ = Poisson's ratio, dimensionless

Longitudinal waves are dilatational or non-distortional, consisting of simple compression and rarefaction waves. Their velocity is often referred to as the "bulk velocity".

Distortional waves polarized at right-angles to the compressional wave are called shear waves. Their velocity   an extended medium is as follows:

$$V_S = \sqrt{\frac{E}{\rho} \quad \frac{1}{2(1 + \mu)}} \quad = \sqrt{\frac{G}{\rho}} \tag{33}$$

where

G   = modulus of rigidity (4.9.1.4).

A third characteristic wave type results when the angle of incidence of the ultrasonic beam is at some critical value so that shear waves are not transmitted into the material. At the critical angle a surface wave called a Rayleigh is generated, similar to wave motion on water. The velocity of these surface waves is dependent on surface condition, being decreased by surface compression and in-

4.8

creased by tension. Small flaws will give rise to back-reflections.

The velocity of Rayleigh waves is given by

$$V_R = \frac{0.87 + 1.12\mu}{1 + \mu} \sqrt{\frac{G}{\rho}} \tag{34}$$

Figure 16 describes the ratio of various mode velocities as a function of Poisson's ratio.

4.8.2 Practical limitations

4.8.2.1 Elastic deflection: The direct use of deflection of a simple beam infers that Young's modulus of elasticity is equal in compression and tension. The assumption must also be made that deflection due to shear may be neglected. Serious error will result in the calculation of elastic modulus from deflection of a short beam. The span should be at least ten and preferably twenty times the depth; for short spans with center-point loading the calculated E will be low.

4.8.2.2 Strain measurements: The temperature limitation on strain gage operation presents a severe restriction on strain-measuring techniques in generating the data usually required. It has also been reported in some cases that the presence of the gage cemented to a tensile surface has influenced the failure stress on that surface, particularly with a porous test piece.

4.8.2.3 Sonic analysis: Some of the practical limitations to accurate determination of resonant frequency are associated with the degree of refinement in the system. Good coupling between driver and specimen must be achieved, and the contact pressure of a mechanically driven system can influence the results. The uniformity of a specimen as to density and geometry will determine the location of nodal points, so that clear definition of the mode of vibration being observed may sometimes be difficult. Calculation of Young's modulus demands an assumption for Poisson's ratio.

A further problem which can obscure precise measurement of resonant frequency is the occurrence of resonance in other parts of the driving-sensing system, such as the signal generator and/or transducer being used to detect the amplitude of vibration.

4.8.2.4 Ultrasonic pulse generation: Scattering due to randomly-oriented discontinuities can cause significant attenuation, so that the pulse may be considerably weakened when it reaches the receiver. Attenuation losses usually decrease with decreasing frequency, but the wavelength must be held to a reasonably small value in relation to the dimensions of the test piece. The
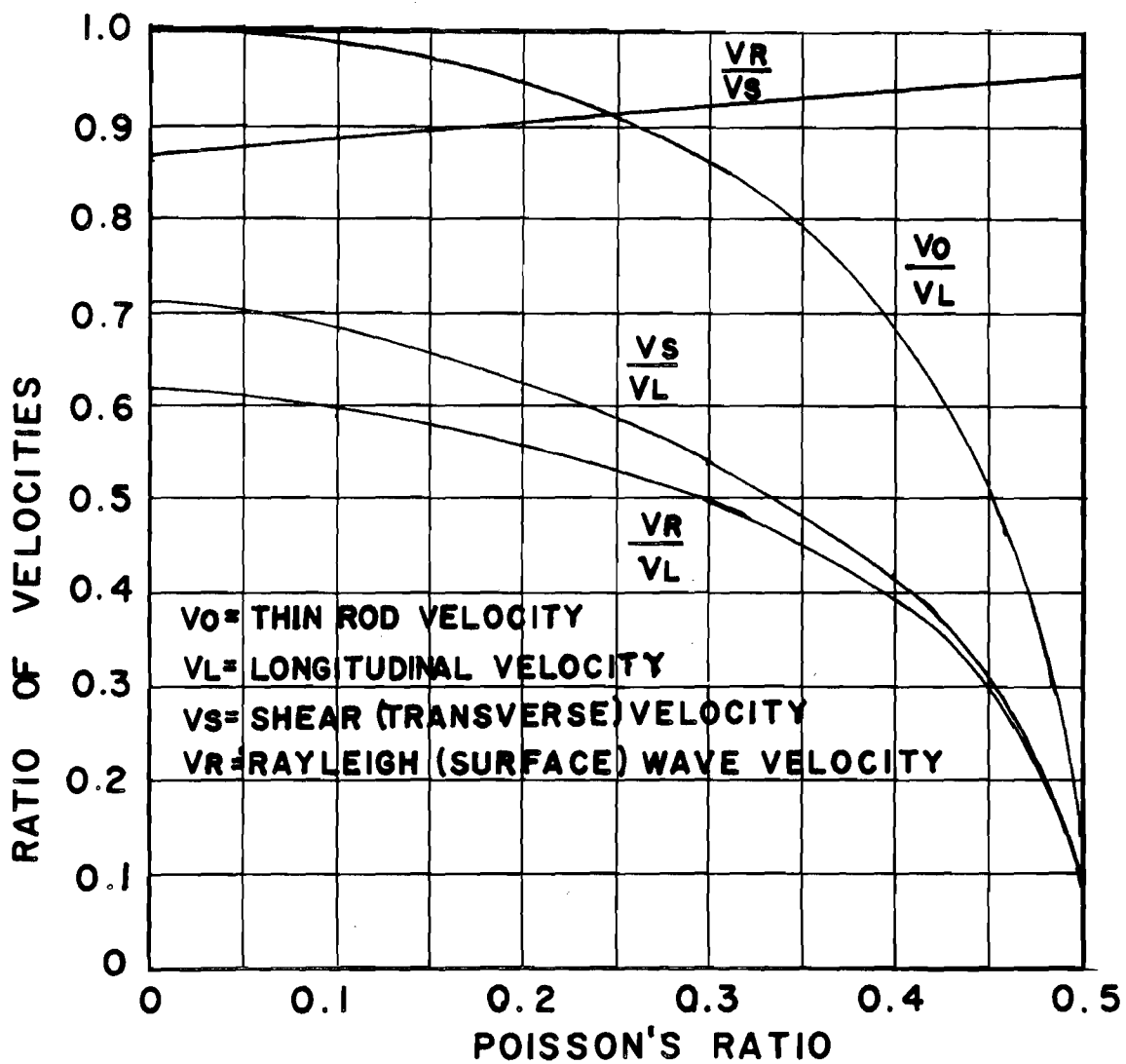
FIGURE 16 - RATIOS OF PROPAGATION VELOCITIES
FOR VARIOUS MODES

internal structure can therefore limit the application of the technique due to grain size, porosity, inclusions, etc.

Anisotropy of structure and of elastic parameters will influence the results. The random orientation of grains with anisotropic elastic properties will yield average numbers for velocity of propagation. The occurrence of boundaries between materials of differing sound velocity will also give rise to reflection and mode conversion, so that background disturbances can become serious in heterogeneous materials.

An upper temperature limitation occurs for transducers, and, the acoustic impedance at elevated temperatures causes signal losses which eventually eliminate detection of a returning pulse.

The coupling between a piezoelectric transducer and the tested material is important in reducing interface losses. Oil or water has been found useful in aiding the transfer of the energy packet into the material, but it is often undesirable to so contaminate a test piece.

Most readout systems utilize an oscillographic technique for observing the detected signal. The time-base usually available at the short times involved in sound transmission may not be of sufficient accuracy, and it is desirable to supply timing marks or compare results against a reference material.

4.8.3 Present practice

4.8.3.1 Beam deflection: Calculation of modulus of elasticity from load-deflection curves is a very common procedure. Many testing machines are equipped with recorders which plot head-movement against load, so that specimen deflection may be measured with appropriate calibration for machine deflections under identical loading conditions. Dial indicators are used, but the much greater resolution and output for direct plotting of linear variable differential transformers has replaced dial-reading in many cases. Optical lever systems permit deflection measurements of sufficient accuracy, and capacitative probes are available for direct displacement readout.

Deflection measurements are used to calculate elastic modulus, but the calculation assumes linearity in stress-strain response for determination of corresponding stress. It was pointed out earlier (4.5.2.4) that the load-deflection curve of a flexure specimen can exhibit greater linearity than the stress-strain curve for the material.

The use of center-point loading is to be discouraged unless the span: depth ratio is large, preferably above 15:1.

4.8.3.2 Strain measurement: Many types of strain gages are available for precise measurements of expansion or contraction at the surface of attachment. The shape used for such measurements should be fairly simple, with uncomplicated loading configurations to avoid strain in directions other than that being measured. It will be evident from a later discussion (4.10.1) that such unrecognized influences can lead to serious error.

Strain gages are commonly used in the reduced section of flexural test specimens subjected to pure bending (4.3.1). An immediate check may be run to determine the similarity between tensile and compressive elasticity by placing gages in the corresponding locations on the flexural specimen. This is impossible in center-point loading, and the tensile data obtained would be dependent to a large extent on the span: depth ratio.

Extensometers find limited application in tensile testing, chiefly at elevated temperatures. These are fastened to the specimen at the extremes of the gage length, and serve to transmit any change in length between attachments for viewing outside the furnace. Optical telescopes or differential transformers are used to sense a change in position of the ends.

Direct viewing of strain on flags positioned at each end of the gage-length can be accomplished with optical telescopes. An automatic follower system which operates with a photosensitive servo system is in successful operation for strain measurements on brittle materials (Ref. 8) to very high temperatures.

4.8.3.3 Sonic analysis:

4.8.3.3.1 Free vibrations: A simple but effective means of sonic analysis for determining Young's modulus of elasticity is mechanical ringing of a bar specimen. The test piece is usually, but not necessarily, supported about the nodal points on soft (sponge rubber) bearings, and subjected to a sharp blow from a solenoid striker or a hand-held suitable device. The resulting pitch is matched to a known frequency by ear or electronically through oscillographic display. Figure 17 (a) illustrates the technique. A time base sweep will permit logarithmic decrement measurements (4.12.1.2) in the latter case, using point nodal supports.

4.8.3.3.2 Forced vibrations: A more sophisticated feature of sonic analysis results with a continuing excitation frequency of mechanical motion impinged on the specimen. When the driving source is operating at a resonant frequency of the specimen, the combined amplitude of vibration becomes a maximum. Figure 17 (b) demonstrates the system. Chief among the advantages of forced vibration methods is the capability of verifying modes of vibration, and further, of forcing a resonant vibration at higher modes in flexural or torsional behavior (4.9.1.3). The width of the frequency-response curve may also be used to calculate internal friction (4.12.1.1). It is also often found that response is
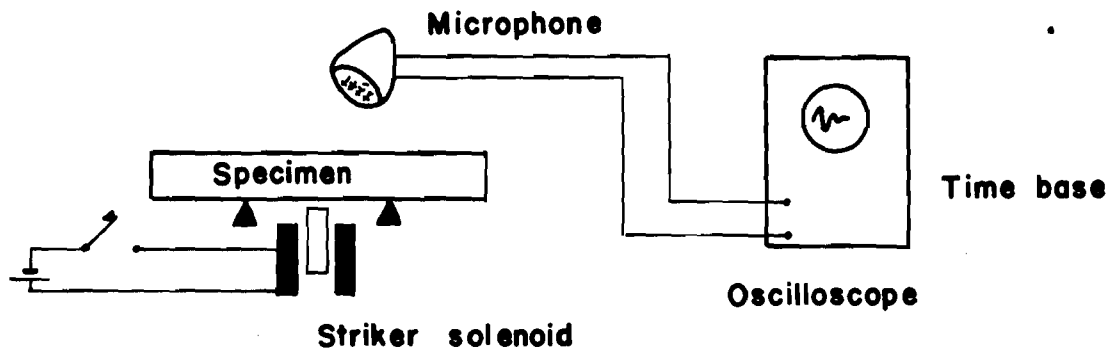
(a) Resonant Frequency by Free Vibrations
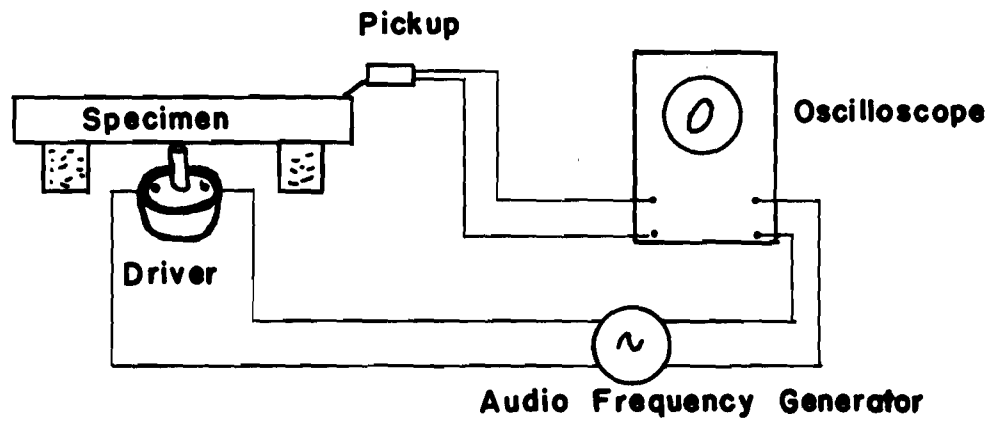
(b) Resonant Frequency by Forced Vibrations
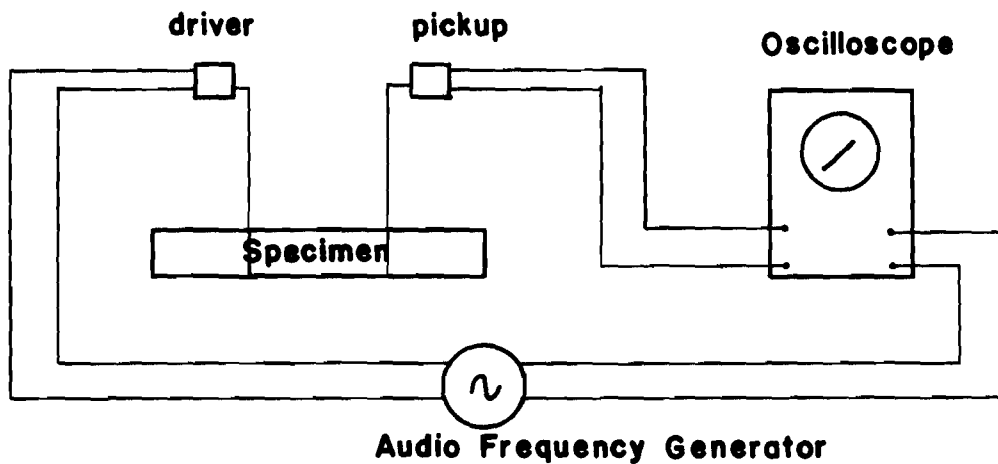
(c) Forced Vibrations in Suspended Specimen

FIGURE 17: Schematic of Various Methods for Resonant
Frequency Measurement

4.8

too poor for adequate measurement in free ringing methods, and resort to forced vibration is essential.

One modification which is very popular in elevated temperature work is illustrated in Figure 17 (c). The specimen is suspended from thin filaments, such as wire or carbon fiber (3M-Pluton B or equivalent) at points slightly off the nodes. One fiber transmits the driving signal and the pickup transducer senses vibration through the other filament. A third centrally-located pickup provides a very useful mode check and extends the capacity to torsional measurements (4.9.1.3).

The driving and pickup units which are most popular are phonographs "cutting heads" normally used to cut the sound track in disk records. Inexpensive cartridge pickups often suffice for sensing, although considerable care must be used to eliminate models which themselves display a resonant frequency within the range of anticipated use. Air-coupling with the specimen from a directional speaker is also utilized in several common designs. Modal configurations are described by Figure 18.

4.8.3.4 Ultrasonic measurements: Commercially available generators and detectors are usually utilized, but ultrasonic techniques are not in widespread use. Considering their relative ease of interpretation and operation, this fact is surprising, especially with the capabilities offered by surface-wave techniques.

Adaptation of a conventional oscilloscope may be accomplished by using its gate output signal as the trigger for pulsing a marker circuit. The transducer of x-cut quartz or piezoelectric ceramic is cut to the proper thickness for the frequency of the wave packet, according to the expression

$$t = 0.1126 \times \frac{1}{f} \qquad \text{for quartz} \qquad (35\ a)$$

$$t = 0.1 \times \frac{1}{f} \qquad \text{for ceramic} \qquad (35\ b)$$

where
t = thickness, inches (for desired frequency)
f = desired frequency, megacycles
The pulse from a receiving piezoelectric is displayed on the vertical plates of the oscilloscope to allow calculation of velocity of transmission.

Another direct reading method is the use of an interval-timer to measure the time lapse between driving pulse and received pulse. One such modification, which has been useful for large shapes, detects the time lapse of surface-wave travel between two stylus-type pickups, the surface wave being generated by a blow with a small hammer.

Nodes

0.224L   0.224L

L

(a) Fundamental Mode , frequency $= \omega$

Nodes

0.14L   0.14L

$L/2$

L

(b) Second Mode , frequency $= n\omega$

n (2nd. mode)

3

2

1

0   0.5   0.1   0.15   0.2

Radius of Gyration / Length
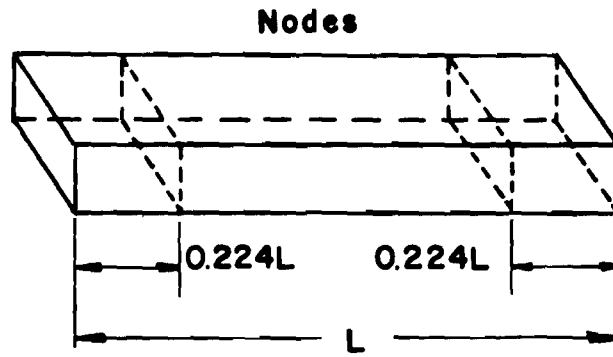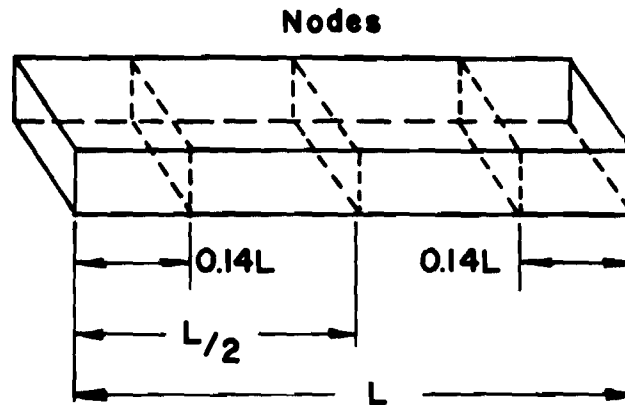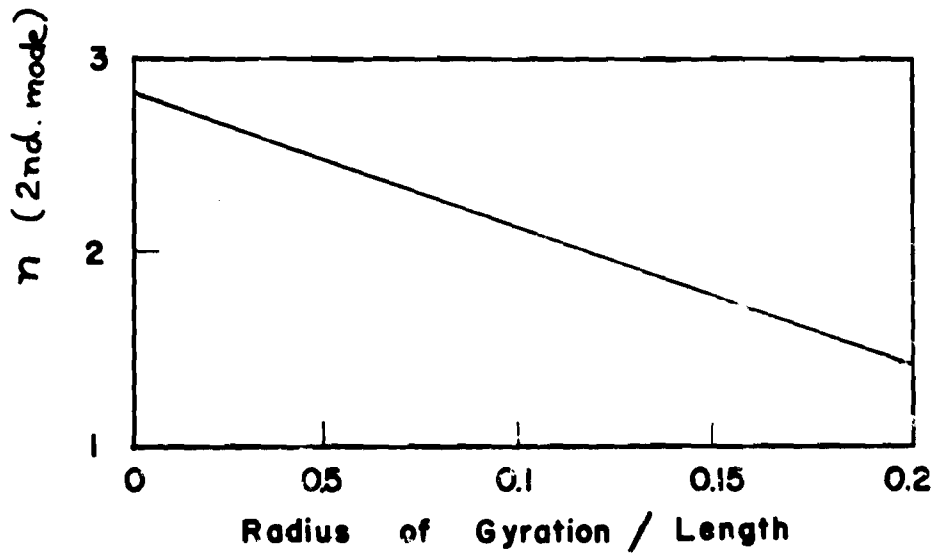
(c) Ratio of Modal Frequencies

FIGURE 18 :   MODES   OF FLEXURAL VIBRATION

The use of ultrasonic methods is commonly restricted to low temperatures, but one ingenious design overcomes the major limitation usually imposed by the maximum permissible transducer temperature. A test piece with two parallel faces at controlled distances from the base is cemented to a carrier material. Pulses reflected from the faces will be received at times different by the interval necessary for the wave packet to travel the known distance. This system is pictured below:
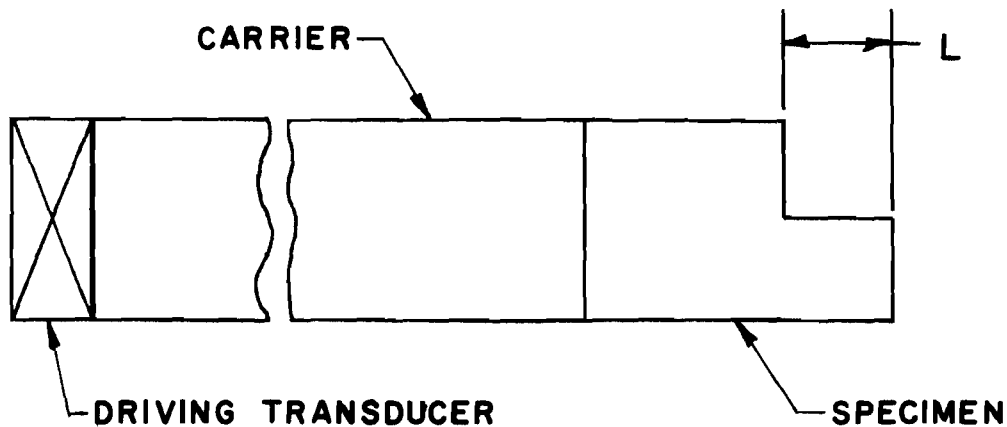
Figure 19. Elevated Temperature Specimen

Normal uses of the method are for measurement of elastic constants and for nondestructive flaw detection. These can be by reflection or transmission systems, as described in Figure 20.

4.9 Modulus of Rigidity

4.9.1 Theoretical basis of the test

The relationship between shearing stress and shearing strain in a material which obeys Hooke's law is expressed by the modulus of elasticity in shear, or modulus of rigidity, G. The proportionality is shown as follows:

$$G = \frac{\tau}{\gamma} \tag{36}$$

where
τ = shearing stress, pound per square inch
γ = shearing strain, radians
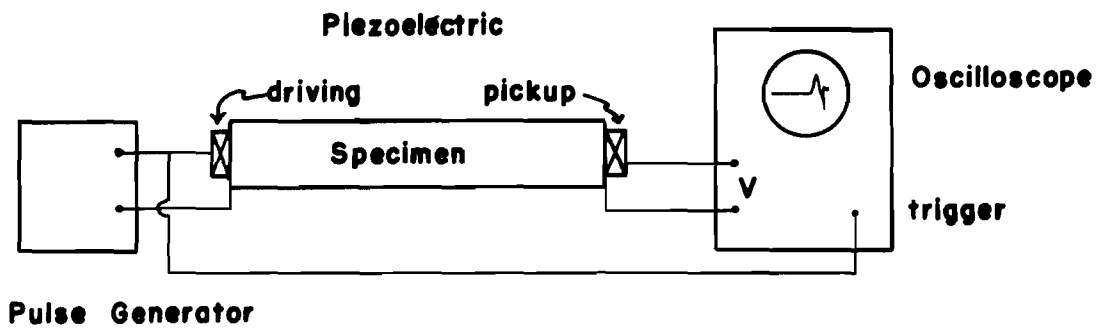
(a) Transmission method
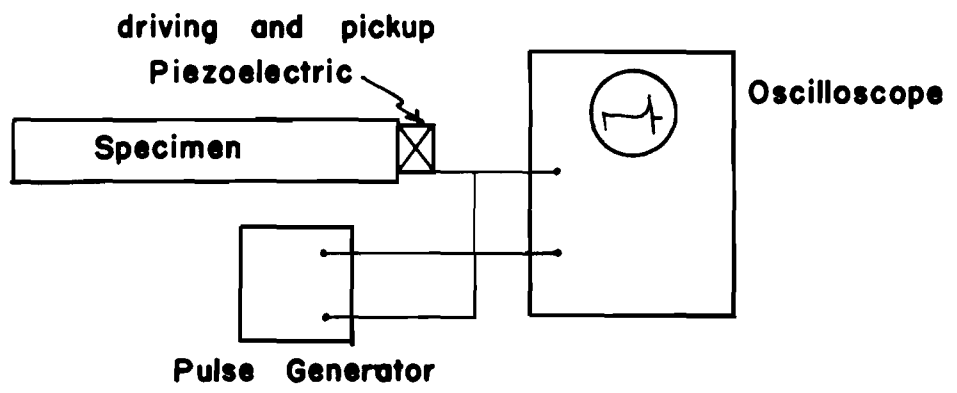
(b) Reflection method
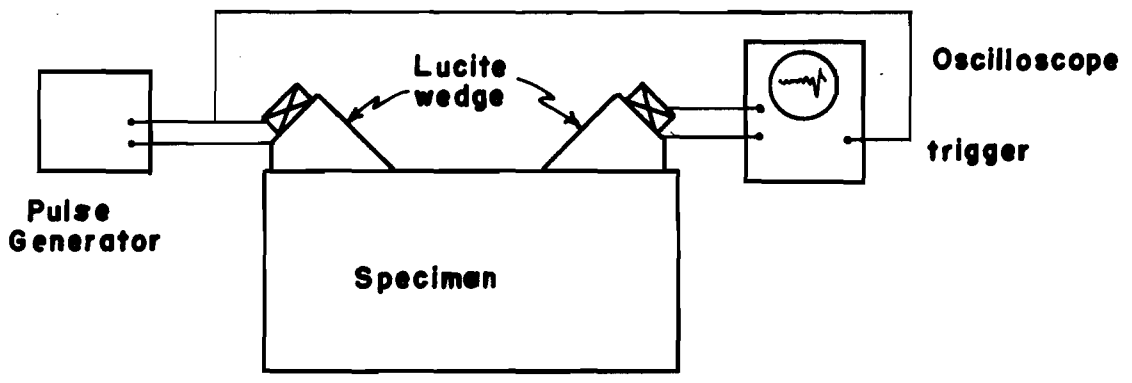
(c) Shear-wave or surface wave measurement

FIGURE 20 : Variations Used in Elastic Property
Determinations by Ultrasonics

65

The physical significance is described by Figure 21, which illustrates the action of a shearing stress and the sliding deformation of a unit cube of material.
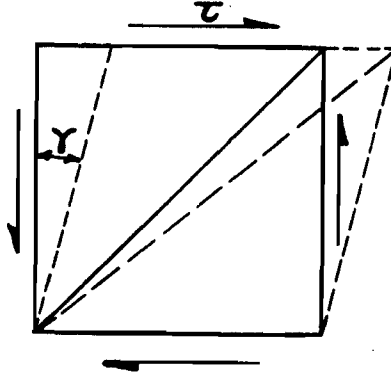
Figure 21. Deformation Associated with a Shearing Stress

The stretching of one diagonal, and compressing of the other, entirely defines the distortion. This leads to the interrelationship of the elastic constants shown by

$$G = \frac{E}{2(1+\mu)} \tag{37}$$

where

G = modulus of rigidity, pounds per square inch

E = Young's modulus, pounds per square inch

μ = Poisson's ratio, dimensionless

The situation described by Figure 21 is one of pure shear, in which only shearing stresses are acting on the faces of the unit cube.

4.9.1.1 Twist angle measurement: The development of pure shear is most easily achieved by placing a cylindrical specimen in torsion. The calculation of magnitude and distribution of stresses has been discussed for this case in section 4.6. The angle of twist may be measured over a known gage length for use in the equation

$$G = \frac{T L}{\theta J} \tag{38}$$

where

G = modulus of rigidity, pounds per square inch

T = twisting moment, inch-pound

L = gage length, inches

θ = angle of twist, radians

J = polar moment of inertia of the cross section, $inch^4$

or, to avoid errors from poorly defined starting conditions, the difference between values is used as

$$G = \frac{(T_2 - T_1)\, L}{(\theta_2 - \theta_1)\, J} \tag{39}$$

where θ_1 is the angular deflection due to T_1 and θ_2 is the angular deflection due to T_2.

4.9.1.2 Strain measurement: The surface of a cylinder subjected to torsion is in a state of pure shear, described by Figure 21.

Strain gages placed on the diagonals of that figure permit direct calculation of shearing stress, since

$$\tau = \sigma = -\sigma_c = \epsilon\, E \tag{40}$$

where

σ = tensile stress, pounds per square inch
σ_c = compressive stress, pounds per square inch
ϵ = measured strain, inches per inch
E = Young's modulus, pounds per square inch

Accompanying angular deformation measurements yield the shearing strain,

$$\gamma = \frac{1}{2}\, \theta\, d \tag{41}$$

where

γ = shearing strain, radians
θ = angle of twist through the gage length, radians per inch
d = diameter, inches

and

$$G = \frac{\tau}{\gamma} \tag{42}$$

4.9.1.3 Resonant frequency: The natural resonant frequency of a beam in its fundamental mode of torsional vibration is related to the modulus of rigidity as follows:

$$G = \rho \left(\frac{\omega\, L}{\pi} \right)^2 \tag{43}$$

where
- G = modulus of rigidity, pounds per square inch
- ρ = mass density, pound-second^2 per inch^4
- ω = resonant frequency (fundamental), cycles per second
- L = length, inches

The modal relationships are determined by inspection of node locations at resonance. Figure 22 pictures the modes and the theoretical relationships of resonant frequency for each.

4.9.1.4 Ultrasonic method: A description of shear-wave propagation through a semi-infinite body has been described by equation 33 section 4.8.1.4.

4.9.2 Practical limitations

4.9.2.1 Assumptions in equations: The assumptions inherent in the mathematical relationships between torsional moment, angle of twist, and specimen dimensions have been discussed in section 4.6.1.2. The implication is that the material follows Hooke's law of linear proportionality between stress and strain. Any deviation from this behavior is necessarily going to invalidate the calculation of modulus of rigidity.

The torque-angle of twist curve for a torsional specimen is analagous to the load-deformation curve from a flexural specimen. Such curves will exhibit more linearity than the stress-strain curve of the material (Ref. 17).

Theoretical relations between resonant vibration frequencies and rigidity moduli have been extended to allow their use in describing the behavior of common test shapes and are described in reference 23. The statement for calculation of G becomes

$$G = B W (n')^2 \qquad (44)$$

where
- G = modulus of rigidity, pounds per square inch
- W = weight, pounds
- n' = a resonant torsional frequency, cycles per second
- B = 4 LR/gAi^2, second^2 per square inch, in which
  - L = length, inches
  - i = unity for first mode, two for second, etc.
  - g = acceleration due to gravity, inches per second^2
  - A = area of the cross section, square inches
  - R = ratio of polar moment of inertia to the shape factor for torsional rigidity, dimensionless
  - R = 1 for a circular cylinder, 1.183 for a square cross section, and

$$\frac{a/b + b/a}{4\,a/b - 2.52\,(a/b)^2 + 0.21\,(a/b)^6} \quad \text{for rectangular cross section}$$

with side   a<b
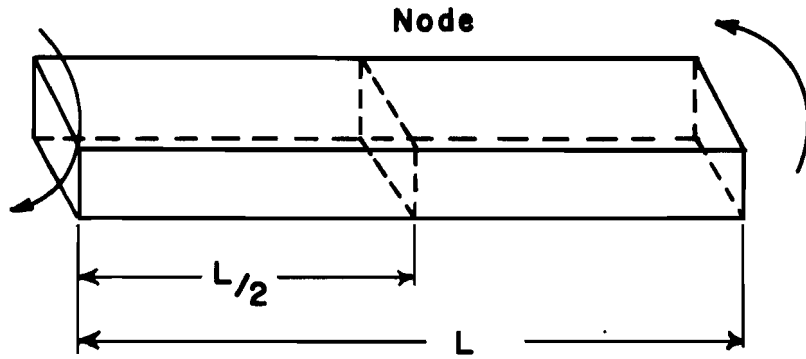
(a) Fundamental Mode , frequency = ω
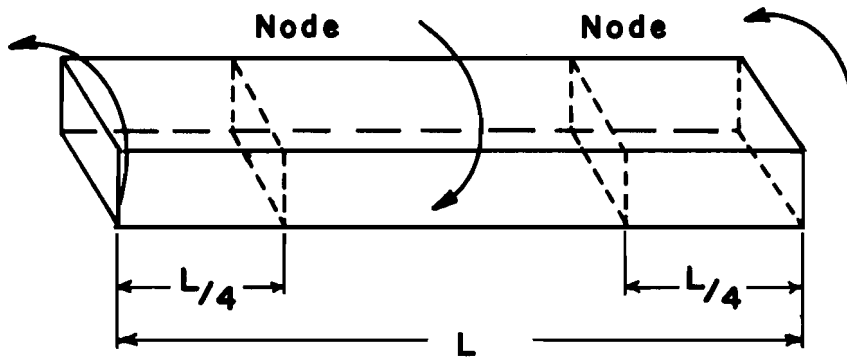
(b) Second Mode , frequency = 2ω
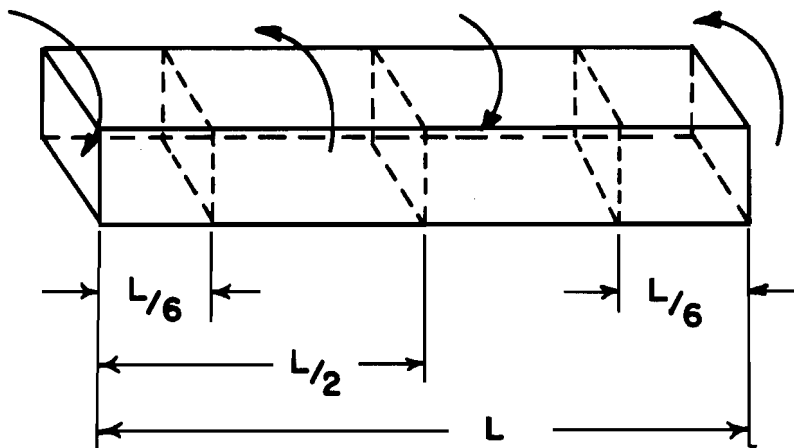
(c) Third Mode , frequency = 3ω

FIGURE·22 : MODE RELATIONSHIPS IN TORSIONAL VIBRATION

4.9

It was pointed out earlier (4.8.2.3) that calculation of E, Young's modulus of
elasticity, by sonic measurement necessitates an assumption for μ , Poisson's
ratio. The validity of this assumption can be checked by torsional vibration de-
termination, and the ratio of shape-adjusted frequencies should yield the identical
value for Poisson's ratio, as follows

$$\mu = \frac{C_1}{2\,B} \left(\frac{n}{n'} \right)^2 - 1 \tag{45}$$

where

μ = Poisson's ratio
C_1 = shape factor for flexural resonance (4.8.1.3), seconds^2 per square inch
B = shape factor for torsional resonance, seconds^2 per square inch
n = flexural frequency (fundamental), cycles per second
n' = torsional frequency, cycles per second

4.9.2.2 Size limitations: Availability of test pieces in sizes amenable to
the performance of torsional tests is often a restricting factor. In the case of
mechanical loading for torque-angle of twist measurement, the gage length needs
to be sufficient for measurable twist. For resonance determination, the ratio of
depth to width may vary widely, but requires less "shape" adjustment as a square
or circular cross section is approached. The length to depth ratio should be kept
below ten for avoidance of confusing overtones. Further, as the specimen weight
decreases, the influence of coupling between driver, specimen, and pickup becomes
more critical if distortion of resonance behavior is to be avoided.

Limitations in size may be more restrictive in ultrasonic work than in resonance
methods.

4.9.3 Present practice

4.9.3.1 Elastic deflection: The common practices for shear-strength de-
termination of brittle materials were presented in section (4.6.3.1) and apply to
the measurement of elastic modulus in torsion. Briefly, specimens of circular
cross section are subjected to a twisting moment and angular twist is observed
over a known gage length.

4.9.3.2 Sonic techniques: Determination of modulus of rigidity by torsional
resonance methods is the most popular procedure, and is easily adapted to high-
temperature work. The description of common sonic configurations is offered in
4.9.1.3.

4.9.3.3 Ultrasonic methods: A shear wave travels through material at a velocity dependent upon mass and rigidity modulus (equation 33). The usual ultrasonic methods are described in 4.8.3.4. Briefly, a packet of distortional waves is caused to travel through a known length of material, and the velocity of that propagation is calculated. This direct measurement of modulus rigidity is surprisingly little used.

4.10 Poisson's Ratio

4.10.1 Theoretical basis of the test

The definition of Poisson's ratio serves to describe the measurements required.

When a material is strained in one direction it undergoes strain of opposite sign in the transverse directions. The ratio of transverse strain to principal strain is known as Poisson's ratio.

For materials with isotropic elastic behavior, Poisson predicted the ratio described above would be 0.25. In this presentation, Poisson's ratio is designation as μ .

The change in volume of a material when subjected to a load can be calculated from its Poisson's ratio. For instance, a tensile strain ϵ in one direction will result in unit volume expansion of $\epsilon(1-2\mu)$. It is not reasonable that tension would cause a reduction in volume, so that the upper limit of Poisson's ratio is generally accepted to be 0.5. The lower limit is zero, which would indicate maximum volume expansion due solely to the increased dimension in the direction of pull with no lateral contraction. ·

The elastic constants of a material are interrelated by Poisson's ratio, such that

$$\mu = \frac{E}{2\,G} - 1 \qquad (46)$$

where
μ = Poisson's ratio
E = Young's modulus of elasticity, pounds per square inch
G = modulus of elasticity in shear, pounds per square inch

4.10.2 Practical limitations

The greatest difficulty in experimentally determining Poisson's ratio is the exceedingly small amount of strain generated in the direction transverse to the load.

Strain gages permit its measurement at room and moderate temperatures, while sonic and ultrasonic methods may often be used for higher temperatures. In the case of resonance techniques, it becomes necessary to assume a value for Poisson's ratio in the calculation of Young's modulus, which can be improved by an iterative technique (4.8.1.3).

4.10.3 Present practice

Resonance testing methods for determination of Young's modulus (4.8.3.3) and modulus of rigidity (4.9.3.2) constitute the most popularly used techniques, utilizing equation (46) or its counterpart, equation (45), section 4.9.2.1.

Strain gage measurements of lateral expansion and axial compression are also used, since

$$\mu = \frac{\epsilon \text{ lateral}}{\epsilon \text{ axial}} \tag{47}$$

where
  μ = Poisson's ratio
  ϵ = strain, inches per inch.

4.11 Bulk Modulus

4.11.1 Theoretical basis of the test

The bulk modulus K is defined as the unit volume contraction under the action of an hydrostatic pressure.

The inter-relationship of elastic parameters provides the usual method of determining bulk modulus, as

$$K = \frac{E}{2(1 - 2\mu)} \tag{48 a}$$

or

$$K = \frac{E}{2(3 - E/G)} \tag{48 b}$$

where

    K = bulk modulus, pounds per square inch

    E   = Young's modulus of elasticity, pounds per square inch

    G   = modulus of rigidity, pounds per square inch

    μ = Poisson's ratio, dimensionless

4.11.2 Practical limitations

The difficulties encountered in direct observation of volume contraction usually prohibit experimental verification of the above equations. The assumptions inherent in these equations are that the material is isotropic and that there are no phase changes.

4.11.3 Present practice

The elastic properties E and G are usually determined by sonic methods or with strain gages, thereafter defining the other elastic parameters.

Direct measurement of bulk modulus has been accomplished by application of hydrostatic load and observation of volume change in the hydrostatic system. This has also been performed under dynamic conditions with piezoelectric sensing of fluctuation in specimen volume.

4.12 Internal Friction

4.12.1 Theoretical basis of the test

In a perfectly elastic material, with stress proportional to and vanishing with strain, there is cyclic energy loss only under adiabatic (dynamic) conditions. Kelvin reasoned by thermodynamics that the difference between the elasticity under adiabatic and isothermal conditions would be

$$E_a - E_i = \frac{\alpha^2 T \; E_i \, E_a}{\rho \; s} \tag{49}$$

where

    E_a = adiabatic elasticity

    E_i = isothermal elasticity

    α = coefficient of thermal expansion

    T   = absolute temperature

    ρ = density

    s   = specific heat

The predicted difference amounts to about 0.01 per cent, whereas the experimentally observed difference amounts to several per cent. The additional mechanism thought to be responsible for this discrepancy is a viscous effect, called internal friction.

4.12

The concept of a complex modulus is used to define the differences between static and dynamic response to stress, such that

$$E_R = \frac{\sigma_0}{\epsilon_R} \qquad (50\ a)$$

$$E_u = \frac{\sigma_0}{\epsilon_0} \qquad (50\ b)$$

where

E_R = relaxed modulus, pounds per square inch
E_u = unrelaxed modulus, pounds per square inch
σ_0 = applied stress, pounds per square inch
ϵ_R = (relaxed) strain observed statically, inches per inch
ϵ_0 = strain observed instantaneously, inches per inch

Since ϵ_R is greater than ϵ_0, the relaxed modulus is less than the unrelaxed value: the material appears more rigid under rapid loading.

Under a periodic stress application there will be an energy dissipation per cycle per unit volume, given by

$$\Delta u = \frac{\sigma_0^2}{E}\ \pi \sin \theta \qquad (51)$$

where

σ_0 = maximum applied stress, pounds per square inch
E = effective modulus, pounds per square inch
θ = phase angle by which strain lags stress, degrees

The relative loss of energy per cycle is determined by comparing the above energy loss with the total energy which may be stored in a unit volume of material, $\sigma_0^2/2E$, and the resulting term is called specific damping capacity:

$$\frac{\Delta u}{u} = 2 \pi \theta \qquad (52)$$

The energy loss per cycle reaches a maximum value when the relaxation time is exactly matched by the period of vibration, so that energy absorption is sensitive to frequency of the test. The mechanisms responsible for damping are temperature dependent or thermally activated, so the internal friction also varies with temperature.

4.12.1.1 Frequency response method: Measurements of internal friction may be accomplished by observation of the width of the resonance peak at a natural frequency of the specimen or the specimen-support system. The width of the response

4.12

curve about resonance at $1/\sqrt{2}$ of maximum amplitude is observed, since

$$\frac{\Delta f}{f_c} = 2 \tan 1/2 \ \theta \simeq \tan \theta \tag{53}$$

where
Δf = frequency spread at $1/\sqrt{2}$ x max. amplitude, cycles per second
f_c = resonant frequency at max. amplitude, cycles per second
θ = phase difference by which strain lags stress, degrees

The internal friction is defined as the tangent of the phase angle, which is the reciprocal of the acoustic magnification:

$$Q^{-1} = \tan \theta = \frac{\Delta f}{f_c} \tag{54}$$

where
f = frequency, cycles per second

4.12.1.2 Logarithmic decrement method: The internal friction may also be determined from measurements of the amplitude of free vibration as the specimen decays from amplitude A_0 to amplitude A_n during N oscillations, as follows:

$$Q^{-1} = \tan \theta = \frac{2.3}{N \pi} \ \log \frac{A_0}{A_n} \tag{55}$$

where
N = ordinal number of vibrations
A_0 = amplitude of first vibration
A_n = amplitude after N vibrations

The logarithmic decrement is the natural logarithm of the ratio of successive amplitudes .

Activation energies associated with the internal friction peaks may be calculated from the observed frequency-dependence of the temperature at which the peak occurs, as follows:

$$H = \frac{R \ T_2 T_1}{T} \ \ln \frac{f_1}{f_2} \tag{56}$$

where
R $\quad$ = gas constant
T_1, f_1 = absolute temperature at which peak occurs at frequency f_1
T_2, f_2 = absolute temperature at which peak occurs at frequency f_2

75

4.12.2 Practical limitations

Measurements of internal friction require a high degree of precision in frequency and amplitude determination, but the capacity is excellent in modern electronic systems. It has been stated that the available accuracy of measurement has exceeded the ability of the experiments to specify the specimen, both in terms of orientation and previous treatment.

4.12.3 Present practice

4.12.3.1 Resonance techniques: Some of these methods are very easy to set up but do not lend themselves to a very wide frequency range of study. The fundamental mode of flexural vibration of a free beam (supported at the nodes) or of a cantilever is most popular. Longitudinal vibrations of a bar specimen have also been utilized. Schematic diagrams of these systems are presented in Figure 23.

4.12.3.2 Torsional pendulum: A very popular method involves the use of a torsional pendulum containing the test specimen as a fiber or thin rod. The logarithmic decrement method permits accurate measurement of both internal friction (by equation 55) and relaxation time. The latter calculation is based on the definition of relaxation time, which is the time required for the amplitude to decrease by the ratio $1/e$, where e is the base of natural logarithms .

The logarithmic decrement method may also be used on a beam specimen freely vibrating, with a trace of amplitude versus time being obtained on an oscillograph. (Sec. 4.8.3.3.1).

The great advantage of torsional pendulum methods is the ability to vary the frequency at which measurement is made, so that frequency-dependent anelastic effects may be clearly seen. Figure 24 demonstrates a typical torsional pendulum machine.

4.13 Fatigue

4.13.1 Cyclic fatigue

Cyclic fatigue, when applied to the mechanical properties of materials, refers to failure under the action of repeated stresses. Fatigue testing essentially involves the application of periodically varying stresses to a test bar by means of mechanical or magnetic devices.

Intimately connected with fatigue is the concept of endurance limit. The endurance limit is the greatest stress which can be applied to a material for an indefinitely large number of times without causing failure. It is determined by making
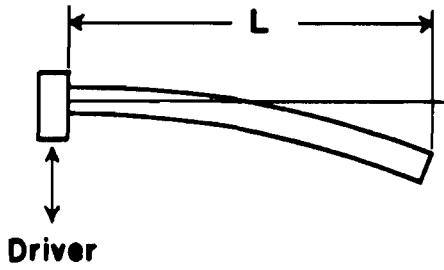
Vibrating Cantilever Method
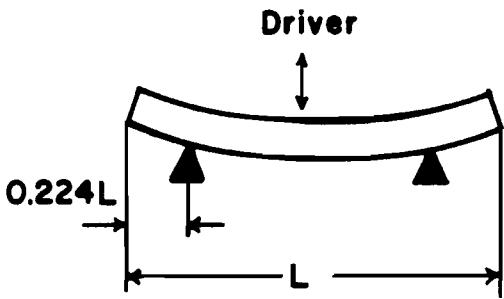
Free — Free Beam Method

0.224L
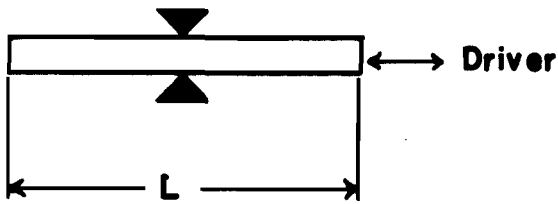
Longitudinal Vibration Method

7.07

Δf
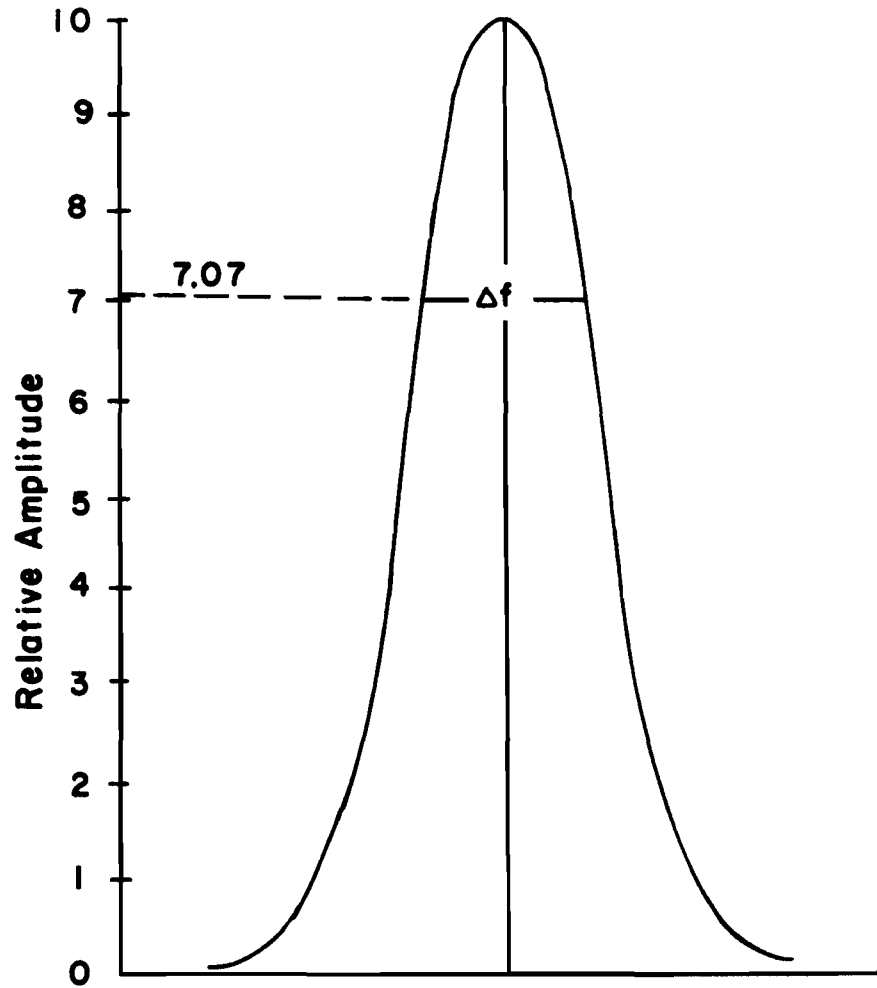
f_c = Resonant Frequency

Driving Frequency

$$\frac{\Delta f}{f_c} = \tan$$

FIGURE 23: COMMON TEST METHODS FOR RESONANT INTERNAL FRICTION MEASUREMENTS
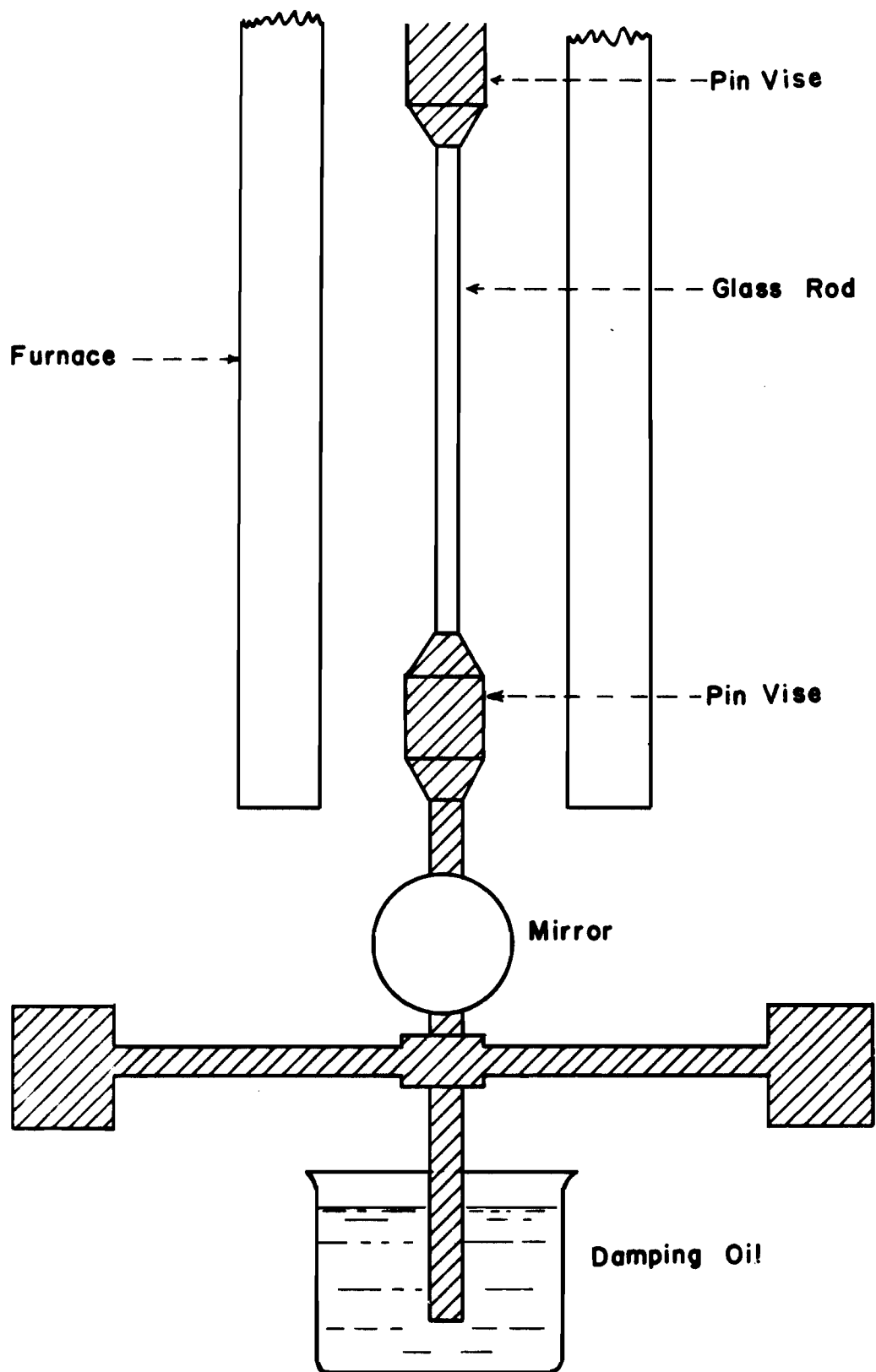
FIGURE 24. Torsional apparatus for measuring the internal friction and dynamic shear modulus of glass specimens.

78

a series of fatigue tests on a number of specimens of the material at different stress values and plotting the stress endured by each versus the logarithm of the number of cycles to failure. By choosing lower and lower stresses, a value may be found which will not produce failure regardless of the number of applied cycles. The diagram plotted is known as the stress-cycle diagram or briefly the S-N diagram. For example:

S
nominal stress   S e

N - log of number of cycles
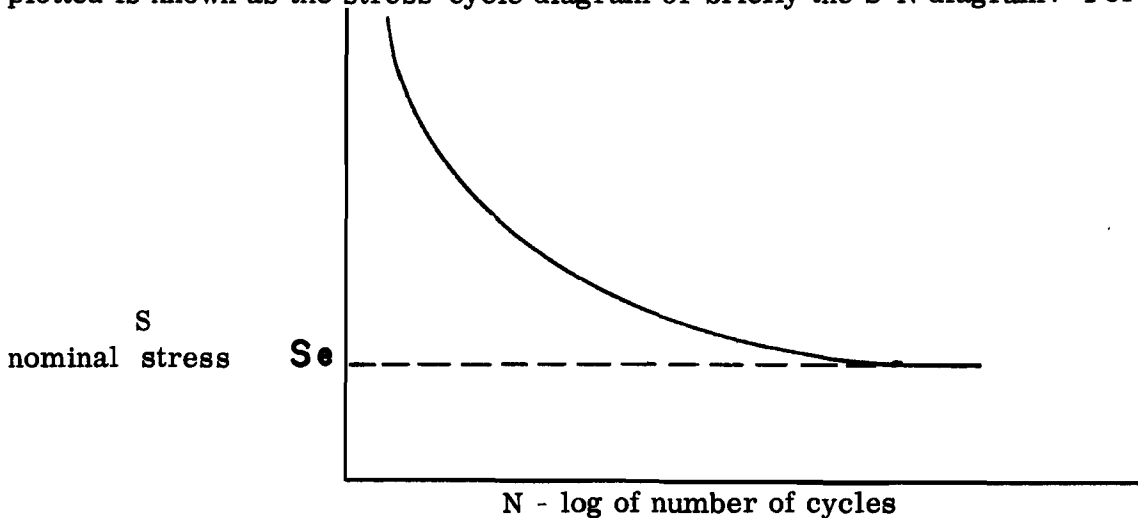
where

S_e = the endurance limit.

It should be noted that due to the statistical nature of brittle failure, the plot will actually have a band width of about one order of magnitude. For example, if a specimen under a certain stress fails after 500 cycles this actually means it may fail anywhere between 100 and 1000 cycles. It should be emphasized that the stress plotted is the nominal stress. Actually local stresses due to stress concentrations will be much higher. The failure can be explained in part by considering hysteresis. That is, for each cycle there will be a net amount of work or energy absorbed by the specimen. This work will be largely absorbed in the local regions of the stress concentrations. At some   critical point in the level of local energy density, failure occurs.

4.13.2 Static fatigue

It has been established that both glasses and polycrystalline oxides of many types exhibit static fatigue. The general characteristic of this type of delayed fracture is a sharp dependence of observed strength on the ambient atmosphere during performance of the test. This influences the measured strength under conditions of dead weight loading or as a function of rate of loading. Slower loading rates generally reduce the resistance to failure. Conditions of the test which have been found important in delayed fracture are temperature, pressure, atmosphere, surface condition, strain rate, and prior thermal history.

Many studies have been conducted to establish the effect of the rate of loading on the strength of given materials. Unfortunately, a significant number of these studies have been performed with one or more of the above influential factors out of control. A useful reference standard for fatigue studies is the observed strength of the material in the absence of fatiguing effects. The two approaches commonly taken toward achieving this goal are testing at cryogenic temperatures, so as to eliminate or minimize thermally activated processes; or the elimination of atmospheric reaction by testing in vacuum or inert atmospheres. The atmospheric constituent most generally recognized for promotion of corrosion fatigue effects is water vapor.

A theory of static fatigue which incorporates the effect of atmospheric corrosion and stress state at points of corrosion has been proposed by Charles and Hillig (Ref. 24), and utilized by Charles in a study of static fatigue in alumina (Ref. 25).

Application of the theory in studies of static fatigue and strain-rate is illustrated by Figure 25. The parameters which are shown to govern the measured strength are as follows:

σ_{th}	=	theoretical strength of the material
V^*	=	effective volume referred to uniaxial stress (see section 3.2)
Γ	=	surface energy between the unreacted solid and its reaction products
V_M	=	molar volume
L	=	initial length of a critical flow
S_N	=	strength of specimen in absence of fatigue
S_L	=	limiting fatigue strength of the material

The normalized frequency distribution curve (Figure 25) may be plotted from the test data to permit evaluation of the slope and limiting strength, as indicated on the diagram. Theory then relates the measured parameters according to the expressions shown, in which R = gas constant and T = absolute temperature.

4.14 Creep

4.14.1 Theoretical basis of the test

The term "creep" is used to define the slow and progressive deformation of a material with time under constant stress. Related phenomena include stress relaxation, internal friction, dynamic elastic modulus relaxation, and grain boundary relaxation in polycrystalline materials. Among the processes recognized as contributing to creep deformation at high temperatures are dislocation climb, diffusional effects, and grain boundary creep, the latter two being of significance in most polycrystalline ceramic materials.
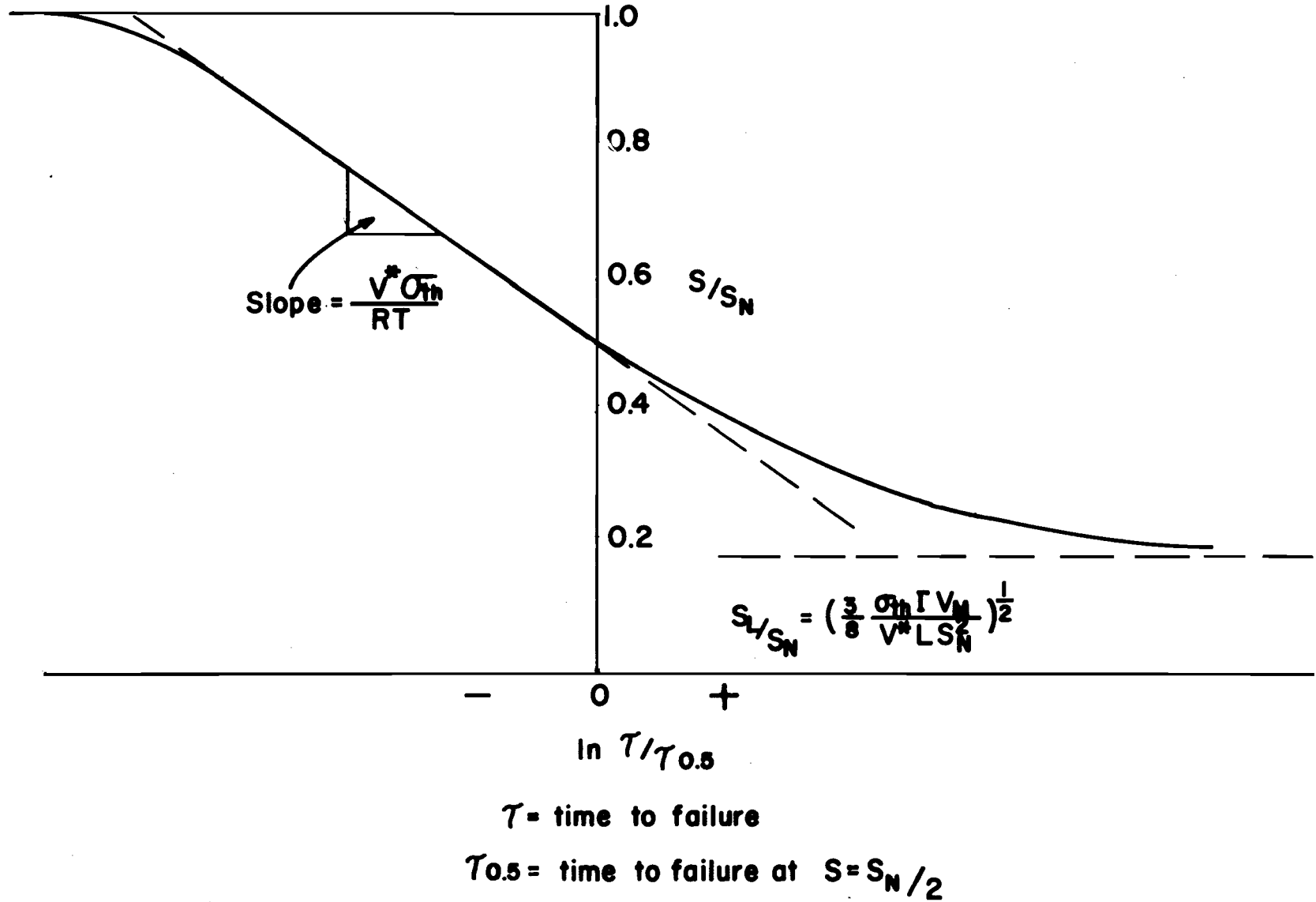
FIGURE 25   Theoretical   Prediction   For   Static   Fatigue

4.14

Diffusional creep is a self-diffusion process in grains. When the material is subjected to an applied stress, diffusional flow takes place within each grain from areas in compression to areas in tension; or conversely, the diffusion of holes takes place from areas of tension to areas of compression. For a polycrystalline sample this leads to a purely viscous flow which is expressed in the following equations:

$$\eta = \frac{k\,T\,r^2}{4\,D\,a} = \left(\frac{3}{32\pi}\right)^{2/3} V_g^{\;2/3} \frac{k\,T}{D\,a} \qquad (57)$$

where

η = viscosity
k = Boltzmann constant
T = absolute temperature
D = diffusion coefficient
a = atomic volume
r = radius of a spherical grain
V_g = grain volume

Diffusional creep of this kind is thought to be the main deformation process at high temperatures, but recent work challenges this concept with evidence of grain boundary effects predominating. (Ref. 26)

The usual method of carrying out creep measurements is to subject the specimens to a constant stress, while maintaining a constant temperature and measuring the extent of deformation with lapse of time. Creep can be determined in tension, compression, shear, and flexure. The time of each test may be a matter of hours, weeks, months or years depending upon the material to be tested. Experimental data are represented by plotting the creep curve as deformation versus lapse of time, as shown in the accompanying Figure 26. Part b of that figure shows typical creep data presented in a log-log plot, which permit calculation of the activation energy for creep from the following equation:

$$\epsilon_{creep} = \alpha\left(\frac{t}{\tau}\right)^m \qquad (58)$$

$$\tau = \tau_0 \exp.\ Q/RT \qquad (59)$$

where

Q = activation energy for creep   T = absolute temperature
ϵ_{creep} = creep strain   R = gas constant
α = constant dependent on applied stress
t = time
τ_0 = time constant
m = slope from time plot

82
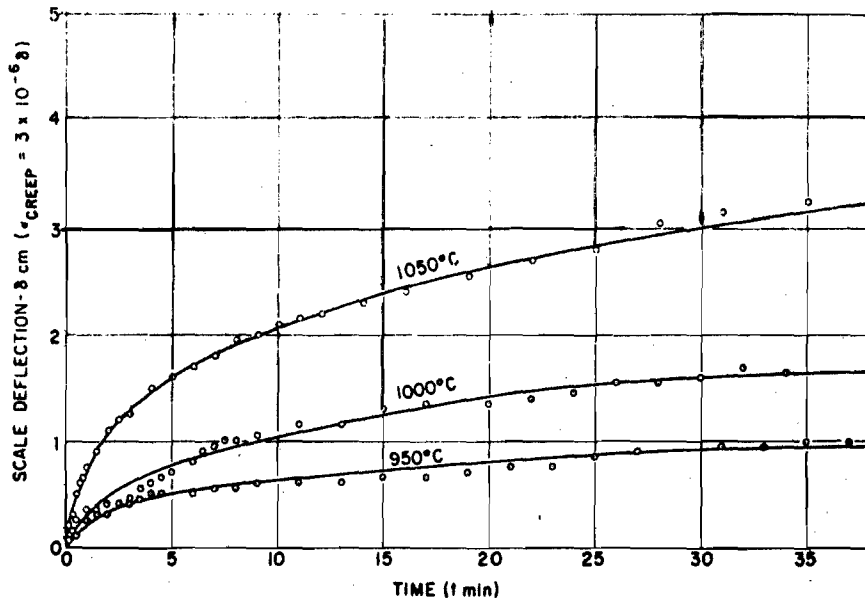
Figure 26 a: Transient Creep, Linear Plot
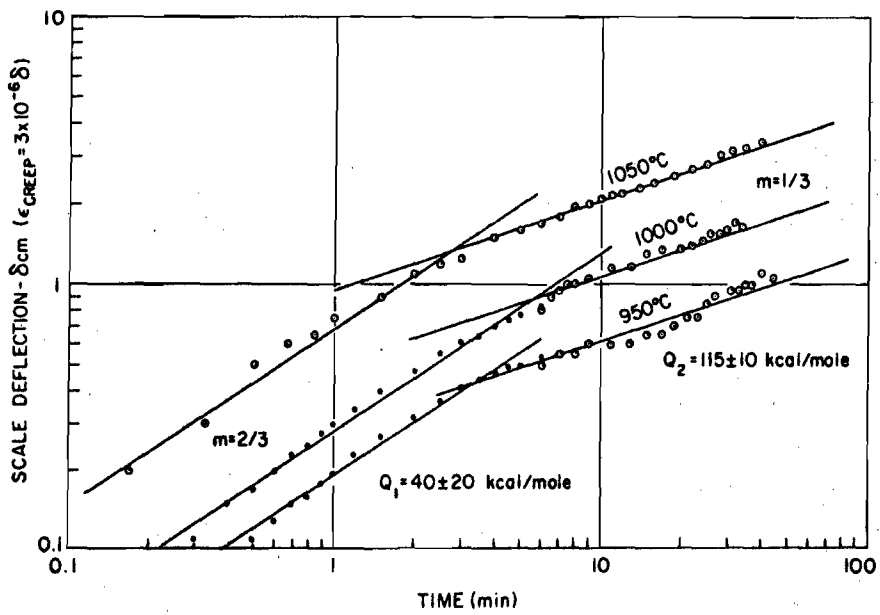
Figure 26 b: Transient Creep, Log-Log Plot

Figure 26. Typical Creep Curve

4.14.2 Practical limitations

The practical limitations inherent in creep studies are associated with the sophistication of the test equipment, such as the sensitivity and recording features of the test machines, the degree of control of ambient conditions during the period of the test, and the number of units needed for measurements under different conditions.

4.14.3 Present practice

Standard procedures for brittle materials usually avoid tensile creep testing in favor of compression or flexural testing. Torsional testing for creep determinations has also been popular.

Systems have been devised which allow concurrent determinations of resonant frequency for modulus of elasticity, logarithmic decrement for internal friction, and bending deformation for transient creep measurements. Such a system is described in Figure 27.

4.15 Thermal Shock Resistance

4.15.1 Theoretical basis of the test

When a material is subjected to conditions which cause a thermal gradient to exist within its boundaries, mechanical strains are developed due to thermal expansion. The severity of the associated stresses will depend on the elastic properties, degree of restraint, magnitude of the thermal expansion coefficient, and character of the thermal gradient.

Manson (Ref. 27) has shown excellent correlation between experimental and theoretical thermal shock resistance of certain brittle materials. The theoretical solution is based on an infinite plate at uniform temperature immersed in a cooling medium, the cooling being expressed in terms of a non-dimensional heat-transfer coefficient β , usually termed Biot's modulus, defined as

$$\beta = \frac{a\,h}{k} \tag{60}$$

where
    a = half thickness of the plate
    h = heat transfer coefficient
    k = thermal conductivity

DIFFERENTIAL
TRANSFORMER

LOAD

WATER COOLED
RADIATION SHIELD

SPECIMEN

MOLYBDENUM WOUND
RESISTANCE FURNACE &
RADIATION SHIELD

WATER-COOLED COLLET
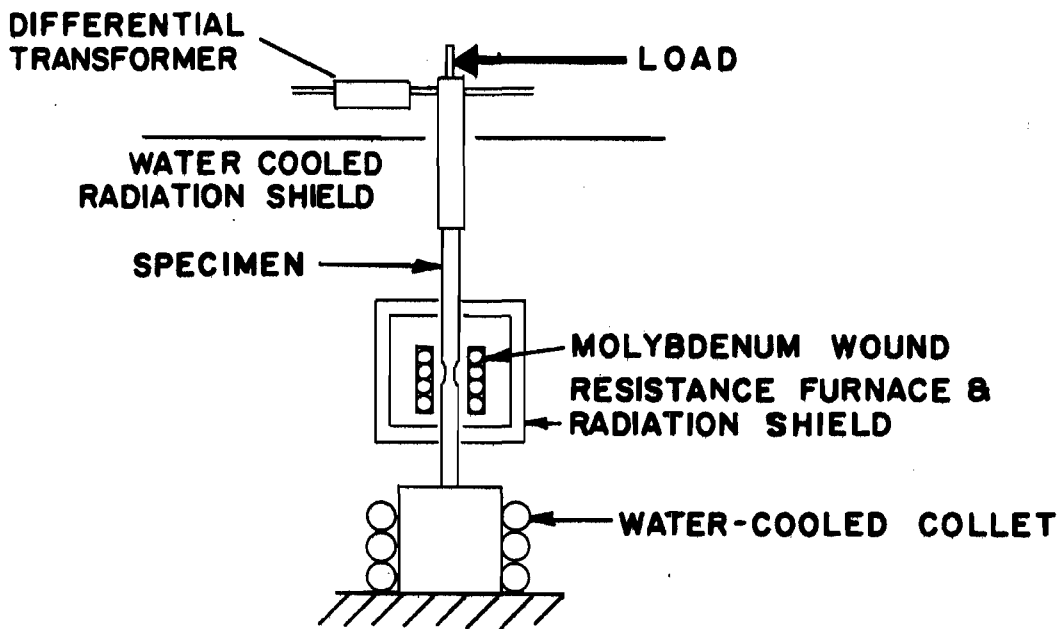
FIGURE 27 : TEST CONFIGURATION FOR INTERNAL
FRICTION, CREEP, AND ELASTIC MEASUREMENTS

4.15

The solution for maximum surface stress as a function of thermal shock environment is shown to follow the expression:

$$\frac{1}{\sigma_{max}} = \frac{(1 - \mu)}{E \, \alpha \, T_0} \left[1.5 + \frac{3.25}{\beta} - 0.5 \exp. \left(\frac{-16}{\beta} \right) \right] \quad (61)$$

where

σ_{max} = maximum surface stress, pounds per square inch
μ = Poisson's ratio
E = Young's modulus of elasticity, pounds per square inch
α = coefficient of thermal expansion, inches per inch per degree
T_0 = initial uniform temperature of plate, degrees F

The maximum temperature differences (between body and fluid in which it is immersed) that can be withstood before failure will depend on the value β. With β very small, this tolerance is proportional to $\frac{k \sigma}{E \alpha}$, and with β large it is

proportional to $\frac{\sigma}{E \alpha}$, where σ = failure stress. Designating these extreme

conditions as P_1 and P_2 respectively, the temperature tolerance for any value of β becomes

$$\Delta T = (1 - \mu) \left[1.5 P_2 + \frac{3.25 P_1}{a h} - 0.5 P_2 \exp. \left(-\left(\frac{16 P_1}{a h P_2} \right) \right) \right] \quad (62)$$

where

ΔT = temperature change causing failure, degrees F
μ = Poisson's ratio
P_1 = $\frac{k \sigma}{E \alpha}$ (for small β)

P_2 = $\frac{\sigma}{E \alpha}$ (for large β)

a = half thickness of plate, inches
h = surface heat transfer coefficient

4.15.2 Practical limitations

The inherent assumptions in the foregoing analysis are that the material obeys Hooke's law to failure and that the elastic properties are independent of temperature. A constant coefficient of thermal expansion is assumed, so that inversions or phase changes are not accounted for. Any anisotropic behavior in elastic or thermal properties, or plastic deformation during the cycling, serves to invalidate the basis for these thermoelastic calculations, and a much more complex analysis is necessary.

86

4.15

The accurate definition of the parameter β for a particular test is essential to interpretation of results and correlation with theory.

One feature of all thermal shock tests which poses a problem to the investigator is a clear definition of an end-point or failure. In cases of complete degredation, this is obvious; but comparative efforts or attempts to show degrees of failure are usually subjective decisions.

4.15.3 Present practice

The great variety of thermal shock tests which are in use would be impossible to describe in detail. Most of these procedures are of a screening type, in which a series of materials or configurations are subjected to some severe thermal environment. Through progressive screening of survivors with increasingly severe conditions, the optimum system may be selected.

Many of the tests are based on a simulation of anticipated service conditions, usually employing test coupons in early screening work, and eventually subjecting an entire prototype design to the test. Systems have been observed which use the following heat and velocity conditions for the test:

Gas-air blast directed onto specimen
Natural gas-air
Natural gas-oxygen
Propane-oxygen
Acetylene-oxygen
Hydrogen-oxygen
Variations by volume consumed and distance
Plasma arc directed onto specimen
Temperature and enthalpy variations by gas control,power
supplied, and distance from tip to specimen
Arc-imaging furnace
Variation by focus, intensity, and distance
Rocket motor exhaust
Variation by distance to specimen and angle of attack
Fused-quartz heating lamps
Variation by electric power supplied, distance, absorptive or
reflective nature of surfaces. Particularly adaptable to program
control
Immersion in, or exposure to, a heating fluid
Immersion in, or exposure to, a cooling fluid

Tests designed to examine the thermal shock resistance of a material are generally based on rapid cooling techniques. Quenching from an equilibrium temperature to a

lower temperature is relatively easily achieved with consistency. An advanced system for this purpose subjects circular disks to controlled peripheral cooling. Any failure is detected in a flexural loading of the disk after removal from the system, an observed decrease in flexural strength indicating damage due to the thermal cycle.

One system of thermal shocking which stresses the test material by rapid heating uses an electron heating source. A wire element is centrally located through the hollow core of a cylindrical shape, the entire configuration is placed in a vacuum, and a high electrical potential is applied across the element-test-piece gap. Extremely high heating rates may be achieved.

Rapid heating of electrically conductive materials is also accomplished by discharging high current densities from a capacitor bank through the test piece.

The wide variety of thermal shock testing reflects the importance of this characteristic as well as the limited ability to define the influence of size and shape. Increasingly severe demands for thermally-resistant materials in high performance vehicles or re-entry situations have surpassed present technical capability.

4.16 Hardness

Hardness of a solid is usually assessed in terms of an indentation or of a scratch depth. A relative hardness measurement is made through comparison with a series of selected minerals.

4.16.1 Indentation or scratch-depth

Various scales have been developed by defining the shape, size, and material of the indenter. Results are expressed by a number which is either proportional to the depth of penetration for a specified load, or proportional to a mean load over the area of the indentation. Common systems are described in the following sections.

4.16.1.1 Brinell hardness test: A vertical hydraulic press forces a hardened steel ball indenter into the surface of the test specimen. The standard test defines a ball of 10 mm. diameter and two test loads, 3000 kg. and 500 kg. Smaller balls and lighter loads are used, maintaining the same ratio of load to square of ball diameter. The Brinell hardness number is calculated as the ratio of the load to the impressed area of indentation, and is calculated by the following equation:

$$ Bhn = \frac{P}{\frac{\pi D}{2} \left(D - \sqrt{D^2 - d^2} \right)} \tag{63}$$

4.16

where

P = test load, kilograms
D = diameter of ball, millimeters
d = diameter of impression, millimeters

4.16.1.2 Rockwell hardness test: The general procedure for a Rockwell test applies a minor load against the test specimen by elevating the specimen, followed by controlled application of a major test load, removal of the test load, and measurement of the penetration caused by the test load. Several overlapping scales of hardness are in common use, each associated with a specific combination of load and indenter. The two indenter shapes are hardened steel balls and diamond cones, 120° included angle. Load ranges from 60 to 150 kg. are employed.

4.16.1.3 Vickers hardness test: A square-based diamond pyramid indenter, with an included angle of 136 degrees between faces, is loaded against the specimen under the controlled action of a dashpot system. Test loads vary from 5 to 100 kg. applied over a loading cycle of 10 to 20 seconds.

Microscopic measurement of the size of the impression is used to define a hardness number, according to the equation

$$DPH = \frac{1.8544\ L}{d^2} \tag{64}$$

where

DPH = diamond pyramid hardness
L = applied load, kilograms
d = length of diagonal of impression, millimeters.

4.16.1.4 Tukon tester: Loads from 25 g. to 50 kg. are applied through either the square-based diamond pyramid described above, or through the "Knoop" type of diamond indenter. The Knoop indenter is a pyramid with a rhombohedral base, the long diagonal of an indentation being 7.11 times the length of the short diagonal.

The test cycle is electronically controlled, the control circuitry being activated by the pressure of specimen against indenter. Following the load application, the specimen is automatically lowered to clear the indenter, then moved into position for microscopic examination and measurement of the indentation size. The long diagonal of the Knoop indentation is measured and used in the following equation for Knoop hardness (Ref. 28)

$$I = \frac{L}{1^2\ C} \tag{65}$$

4.16

where
I = Knoop hardness number
L = load applied to the indenter, kilograms
1 = length of long diagonal, millimeters
C = constant for each indenter, supplied by manufacturer

When a square-based indenter is used, the DPH equation (section 4.16.1.3) applies to definition of the hardness number.

4.16.1.5 Bierbaum microcharacter: A diamond tool is caused to move over a surface with controlled loading conditions on the tool. This scratch test has found wide application in defining the hardness of brittle materials, generally of a glass-type.

The cutting tool is a corner of a diamond cube. The surface is drawn under this loaded point, and the resulting scratch width is determined by measurement with a microscope fitted with an ocular micrometer.

The standard load is 3 grams. Calculation of the hardness number is made according to the equation

$$ K = \frac{10^4}{\lambda^2} \tag{66} $$

where
K = hardness number
λ = width of scratch, microns

4.16.2 Relative hardness measurement

A selection of minerals of varying hardness has been used for many years for hardness classification. The selection, known as Mohs scale, is as follows:

Mineral	Mohs Hardness Number
Talc	1
Gypsum	2
Calcite	3
Fluorite	4
Apatite	5
Orthoclase	6
Quartz	7
Topaz	8
Corundum	9
Diamond	10

90

4.16

The relative scratch hardness of a material is determined by locating the softest mineral which will scratch the unknown. A subjective decision is then reached by the experimenter to determine whether the unknown compares closest with one of the standard minerals, or whether it is better described as midway between the two bracketing minerals. Although the test is qualitative in nature, the standard minerals are wisely chosen to provide a uniform gradient in hardness qualities.

4.16.3 Indentation strength

Variations of the Brinell method have been used to measure the failure stress at glass surfaces. The "microstrength" (Ref. 29) is calculated according to the Hertz formula for stresses in a contact region, as follows:

$$\sigma_r = \frac{1}{r^2} \frac{(1 - 2\mu)P}{2\pi} \qquad \text{for } r > a \qquad (67)$$

where

σ_r = radial stress, pounds per square inch

r = distance from center of indentation, inches

μ = Poisson's ratio of the glass

P = load, pounds

a = radius of contact zone, inches

The failure occurs in a region outside the observed contact area. (Ref. 30 a) This fact may be a reflection of the flaw-sensitive failure of a brittle material, since equation (67) indicates that stresses would be maximum at the circumference of the contact area, where $r = a$ (see equation 68). The form of the stress equation has been confirmed (Ref. 30 b) through an analysis of curvature under the indenter, arriving at the equation

$$\sigma_r = \frac{1}{r^2} \frac{4G^2 A a}{(K + 2G)\pi} \qquad \text{for } r > a \qquad (68)$$

where

σ_r = radial stress, pounds per square inch

r = radius of fracture circle, inches

a = radius of contact region, inches

G = rigidity modulus, pounds per square inch

K = bulk modulus of elasticity, pounds per square inch

A = maximum indentation depth, inches

A comparison of equations (67) and (68) illustrates their similar dependency on the parameter $1/r^2$, indicating a maximum stress when $r = a$.

4.17 Flaw Detection

It has been emphasized that many brittle material properties are highly dependent on flaws and cracks. There are many means by which internal and surface flaws may be detected; but except for very large flaws the determination of size and orientation cannot at the present time be used to compute adjusted strengths and properties of the material.

Some of the methods of flaw detection are as follows:

1. γ or X-rays: limited to relatively thin sections due to absorption of energy.

2. Ultrasonic Vibrations: this method possesses a penetration depth.

Both of the above methods can also locate the detected flaw by a means similar to radio triangulation.

3. Magnetic crack detection: limited to surface cracks and of course magnetic materials.

4. Penetrant methods: for surface cracks, such as: oil and chalk, fluorescent and chalk, fluorescent penetrant, and dye penetrant.

Vacuum immersion in dye penetrant is a powerful qualitative selection or inspection method for dense (low porosity) materials. Many uncontrolled material variables introduced into mechanical testing programs may be detected by such inspection, and have been brought to light only by such means. The liberal use of these inspection techniques is particularly advisable in special testing environments which are usually very costly.

A very thorough and useful reference manual for non-destructive testing is the Non-destructive Testing Handbook, Reference 31.

REFERENCES

1. Griffith, A.A., "The Phenomena of Rupture and Flow in Solids," Phil. Trans. Royal Soc., 221A, 163 (1920).

2. Orowan, E., "Energy Criteria of Fracture," Welding Journal, 34 pages 157-160 (Suppliment) (1955).

3. Weibull, W., "A Statistical Theory of the Strength of Materials," Ing. Vetenskaps Akard. Handl, No. 151, Stockholm (1939), and "A Statistical Distribution Function of Wide Applicability," J. Applied. Mech. 18, 293-97 (1951).

4. Daniels, I.M. and Weil, N.A., "Task 3-Effect of Non-Uniform Stress Fields, Studies of the Brittle Behavior of Ceramic Materials," Technical Documentary Report No. ASD-TR-61-628, April, 1962.

5. Bortz, S.A., "Task 1-Effect of Structural Size: The 'Zero Strength', Studies of the Brittle Behavior of Ceramic Materials," Technical Documentary Report No. ASD-TR-61-628, April 1962.

6. Gregory, L.D. and Spruill, C.E., "Structural Reliability of Re-entry Vehicles Using Brittle Materials in Primary Structure," Presented to the Aerospace Systems Reliability Symposium, Inst. of Aerospace Sciences, Salt Lake City, Utah (1962).

7. Salmassy, O.K., Bodine, E.G., Duckworth, W.H., and Manning, G.K., "The Behavior of Brittle-State Materials," WADC Technical Report No. 53-50, Part 2 (1953).

8. Pears, C.D. and Thomas, A.L., "The True Stress-Strain Properties of Brittle Materials to 5500°F.," Southern Research Institute, Birmingham, Alabama, March 20, 1962.

9. Bressman, J.R., "A Method for Determining Tensile Properties of Refractory Materials at Elevated Temperatures," J. Amer. Ceram. Soc., 30, 145 (1947).

10. Bortz, S.A., Master of Science Thesis, Illinois Institute of Technology, 1963.
----"A Means of Obtaining Axial Tension from a Bending Test," paper presented to American Ceramic Society, Pittsburgh, Pa., April, 1963.

11. Rudnick, A., Hunter, A.R., and Holden, F.C., "An Analysis of the Diametral-Compression Test," paper presented to A.S.T.M., New York, New York, June, 1962.

12. Moore, R.E., Ph.D. dissertation, University of Missouri, 1962.

13. Lee, G.H., "An Introduction to Experimental Stress Analysis," Chapter 7, Wiley, New York (1950).

14. Sedlacek, R., and Holden, F.C., "Method for Tensile Testing of Brittle Materials," Rev. Sci. Inst., 33, 3, 298-300 (1962).

15. Timoshenko, S., Strength of Materials, Part II, pg. 59, D. Van Nostrand (1956).

16. Duckworth, W.H., "Precise Tensile Properties of Ceramic Bodies," J. Amer. Ceram. Soc., 34, 1, 1-9 (1951).

17. Baldwin, J.R., "The Behavior in Tension, Torsion, and Flexure of Members Made of Brittle Materials," dissertation, University of Illinois (1961).

18. Duckworth, W.H., Schwope, A.D., Salmassy, O.K., Carlson, R.L., and Schofield, H.Z., "Mechanical Property Tests on Ceramic Bodies," WADC Technical Report 52-67, p. 68, March 1952.

19. (a) Milligan, L.H., "Modulus of Rupture of Cylindrical Ceramic Rods When Tested on a Short Span," J. Amer. Ceram. Soc. 36, 5, 159-60 (1953).

    (b) Patton, W.R. and Shevlin, T.S., "An Investigation of the Modulus of Rupture Test," Bachelor of Science Thesis, Ohio State University, (1942).

20. Bortz, S.A. and Lund, H.H., "The Brittle Ring Test," pp. 383-404 in Mechanical Properties of Engineering Ceramics, Kriegel, W.W. and Palmour, H., Eds., Interscience Publishers, New York, 1961.

21. Green, L., jr., Stehsel, M.L., Waller, C.E., "Techniques for Tensile and Torsional Testing of Refractory Materials," J. H. Weisbrook, Editor Mechanical Properties of Intermetallic Compounds, Wiley, New York (1960).

22. Shook, W.B., "Impact Stress Measurements in Brittle Materials," dissertation, Ohio State University, 1961.

23. Pickett, G. "Equations for Computing Elastic Constants from Flexural and Torsional Resonant Frequencies of Vibration of Prisms and Cylinders," Proc. ASTM 45, 846 (1945).

24.   Charles, R.J., Hillig, W.B., "The Kinetics of Glass Failure by Stress Corrosion," Symposium on Mechanical Resistance of Glass and Causes of Its Lowering, Florence, Italy, September, 1961.

25.   Charles, R.J., "Static Fatigue: Delayed Fracture, Task 9" in "Studies of the Brittle Behavior of Ceramic Materials," ASD Report 61-628, April 1962.

26.   Chang, R. and Graham, L.J., "Transient Creep and Associated Grain-Boundary Phenomena in Polycrystalline Alumina and Beryllia," NAA-SR-6483, Atomics International, September 30, 1961.

27.   Manson, S.S., "Thermal Stresses and Thermal Shock," p. 393-418 in Mechanical Behavior of Materials, Dorn, J.E., Ed., McGraw-Hill, New York, New York (1961).

28.   Knoop, F., Peters, C.G., and Emerson, W.B., "Sensitive Pyramidal Diamond Tool for Indentation Measurements," J. Res. Nat. Bur. Standards, 23 (1) 39-62 (1939); RP 1220.

29.   Powell, H.E., and Preston, F.W., "Microstrength of Glass," J. Amer. Ceram. Soc., 28 (6) 145-49 (1945).

30.   (a) Sucov, E.W., "New Statistical Treatment of Ball Indentation Data to Determine Distribution of Flaws in Glass," J. Amer. Ceram. Soc., 45 (5) 214-18 (1962).

        (b) Sucov, E.W., "Elastic Stresses Produced by Indentation of Plane Surface," J. Amer. Ceram. Soc., (45) 575-78 (1962).

31.   McMaster, R.C., Editor, Non-Destructive Testing Handbook, Ronald Press Company, New York, Volumes I and II, (1959).

Section 1.3, page 1
General References Pertaining to Brittle Behavior.

APPENDIXES I AND II

APPENDIX I

CONDUCT OF THE SURVEY

Phase I. Letter Survey

A comprehensive mailing list was compiled from the National Science Foundation listing of Industrial Research Laboratories and the 1962 Yearbook of the Journal of Engineering Education. A total mailing of 1389 letters was sent to the materials interests, 781 being industrial concerns and 708 educational institutions. A later listing of equipment manufacturers and associated instrumentation suppliers was used to obtain representative information on the availability and capability of testing devices. Figures 28, 29, and 31 show the form letters mailed to the various information sources, and Figure 30 illustrates the questionnaires mailed to industrial and educational materials interests.

A tabular listing of selected replies to the questionnaire is shown on pages 99 through 124. Those marked with an asterisk were visited during the course of the data-collection for this survey. Many of the other participants were helpful in supplying further information in response to specific questions.

In keeping with the work statement for this program, an attempt was made to gather economic information pertaining to the cost of test equipment and cost allowances for test performance. The price schedules for standard testing procedures are available from most commercial testing laboratories, and quotations for non-standard tests may also be obtained. In-house testing costs are not clearly resolved for most industrial and research concerns involved with brittle materials studies, as such expenses are generally interwoven in complex ways with the overall development program.

THE OHIO STATE UNIVERSITY
ENGINEERING EXPERIMENT STATION
156 WEST 19TH AVENUE
COLUMBUS 10, OHIO

CERAMIC RESEARCH

CYPRESS 3-2365

File: RF 1420

Gentlemen:

The Engineering Experiment Station is conducting a comprehensive survey of testing methods for brittle materials. This is in cooperation with the Aeronautical Systems Division at Wright-Patterson Air Force Base.

The purpose of this project is to develop a reference handbook on the mechanical property evaluation of non-metallic, inorganic materials, including intermetallic compounds and graphite. We are confident that such an effort can contribute substantially to the present state of the art, and therefore solicit your aid in this survey.

We will write for more details on the basis of the enclosed questionnaire.

Yours very truly,

ENGINEERING EXPERIMENT STATION

William B. Shook
Director
Ceramic Research

WBS:rmc
Encl.

AN INVESTMENT IN　　　　HUMAN RESOURCES

FIGURE 28. Survey Mailed to Industrial Interests.

100

THE OHIO STATE UNIVERSITY
ENGINEERING EXPERIMENT STATION
156 WEST 19TH AVENUE
COLUMBUS 10, OHIO

CERAMIC RESEARCH

CYPRESS 3-2365

File: RF 1420

In cooperation with the Aeronautical Systems Division, Wright-Patterson Air Force Base, we are conducting a comprehensive survey of testing methods used to evaluate brittle materials. The materials and property measurements of specific interest are listed on the enclosed sheet.

The results of this survey will be incorporated in a reference handbook to be made available by the Air Force. The success of this program in producing a meaningful reference source will depend on your help.

We hope to correspond with members of your staff who are involved with these materials and tests, and possibly arrange our visit to the appropriate laboratories.* Would you therefore direct this request through the proper channels for this purpose?

We shall look forward to our further correspondence.

Very truly yours,

ENGINEERING EXPERIMENT STATION

William B. Shook
Director
Ceramic Research

WBS:RMC
*A security clearance of SECRET is available in case the testing procedures or material studies are classified.

FIGURE 29. Survey Letter Mailed to Institutions.

101

SURVEY OF TESTING METHODS
OHIO STATE UNIVERSITY-WRIGHT PATTERSON AIR FORCE BASE

Organization

Name_____   Name of person with whom we should
                                    correspond

Address_____

City, State_____   _____

The materials and tests of interest are listed below. Please check those which
define your activities.

Materials   **Tests**

___ Oxides (mixed oxides)   ___   Tensile
___ Glass and/or glass-ceramics   ___   Compressive
___ Intermetallics (aluminum, silicides ___ Flexural
     beryllides, etc.)   ___   Impact
___ Borides   ___   Creep (all types)
___ Carbides   ___   Hardness
___ Nitrides   ___   Fatigue
___ Sulfides   ___   Modulus of Elasticity
___ Graphite   ___   Modulus of Rigidity
___ Ceramic composites (adaptable   ___   Poisson's Ratio
     to generalized tests   ___   Bulk Modulus
___ Vitrified ceramics   ___   Internal Friction
___ Cermets   ___   Thermal Shock
                                        ___   Porosity and absorption
Comments_____   ___   Grain size
_____   ___   Softening point
_____   ___   Others

Would you permit a visit to your laboratories for further information?_____
Security clearance required_____

Return to   Dr. William B. Shook   (Return envelope enclosed)
                 Ceramic Research
                 156 W. 19th Avenue
                 The Ohio State University
                 Columbus 10, Ohio

FIGURE 30. Survey Questionnaire.

102

THE OHIO STATE UNIVERSITY
ENGINEERING EXPERIMENT STATION
156 WEST 19TH AVENUE
COLUMBUS 10, OHIO

September 19, 1962

Gentlemen:

The Engineering Experiment Station, in cooperation with Wright
Patterson Air Force Base, is conducting a survey of testing methods for
brittle materials. Many manufacturers and users of such materials have
been contacted with a general expression of willingness to help in this
effort.

For the sake of completeness, we are anxious to include informa-
tion about testing machines, environmental control (especially high tempera-
ture conditions), and special features of testing equipment. The ultimate
goal is to make this information available in the form of a Reference Handbook
to brittle materials interests.

We would appreciate any information you may supply us regarding
your products, and hope that this communication can eventually lead to more
personal contact.

Very truly yours,

ENGINEERING EXPERIMENT STATION

William B. Shook
Director
Ceramic Research

WBS:rmc

FIGURE 31. Survey Letter Mailed to Equipment Suppliers.

103

TABLE 2. Selected Returns from Questionnaire.

Company	Oxides	Glass	Intermetallics	Borides	Carbides	Nitrides	Sulfides	Graphite	Ceramic composites	Vitrified ceramics	Cermets	Tensile	Compressive	Flexural	Impact	Creep	Hardness	Fatigue	Elasticity	Rigidity	Poisson's Ratio	Bulk Modulus	Internal Friction	Thermal Shock	Porosity and absorption	Grain size	Softening point	Others
ALABAMA																												
* Southern Research Institute	x	x	x	x	x	x		x	x	x	x	x	x	x		x	x	x	x		x	x		x	x	x	x	
University of Alabama, Dept. Engineering Mechanics								x				x					x							x				
ALASKA																												
University of Alaska												x	x	x		x	x											
ARIZONA																												
Sperry Phoenix Company		x															x	x						x	x			
Research Chemicals, Inc.	x	x	x	x		x	x						x				x								x	x	x	x
A.R.C. Laboratories	x							x		x		x	x	x			x										x	
University of Arizona, College of Engineering	x	x	x	x	x			x	x		x	x	x	x	x	x	x	x			x	x						x
CALIFORNIA																												
Seruomechanics		x											x						x	x				x				
* Hughes Aircraft Co.	x	x		x					x															x	x	x	x	x
* University of California																												
Dept. Mineral Technology	x	x						x				x	x	x	x	x			x	x	x		x			x		
Dept. Engineering	x	x	x					x	x	x			x	x			x									x		
Lawrence Radiation Laboratory	x	x		x				x	x	x			x	x		x									x	x		
Beckman Instruments Inc.	x	x										x													x	x		
Ampex Computer Products Co.	x												x													x		
* U.S. Borax Research Corporation	x	x	x								x	x	x	x	x		x							x				x
Smith-Emery Company	x		x	x	x	x	x	x		x		x	x	x			x		x	x	x	x				x	x	
Western Gold and Platinum Co.	x								x				x															

104

TABLE 2. (Contd.)

105

Company	Oxides	Glass	Intermetallics	Borides	Carbides	Nitrides	Sulfides	Graphite	Ceramic composites	Vitrified ceramics	Cermets	Tensile	Compressive	Flexural	Impact	Creep	Hardness	Fatigue	Elasticity	Rigidity	Poisson's Ratio	Bulk Modulus	Internal Friction	Thermal Shock	Porosity and absorption	Grain size	Softening point	Others
Pacific Semiconductors, Inc.		x																										x
Metal Control Laboratories Inc.	x				x			x				x	x		x	x	x	x								x		
Fairchild Semiconductor	x	x	x																								x	x
* North American Aviation, Inc.	x	x				x		x				x		x	x									x			x	
* General Dynamics/Pomona	x	x	x		x				x					x	x									x	x		x	
* H.I. Thompson Fiberglass Co.	x	x		x	x	x	x	x	x	x		x	x	x	x		x	x	x				x	x	x	x	x	x
Gladding, McBean and Company								x		x			x	x	x				x						x	x	x	
* General Dynamics/Astronautics	x	x							x			x	x	x	x	x			x	x	x					x	x	
Cratex Manufacturing Co. Inc.	x				x							x						x	x	x	x					x		
Western Gear Corporation	x		x	x	x	x			x																			
* Stanford University																												
Dept. Materials Science								x			x	x	x		x		x					x				x		
Stanford Research Institute	x	x	x	x	x	x		x			x	x	x	x			x	x	x	x	x				x	x	x	
Kaiser Gypsum Company, Inc.		x						x				x	x	x	x	x	x		x	x	x				x	x	x	
Lockheed Propulsion Co.					x				x	x																x		x
Lockheed Missiles and Space Co.									x			x																
Commercial Minerals Company																												x
Bermite Powder Company	x	x			x			x	x	x	x																	
* American Better Chemicals				x	x	x	x	x				x	x	x	x		x		x						x	x	x	x
Almay Research and Testing Corp.												x	x			x	x	x	x							x		
* The Payne Co./Day and Night Mfg. Co.	x	x						x		x	x	x	x	x	x				x						x	x	x	x
* Bell and Howell Research Center	x	x	x		x					x		x	x	x					x					x	x	x	x	
G.E. Vallecitos Atomic Laboratory	x		x	x				x				x				x									x	x	x	x

TABLE 2. (Contd.)

Company	Oxides	Glass	Intermetallics	Borides	Carbides	Nitrides	Sulfides	Graphite	Ceramic composites	Vitrified ceramics	Cermets	Tensile	Compressive	Flexural	Impact	Creep	Hardness	Fatigue	Elasticity	Rigidity	Poisson's Ratio	Bulk Modulus	Internal Friction	Thermal Shock	Porosity and absorption	Grain size	Softening point	Others
*General Dynamics/General Atomic	x		x	x	x		x	x			x	x	x	x	x		x		x	x	x		x	x		x		
C.F.Braun and Co.	x	x			x			x									x	x						x				x
Litton Systems Inc.	x	x	x											x	x		x						x	x			x	x
Consolidated Electrodynamics		x																					x	x			x	
McCormick Selph Associates, Inc.	x	x								x		x	x										x					
Vidya, Inc.	x	x	x	x	x	x	x	x	x	x	x												x				x	x
*Sloan Research Industries	x	x	x	x	x			x	x	x																x		x
COLORADO																												
*Denver Research Institute	x	x	x						x					x		x			x	x							x	x
*Coors Porcelain Company	x								x			x	x	x	x		x		x	x	x		x	x		x	x	
Automation Industries									x														x					x
Automation Industries/Electro-Ceramics	x								x																			x
Ideal Cement Co.												x	x	x					x							x		
CONNECTICUT																												
Tilo Co. Inc.														x	x				x					x				x
R. T. Vanderbilt Co. Inc.								x	x					x										x		x	x	x
Fafnir Bearing Company	x	x			x		x	x		x				x			x	x						x				x
Materials Development Laboratory	x			x	x					x	x	x		x							x	x	x		x	x	x	x
Emhart Glass Testing Labs		x													x								x				x	x
Entoleter, Inc.	x				x			x			x	x	x	x	x				x							x	x	
DELAWARE																												
L. D. Caulk Company	x							x					x		x		x		x									
E. I. duPont deNemours	x		x					x					x	x	x		x						x			x		

TABLE 2. (Contd.)

Company	Oxides	Glass	Intermetallics	Borides	Carbides	Nitrides	Sulfides	Graphite	Ceramic composites	Vitrified ceramics	Cermets	Tensile	Compressive	Flexural	Impact	Creep	Hardness	Fatigue	Elasticity	Rigidity	Poisson's Ratio	Bulk Modulus	Internal Friction	Thermal Shock	Porosity and absorption	Grain size	Softening point	Others
FLORIDA																												
Metallurgical Research Lab.												x				x												
University of Florida																												
Sun Tests Unlimited Inc.		x							x	x					x	x	x							x				x
Winder Aircraft Corp.		x	x	x	x				x	x		x		x	x	x	x	x	x					x				
Exposure Research Inc.		x							x	x																		
GEORGIA																												
* Lockheed Georgia Co.	x		x					x	x		x	x					x							x				x
* Georgia Institute of Technology																												
School of Ceramic Engineering	x											x	x				x		x		x			x	x	x	x	
* Engineering Experiment Station	x	x	x	x	x	x			x	x	x	x	x	x	x		x		x	x	x	x		x	x	x	x	
IDAHO																												
University of Idaho																												
Engineering Experiment Station												x	x	x			x	x	x	x	x	x					x	
ILLINOIS																												
* Armour Research Foundation	x		x									x		x	x				x	x	x	x	x	x	x	x		
Structural Clay Products										x		x	x	x					x					x	x	x	x	
F. Lasala		x								x		x		x					x						x			
Engineered Ceramics Mfg. Co.	x	x	x		x	x		x	x	x		x	x												x	x	x	
American Machine and Foundry Co.		x				x				x																		x
University of Illinois																												
* Dept. of Theo. and Applied Mech.		x										x		x	x		x											
* Dept. Ceramic Engineering	x	x	x	x	x	x	x	x	x	x	x	x	x	x	x	x	x	x	x	x	x	x	x	x	x	x	x	x

TABLE 2. (Contd.)

Company	Materials											Tests																
	Oxides	Glass	Intermetallics	Borides	Carbides	Nitrides	Sulfides	Graphite	Ceramic composites	Vitrified ceramics	Cermets	Tensile	Compressive	Flexural	Impact	Creep	Hardness	Fatigue	Elasticity	Rigidity	Poisson's Ratio	Bulk Modulus	Internal Friction	Thermal Shock	Porosity and absorption	Grain size	Softening point	Others
Northwestern University Technological Institute *	x		x	x	x	x	x	x				x	x		x								x			x		
M. H. Detrick Co.	x								x			x	x	x	x		x							x	x	x	x	
Continental Can Co.		x																								x		
Bell and Gosseth Co.	x			x	x						x	x	x	x	x		x									x		
Hazel-Atlas Glass Div.		x											x		x									x			x	x
Amphenol Borg Electronics Corp.	x	x								x		x		x			x		x					x	x	x	x	x
Crane Packing Co.								x				x	x	x	x	x	x	x	x					x	x	x		
Chicago Vitreous Corporation		x											x	x	x									x			x	x
Sumner Sollitt Co.												x	x	x							x			x				
Sears Roebuck and Co.		x							x	x		x	x	x	x		x		x					x	x			
Portland Cement Association												x	x	x		x			x	x								
INDIANA																												
Linde Company	x				x								x				x		x									
Linde Co./Speedway Research Lab.	x		x	x	x	x						x					x		x					x	x	x	x	
Haynes Stellite Co.						x					x			x										x				
CTS Corporation	x	x							x	x	x													x	x			
Delco Radio Div., GMC	x		x			x		x													x			x	x			
P. R. Mallory and Co. Inc.	x		x						x			x	x	x	x		x		x					x		x	x	
Louisville Cement Co.		x										x	x	x														
Rostone Corporation	x		x						x			x	x	x	x										x			
Raybestos-Manhattan, Inc.											x	x	x				x							x	x			x
Link-Belt Co.					x			x			x	x	x		x													

TABLE 2. (Cont'd.)

Company	Oxides	Glass	Intermetallics	Borides	Carbides	Nitrides	Sulfides	Graphite	Ceramic composites	Vitrified ceramics	Cermets	Tensile	Compressive	Flexural	Impact	Creep	Hardness	Fatigue	Elasticity	Rigidity	Poisson's Ratio	Bulk Modulus	Internal Friction	Thermal Shock	Porosity and absorption	Grain size	Softening point	Others
IOWA																												
Iowa State University																												
* * Dept. Mech. Engr.		x			x			x	x	x	x	x	x	x	x	x	x	x	x	x	x		x	x	x	x	x	
* * Ames Laboratory for AEC	x	x	x		x			x	x	x			x	x	x	x		x					x			x	x	
Patzig Testing Laboratories		x										x		x	x												x	
KANSAS																												
* The Boeing Company	x	x	x					x	x		x	x	x	x	x		x		x		x			x	x	x	x	
*University of Wichita																												
Dept. Metallurgical Engineering	x	x	x						x	x		x	x	x	x									x	x	x	x	
School of Engineering		x						x	x		x	x	x	x	x		x	x	x	x	x	x			x	x		x
KENTUCKY																												
University of Louisville													x	x											x			
Henry Vogt Machine Co.												x	x		x		x									x		
University of Kentucky																												
Dept. Min.-Metallurgical Engr.																x												
Cohart Refractories	x	x											x				x								x	x	x	x
American-Standard	x	x						x		x	x	x	x	x	x		x								x	x	x	
MARYLAND																												
Martin Co.-Nuclear Div.	x		x	x	x	x		x	x		x														x	x		
Thiokol Chemical Corp.	x							x				x	x			x			x									
Trans Tech. Inc.	x									x		x	x	x	x		x								x	x	x	x
General Refractories Co.	x											x	x	x		x	x	x	x						x	x	x	x
American Instrument Co.																									x			x
Koppers Company Inc.												x			x		x	x	x									

109

TABLE 2. (Contd.)

Company	Materials											Tests																
	Oxides	Glass	Intermetallics	Borides	Carbides	Nitrides	Sulfides	Graphite	Ceramic composites	Vitrified ceramics	Cermets	Tensile	Compressive	Flexural	Impact	Creep	Hardness	Fatigue	Elasticity	Rigidity	Poisson's Ratio	Bulk Modulus	Internal Friction	Thermal Shock	Porosity and absorption	Grain size	Softening point	Others
Pemco Div., Glidden Company	x	x								x																		
MASSACHUSETTS																												
Aerovox Corporation		x								x																x		
Manlabs Inc.			x	x								x					x		x	x				x		x		
Plas-Tech Equipment Corp.		x							x	x	x	x	x		x	x			x	x								
Mass. Inst. of Technology																												
Dept. of Metallurgy	x	x							x	x	x					x	x		x						x		x	
Ceramics Division	x	x	x		x		x			x	x	x	x	x			x	x		x	x			x		x	x	
Worcester Poly. Institute							x	x			x	x	x	x	x			x	x	x	x	x				x	x	
Northeastern University	x	x			x			x	x		x	x	x	x	x			x	x	x	x	x				x		x
LTI Research Foundation												x	x	x	x	x	x	x	x	x	x					x		
United Shoe Machinery Corp.		x			x			x		x							x		x					x			x	
Ionics Incorporated	x	x	x	x	x	x	x	x	x	x														x				
Arthur D. Little, Inc.									x					x					x									
Raytheon Co.	x				x	x		x	x			x	x	x			x	x		x	x	x		x		x	x	
Nortronics		x			x			x	x	x		x					x		x									
Electronized Chemicals Corp.																												x
Factory Mutual Engineering Div.																												
Alloyd Electronics Corp.	x	x	x	x	x	x	x	x	x			x					x	x	x	x	x			x	x	x	x	
Arnold Greene Testing Lab.		x			x				x	x		x	x	x	x		x									x	x	
Cabot Corp.	x	x														x						x		x		x		
Lukens Laboratories	x		x	x																						x	x	
Myerson Tooth Corp.										x			x	x									x	x	x	x		
American Optical Co.		x										x	x		x		x		x		x						x	x

TABLE 2. (Contd.)

Company	Oxides	Glass	Intermetallics	Borides	Carbides	Nitrides	Sulfides	Graphite	Ceramic composites	Vitrified ceramics	Cermets	Tensile	Compressive	Flexural	Impact	Creep	Hardness	Fatigue	Elasticity	Rigidity	Poisson's Ratio	Bulk Modulus	Internal Friction	Thermal Shock	Porosity and absorption	Grain size	Softening point	Others
Baystate Abr. Products Co.									x	x		x	x	x	x			x	x		x					x	x	
General Electric Co.	x	x													x			x										
Boston Edison Co.		x					x					x	x		x			x						x				
Mass. Inst. of Technology	x	x										x	x	x		x	x						x					
MICHIGAN																												
Dow Corning Corporation	x		x									x	x	x	x			x	x							x		
University of Michigan																												
Chemical and Metall. Engr.	x					x					x						x									x		x
Sealed Power Corporation												x					x	x	x									
Kawneer Company										x																		x
Ford Motor Co.	x	x	x	x	x	x		x	x		x	x	x	x	x		x	x	x	x	x	x		x	x	x		
Wayne State University		x													x													
Temco Aircraft Co.													x															
Champion Spark Plug Company	x												x	x	x				x									
Besser Technical Center										x			x	x	x				x		x					x	x	x
Brooks and Perkins Inc.			x	x	x	x		x	x		x		x	x					x	x				x	x	x		
Industrial Tectonics Inc.	x	x	x	x	x	x		x	x	x	x						x											
Ford Motor Co./Glass Div.		x															x	x	x								x	
American Metal Products	x	x	x	x	x	x	x	x	x	x	x	x	x	x			x									x	x	x
Research Laboratories, GMC	x	x		x	x			x			x																	
Chrysler Corporation	x	x	x	x	x	x		x	x	x	x	x	x	x	x		x		x						x	x	x	
Detroit Testing Lab. Inc.		x			x	x	x	x	x	x		x	x	x	x	x	x		x						x	x	x	
Laboratory Equipment Corp.	x		x						x	x																x		

TABLE 2. (Contd.)

Company	Oxides	Glass	Intermetallics	Borides	Carbides	Nitrides	Sulfides	Graphite	Ceramic composites	Vitrified ceramics	Cermets	Tensile	Compressive	Flexural	Impact	Creep	Hardness	Fatigue	Elasticity	Rigidity	Poisson's Ratio	Bulk Modulus	Internal Friction	Thermal Shock	Porosity and absorption	Grain size	Softening point	Others
MINNESOTA																												
University of Minnesota	x																						x					
Research Incorporated												x	x	x	x	x		x										
*Honeywell Research Center	x	x		x					x	x	x	x	x	x		x		x						x	x	x	x	
Northern States Power Company										x																		x
MISSISSIPPI																												
Mississippi State University	x	x	x	x	x	x	x	x	x	x	x	x	x	x	x	x	x	x	x		x	x	x	x	x	x	x	
MISSOURI																												
University of Missouri																												
Dept. Civil Engr.									x			x																
Missouri School of Mines																												
Dept. Metallurgical Engr.						x											x									x		
*Dept. Ceramic Engineering	x	x		x	x	x	x		x			x	x	x		x	x		x	x			x	x	x	x	x	
A. P. Green Fire Brick Co.	x			x					x			x	x			x								x	x	x	x	x
*James W. Weldon Lab.	x		x	x	x	x						x	x		x	x	x	x	x			x				x		
Industrial Research and Testing	x					x			x			x	x	x	x		x							x		x	x	
Gustin Bacon Manufacturing Co.		x										x															x	
MONTANA																												
Montana State College										x	x													x	x	x	x	
Montana School of Mines																												
Dept. Mineral Dressing	x	x	x	x	x	x	x	x	x	x			x		x							x				x		
NEBRASKA																												
Dale Electronics Inc.	x	x							x			x	x											x	x			

112

TABLE 2. (Contd.)

Company	Oxides	Glass	Intermetallics	Borides	Carbides	Nitrides	Sulfides	Graphite	Ceramic composites	Vitrified ceramics	Cermets	Tensile	Compressive	Flexural	Impact	Creep	Hardness	Fatigue	Elasticity	Rigidity	Poisson's Ratio	Bulk Modulus	Internal Friction	Thermal Shock	Porosity and absorption	Grain size	Softening point	Others
NEW HAMPSHIRE																												
Richard D. Brew and Company												x	x	x	x	x	x							x		x	x	
N. H. Ball Bearings, Inc.	x	x	x	x	x	x	x	x	x	x	x	x	x	x	x	x	x	x	x					x		x	x	
NEW MEXICO																												
New Mexico State University																												
Dept. Mech. Engineering			x														x											
University of New Mexico																												
NEW JERSEY																												
* Wright Aeronautical Div.	x	x	x	x	x	x	x	x	x		x	x	x	x	x	x	x	x	x	x	x			x		x	x	x
* National Moldite Co.	x																x	x						x			x	
* Newark College of Engineering	x	x								x		x	x	x	x		x		x	x								
T. A. Edison Research Laboratory	x	x																										x
* Mycalex Corporation of America												x	x	x	x									x	x	x	x	
* Austenal Company	x	x						x					x													x	x	
National Radiac Inc.																										x		
Ronthor Reiss Corporation												x		x			x											
Bart Laboratories and Design Inc.												x					x	x					x					
Stevens Inst. of Technology																												
Metallurgical Dept.												x		x	x		x											
Isolantite Manufacturing Corp.										x		x	x	x												x		
Princeton University																												x
Bell Telephone Laboratories	x	x				x			x			x						x	x	x	x		x				x	
Thiokol Chemical Corporation	x		x	x	x	x		x	x	x	x	x	x	x			x		x							x		x
ITT Federal Laboratories	x									·																x		x

113

TABLE 2. (Contd.)

114

Company	Oxides	Glass	Intermetallics	Borides	Carbides	Nitrides	Sulfides	Graphite	Ceramic composites	Vitrified ceramics	Cermets	Tensile	Compressive	Flexural	Impact	Creep	Hardness	Fatigue	Elasticity	Rigidity	Poisson's Ratio	Bulk Modulus	Internal Friction	Thermal Shock	Porosity and absorption	Grain size	Softening point	Others
Materials												**Tests**																
Rutgers University																												
School of Ceramics		x							x			x		x	x				x	x	x			x			x	
School of Ceramics		x														x				x	x		x					
National Beryllia Corp.	x								x	x	x	x	x	x					x					x	x		x	
Joseph Dixon Crucible Co.								x																				
Carbone Corp.					x			x				x	x	x			x	x	x					x	x			
Johns Manville Corp.		x							x			x	x	x	x	x	x		x	x	x			x	x	x	x	
Gulton Industries										x			x						x									
Associated Testing Laboratories		x							x	x														x	x			
Columbian Carbon Company	x																								x	x		
Asbury Graphite Mills Inc.								x																				
Frenchtown Porcelain Co.	x								x	x		x	x	x	x								x	x	x	x		
United Clay Mines Corp.										x		x														x		
Victory Engineering Corporation	x	x		x																				x				
Engelhard Industries, Inc.	x							x																x				x
NEW YORK																												
* Union Carbide Research Institute			x	x	x			x				x					x	x	x				x				x	x
* Servo Corporation of America	x	x	x				x			x		x		x					x	x	x			x	x		x	
* Amperex	x	x		x				x	x	x		x	x		x				x					x	x	x	x	
* Lucius Pitkin Inc.	x	x	x					x	x	x		x	x	x					x		x					x	x	x
* Tempil Corporation	x								x	x																		
New York University																												
Dept. Civil Engineering												x	x	x	x	x	x	x										
* New York University								x																				

TABLE 2. (Contd.)

Company	Oxides	Glass	Intermetallics	Borides	Carbides	Nitrides	Sulfides	Graphite	Ceramic composites	Vitrified ceramics	Cermets	Tensile	Compressive	Flexural	Impact	Creep	Hardness	Fatigue	Elasticity	Rigidity	Poisson's Ratio	Bulk Modulus	Internal Friction	Thermal Shock	Porosity and absorption	Grain size	Softening point	Others
Alco Products Inc.												x	x		x		x	x						x		x		
Carlson Company												x	x	x			x	x	x	x	x							
University of Buffalo		x																										
Webb Institute of Naval Arch.												x	x						x									
Sperry Gyroscope Co.	x	x		x	x	x		x	x	x	x						x	x						x	x	x		x
Morganite Inc.								x				x	x	x					x							x		
Polytechnic Inst. of Brooklyn Dept. Metallurgical Engr.			x	x													x											
City Testing and Research Labs.												x	x	x	x	x	x	x	x	x				x	x	x	x	x
Materials Research Corp.	x			x	x							x	x	x		x												
United Nuclear Corp.				x	x						x						x									x		x
Sintercast Div./Chromalloy				x							x			x	x		x							x	x			
Pfaudler Co.		x	x					x						x			x		x	x			x	x			x	x
Speer Carbon Company, Inc.	x	x		x	x	x	x	x				x	x	x	x		x		x		x			x	x	x		x
Cornell Aero. Lab.	x	x	x	x								x							x	x	x	x	x	x		x		
Errol B. Shand	x	x						x	x			x		x	x				x							x		
Corning Glass Works	x	x						x	x			x	x	x	x	x	x	x	x	x	x	x	x	x	x	x		
Electro Refractories and Abrasives	x		x	x	x			x	x			x	x	x					x						x	x	x	
Scintilla Div./Bendix Aviation Corp.	x	x						x						x					x						x		x	
Erie County Technical Institute		x		x	x			x			x	x	x	x	x	x	x		x	x						x	x	
National Lead Company	x			x	x	x				x							x		x	x				x				
IBM	x														x			x					x					
Marlin-Rockwell	x	x	x	x	x	x	x	x	x	x	x		x				x		x					x		x	x	
Carborundum Co.	x		x	x	x			x	x					x	x	x	x		x		x			x		x		x

115

TABLE 2. (Contd.)

Company	Oxides	Glass	Intermetallics	Borides	Carbides	Nitrides	Sulfides	Graphite	Ceramic composites	Vitrified ceramics	Cermets	Tensile	Compressive	Flexural	Impact	Creep	Hardness	Fatigue	Elasticity	Rigidity	Poisson's Ratio	Bulk Modulus	Internal Friction	Thermal Shock	Porosity and absorption	Grain size	Softening point	Others
Syracuse China Corp.									x	x			x	x	x		x	x						x	x	x	x	
* Manhattan College		x							x	x	x	x	x	x	x		x	x	x	x	x	x					x	
Alfred University																												
College of Ceramics	x	x	x		x	x	x		x	x	x	x	x	x	x		x	x		x	x	x	x	x	x	x	x	x
NORTH CAROLINA																												
* Duke University																												
College of Engineering									x						x													x
Dept. Civil Engr.	x				x				x			x	x	x			x											
North Carolina State College																												
* Dept. Engineering Research	x	x	x	x	x	x	x	x	x	x	x	x	x	x	x	x	x	x	x	x	x	x	x	x	x	x	x	x
Lithium Corp. of America			x																									
OHIO																												
Basic Incorporated	x												x	x										x		x	x	x
Cambridge Tile Mfg. Co.										x			x	x			x		x					x			x	
Aeronca Mfg. Corp.	x	x							x			x	x	x	x		x							x	x	x		x
Mosaic Tile Co.		x											x		x							x		x	x	x		
Metcut Research Associates												x	x			x	x	x	x	x	x			x	x	x	x	x
Monsanto Research Corporation	x	x	x	x	x	x	x	x	x	x	x	x	x	x	x	x	x	x	x	x	x	x	x	x	x	x		x
Owens Illinois Tech. Center		x												x	x		x		x				x	x			x	x
Armco Steel Corporation	x												x				x							x			x	
* North American Aviation	x	x	x				x	x	x	x	x	x	x				x	x	x	x	x			x	x	x	x	x
* Republic Steel Corp.	x		x	x	x	x	x	x					x	x			x							x	x	x	x	
* Zirconium Corp. of America	x									x			x	x			x							x	x		x	
* Clevite Corporation	x												x		x		x				x		x			x		

TABLE 2. (Contd.)

Company	Materials											Tests															
	Oxides	Glass	Intermetallics	Borides	Carbides	Nitrides	Sulfides	Graphite	Ceramic composites	Vitrified ceramics	Cermets	Tensile	Compressive	Flexural	Impact	Creep	Hardness	Fatigue	Elasticity	Rigidity	Poisson's Ratio	Bulk Modulus	Internal Friction	Thermal Shock	Porosity and absorption	Grain size	Softening point	Others
S. K. Wellman Co.													x				x								x			x
Barium and Chemicals Co.	x	x			x	x	x																					
Borg Warner Corp.		x								x															x	x		
* Brush Beryllium Co.	x	x	x	x	x	x	x	x	x	x	x	x	x	x	x	x	x	x	x	x	x	x	x	x	x	x	x	x
Ohio Carbon Company								x				x	x	x			x		x				x		x	x		
The Siegler Corp.	x	x						x				x	x	x					x						x	x		x
Cleveland Twist Drill Co.					x												x								x	x		x
* National Carbon Research Lab.			x	x	x	x	x	x				x	x	x		x	x		x	x	x		x	x	x	x		x
Ohio Brass Co.										x			x		x		x								x			
General Electric	x	x			x			x			x	x		x	x				x						x			
Kimble Glass Co.		x								x		x	x				x		x	x				x	x	x	x	x
Westinghouse Elec. Corp.	x	x	x	x	x	x	x	x	x	x	x	x	x	x	x	x	x	x	x	x	x	x			x	x	x	x
Philip Carey Mfg. Co.	x	x	x																									
University of Toledo College of Engineering	x																											x
University of Dayton Res. Inst.	x		x				x	x			x	x						x							x			
OKLAHOMA																												
Oklahoma State University School of Civil Engr.												x	x	x	x	x	x	x	x	x	x	x				x	x	x
OREGON																												
Oregon State University												x	x	x	x	x	x											
PENNSYLVANIA																												
Pittsburgh Plate Glass Co.		x										x		x	x				x						x		x	
Mellon Institute													x						x		x	x			x	x	x	x

TABLE 2. (Contd.)

118

Company	Materials											Tests																
	Oxides	Glass	Intermetallics	Borides	Carbides	Nitrides	Sulfides	Graphite	Ceramic composites	Vitrified ceramics	Cermets	Tensile	Compressive	Flexural	Impact	Creep	Hardness	Fatigue	Elasticity	Rigidity	Poisson's Ratio	Bulk Modulus	Internal Friction	Thermal Shock	Porosity and absorption	Grain size	Softening point	Others
Carnegie Tech.		x										x																
Swarthmore College												x	x	x	x	x	x	x	x	x	x							x
Temple University												x					x											
Westinghouse Electric Corp.	x	x	x	x	x			x	x	x		x	x	x	x	x	x	x	x		x			x	x	x	x	
U.S.Steel Corp.	x	x		x	x	x		x	x	x	x		x	x		x	x					x		x	x	x	x	x
Westinghouse/Atomic Fuel Div.	x				x						x		x															
Kennametal Inc.					x						x	x	x		x		x	x	x	x	x	x		x		x		
Foote Mineral Company	x	x								x		x	x	x	x									x	x		x	
A. P. Green Firebrick Co.	x	x	x		x								x	x										x	x	x	x	x
Elliott Co.		x			x	x		x		x		x	x	x	x	x	x	x	x	x	x			x	x		x	
Aeroprojects Inc.	x	x						x				x	x				x								x	x		x
G. and W. H. Corson, Inc.													x					x							x	x		
Harbison Walker Refractories	x				x				x	x		x	x			x	x		x		x			x	x	x	x	x
Speer Carbon Co. Inc.		x						x	x	x		x	x	x	x	x	x	x	x	x	x		x	x	x	x		
Lehigh Portland Cement Co.	x		x									x	x	x														
Saxonburg Ceramics Inc.	x								x	x			x	x	x										x	x	x	
Magnetics Inc.	x									x		x	x		x										x	x		
Garber Research Center	x												x	x		x			x						x	x		x
Nuclear Materials and Equip.Co.	x				x	x		x	x	x			x												x	x	x	x
American Glass Research Inc.		x												x	x				x	x	x				x			
International Resistance Co.						x	x																					x
Stackpole Carbon Co.	x							x		x		x	x	x			x		x	x			x		x	x		
Findlay Refractories Co.	x															x									x	x	x	x
Shenango China, Inc.											x			x	x									x	x	x		

TABLE 2. (Contd.)

Company	Oxides	Glass	Intermetallics	Borides	Carbides	Nitrides	Sulfides	Graphite	Ceramic composites	Vitrified ceramics	Cermets	Tensile	Compressive	Flexural	Impact	Creep	Hardness	Fatigue	Elasticity	Rigidity	Poisson's Ratio	Bulk Modulus	Internal Friction	Thermal Shock	Porosity and absorption	Grain size	Softening point	Others
Beryllium Corporation	x		x					x	x		x	x	x	x										x		x		
Ceramic Color and Chem. Mfg.	x	x	x						x															x	x	x	x	
C. K. Williams and Co.																									x	x		
Westinghouse/Semiconductor		x	x						x			x	x	x	x			x	x			x	x	x	x	x	x	
Westinghouse/Atomic Power	x		x	x	x	x	x	x	x		x		x				x							x		x	x	
Borolite Corporation				x	x						x		x				x							x				
The Budd Company												x	x	x		x		x	x		x							
SKF Industries		x			x			x		x	x							x	x	x								
Franklin and Marshall College																			x	x	x	x	x					
Bethlehem Steel Co.		x								x								x	x						x	x	x	
Lehigh University																												
Dept. Metallurgy	x			x								x	x	x	x	x	x	x	x	x	x	x	x	x	x	x	x	x
Pure Carbon Company Inc.			x	x	x			x				x	x	x	x	x	x	x	x	x	x			x	x	x		
Firth Sterling Inc.			x	x	x						x	x	x		x		x	x						x		x		
Brockway Glass		x															x							x			x	x
Armstrong Cork Co.		x						x				x	x	x	x													
University of Pennsylvania																												
School of Met. Engr.	x	x	x	x	x	x	x	x	x	x	x	x	x	x	x	x	x	x	x	x	x	x	x	x	x	x	x	x
Pennsylvania State University																												
Dept. Ceramic Technology	x	x						x	x					x			x							x		x	x	x
Dept. Engineering Mechanics												x	x	x	x	x	x	x	x	x				x				
University of Pittsburgh																												
Civil Engr. Dept.								x				x	x	x				x	x						x			
Westinghouse Electric/Atomic	x																x								x	x		x

119

TABLE 2. (Contd.)

Company	Materials											Tests																
	Oxides	Glass	Intermetallics	Borides	Carbides	Nitrides	Sulfides	Graphite	Ceramic composites	Vitrified ceramics	Cermets	Tensile	Compressive	Flexural	Impact	Creep	Hardness	Fatigue	Elasticity	Rigidity	Poisson's Ratio	Bulk Modulus	Internal Friction	Thermal Shock	Porosity and absorption	Grain size	Softening point	Others
Lehigh University Metallurgical Dept.	x		x						x		x	x	x		x	x	x	x	x				x			x	x	
PUERTO RICO																												
University of Puerto Rico College Station									x	x		x	x	x	x		x		x	x					x	x	x	
RHODE ISLAND																												
Raytheon Co.		x			x				x		x	x	x	x				x	x	x	x		x	x	x			
SOUTH CAROLINA																												
* Clemson College Ceramic Engineering Dept.	x	x							x	x		x	x	x	x	x	x							x	x	x	x	
SOUTH DAKOTA																												
S.D. State College Engineering Experiment Sta.												x	x		x		x		x	x	x	x						
S.D. School of Mines and Tech. Dept. Metallurgy												x	x		x		x	x	x									
TENNESSEE																												
Vanderbilt University	x		x										x				x		x									
American-Saint Gobain Corp.		x										x	x				x		x	x	x					x		
TEXAS																												
Texas Nuclear Corporation	x	x	x	x	x	x	x	x	x	x	x																	x
Southwestern Laboratories												x	x	x	x		x											
* Aeronetics, Inc.			x					x			x	x	x	x	x		x						x	x	x	x	x	x
* Chance Vought Corp.	x		x	x	x	x		x	x			x	x	x	x	x	x	x	x					x	x	x	x	
* Texas Instruments Inc.			x		x						x	x	x				x		x	x				x		x		

120

TABLE 2. (Contd.)

Company	Oxides	Glass	Intermetallics	Borides	Carbides	Nitrides	Sulfides	Graphite	Ceramic composites	Vitrified ceramics	Cermets	Tensile	Compressive	Flexural	Impact	Creep	Hardness	Fatigue	Elasticity	Rigidity	Poisson's Ratio	Bulk Modulus	Internal Friction	Thermal Shock	Porosity and absorption	Grain size	Softening point	Others
* Chance Vought Corporation	x				x			x	x			x	x	x			x		x					x	x	x	x	
University of Houston																												
Dept. Chemical Engineering	x												x															
Shilstone Testing Laboratory					x												x											
University of Texas																												
Dept. Chemical Engineering	x		x																									
UTAH																												
University of Utah																												
Dept. Ceramic Engineering	x	x		x	x	x						x	x			x	x							x		x	x	
Sperry Utah Company												x	x		x		x									x		
VERMONT																												
University of Vermont		x			x					x		x		x				x	x					x				
VIRGINIA																												
VMI--Civil Engineering												x	x	x	x				x	x	x		x					
VPI--Engr. Mech. Dept.										x		x	x	x	x	x	x	x	x	x	x	x						x
WASHINGTON																												
Electro-Chemical Corp.	x																											x
* Boeing Company		x									x	x	x	x	x	x		x	x	x	x	x		x				
* Boeing Co./Materials and Process	x	x	x	x	x	x		x	x	x	x		x	x	x			x						x	x	x	x	
* Boeing Co./Aerospace Div.	x				x			x	x			x	x	x	x			x					x		x		x	x
University of Washington																												
School of Mineral Engr.	x	x	x					x	x	x		x	x	x	x	x		x	x	x	x		x	x	x		x	x
Ceramic Engr. Dept.													x	x	x				x								x	

121

TABLE 2. (Contd.)

Company	Oxides	Glass	Intermetallics	Borides	Carbides	Nitrides	Sulfides	Graphite	Ceramic composites	Vitrified ceramics	Cermets	Tensile	Compressive	Flexural	Impact	Creep	Hardness	Fatigue	Elasticity	Rigidity	Poisson's Ratio	Bulk Modulus	Internal Friction	Thermal Shock	Porosity and absorption	Grain size	Softening point	Others
WEST VIRGINIA																												
Fostoria Glass Co.		x																						x			x	
Homer Laughlin China Co.									x	x				x	x									x	x			
National Steel Corporation	x												x	x		x									x	x	x	
West Virginia University																												
College of Engineering									x			x																x
Engineering Experiment Station		x							x	x	x	x		x	x		x	x	x	x	x	x				x	x	
WISCONSIN																												
Allen-Bradley Co.	x											x		x	x		x							x	x	x		
* Allis-Chalmers			x		x				x		x		x				x		x	x	x			x				
* Centralab Inc.	x								x	x		x	x	x	x		x							x	x	x	x	x
Kearney and Tecker Corp.				x													x	x										
Bjorksten Research Labs.	x	x	x	x	x	x	x	x	x	x	x	x	x	x	x		x		x			x		x	x	x	x	
Marquette University																												
College of Engineering	x		x			x					x	x	x	x	x	x	x		x	x	x							
College of Engineering	x											x	x	x		x	x		x	x								
University of Wisconsin																												
Dept. Minerals and Metals			x										x	x	x		x			x								

TABLE 2. (Contd.)

Company	Oxides	Glass	Intermetallics	Borides	Carbides	Nitrides	Sulfides	Graphite	Ceramic composites	Vitrified ceramics	Cermets	Tensile	Compressive	Flexural	Impact	Creep	Hardness	Fatigue	Elasticity	Rigidity	Poisson's Ratio	Bulk Modulus	Internal Friction	Thermal Shock	Porosity and absorption	Grain size	Softening point	Others
CALIFORNIA																												
* Douglas Aircraft		x	x		x			x				x		x	x				x					x	x	x		
* Atomics International	x		x	x	x	x		x			x		x	x	x	x	x		x	x	x		x		x	x		x
MINNESOTA																												
* Minnesota Mining and Mfg. Co.	x				x									x					x	x	x		x	x	x	x		
MISSOURI																												
* McDonnell Aircraft	x							x						x										x				
NEW YORK																												
Yudewitz	x	x	x	x	x	x	x	x	x	x	x																	
OHIO																												
University of Cincinnati Dept. Chem. and Met'l Engr.	x		x	x	x	x		x											x	x			x	x		x		
PENNSYLVANIA																												
Bucknell University		x	x		x	x						x	x	x			x	x	x	x	x							x
TEXAS																												
Texas Western College												x			x		x		x							x		

123

*Visited by author for tour of facilities and discussion with materials personnel.

Phase 2. Personal Visits and Discussion

As a major part of the survey, sixty-five conducted tours of research and testing facilities were arranged. Each of these visits included a discussion of testing philosophy, procedures, personnel, physical equipment, current active materials interests, and suggestions for areas of major need in advancing the technology of brittle materials.

In order of approximate priority and frequency of occurrence, the suggested major needs of further research endeavor by various groups is as follows:

Design and allowables:
1. Materials suppliers must provide more information regarding the entire spectrum of mechanical-thermal behavior, including sufficient statistical information for high reliability-minimum weight use.
2. Variability in these statistics is also in need of clarification.
3. Development must supply materials with greater ductility and better definition of stress-strain relationships.

Materials research and development:
1. Purity levels of majority of raw materials are not sufficiently specified or materials are not available at needed specifications.
2. Present analytical requirements have exceeded many classical chemical determination sensitivities.
3. Stricter minimum descriptions of materials, including surface condition, environment, and fine structure, are needed in published research.

Materials testing and specifications:
1. Standards for testing procedures with methods for complete specification of the material and its environment are needed.
2. Accurate and realistic descriptions of service requirements must be provided.
3. Statistical descriptors of brittle failure for all stress-states need clarification.

Systems fabricators:
1. Joining methods for brittle materials need research support.
2. Weight reductions and improved thermal shock characteristics are required.

The general philosophies and practices in working with the various materials have been portrayed within the body of this report.

APPENDIX II

EQUIPMENT

This appendix describes the operating principles of general types of equipment which are commonly associated with mechanical property measurements of brittle materials. The use of trade names and reference to specific manufacturers has been avoided.

The measurements necessary to the evaluation of mechanical properties are force (weight), displacement (length or angle), time (frequency), and temperature. Many measuring techniques are available for each of these parameters, and a complete catalogue of equipment types is beyond the scope of this work. It is rather intended that the principles of measurement are sufficiently described to permit an understanding of the various degrees of complexity in available testing devices.

1. Measurement of Force

The most convenient measure of force is the gravitational attraction between the earth and a mass, or the weight of that mass. Measurement of force is accomplished by direct weighing or by indirect comparison through calibrated transducers.

1.1 Mechanical weighing systems

1.1.1 Equal arm balance

The simplest weighing system for direct measurement is an equal arm balance. The common analytical balance is an example of this type of machine. The moment produced by the unknown mass is directly compared to the moment of a known mass, with suitable adjustments being made to effect a perfect balance. The equivalence of the balance arms may be checked by interchanging the two weights at balance, which is known as the method of symmetry.

1.1.2 Unequal arm balance

Measurement of larger weights may be conveniently accomplished on unequal arm balances, in which the moment arm of the known force is larger than the moment arm of the unknown force. Frictional forces in the weighing system are also magnified by unequal arm balances. Some of the most common cross-breaking machines in ceramic work are constructed on this principle, schematically pictured in Figure 32. Such loading frames are popularly used in elevated-temperature strength tests, wherein the specimen, supports, and loading members are confined within a furnace enclosure. The load is usually transmitted through a refractory rod in compression, as shown by the dashed alternate mechanism in Figure 32.
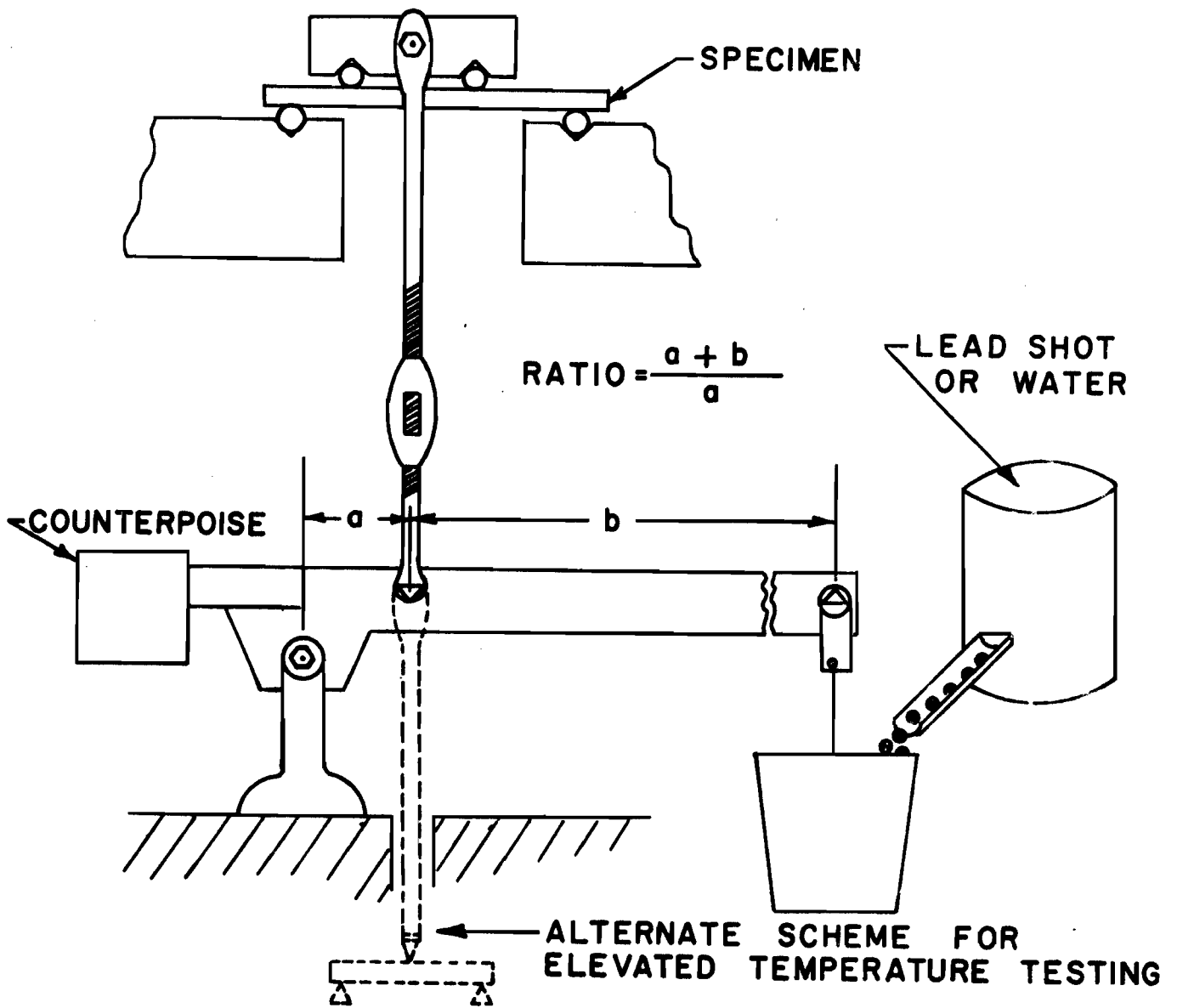
RATIO $= \dfrac{a + b}{a}$

FIGURE 32: UNEQUAL ARM CROSS-BREAKING MACHINE

126

1.1.3 Multiple lever balance

A system of multiple levers is shown schematically in Figure 33. Such a system allows the measurement of large weights in terms of much smaller weights (or moments). The frictional forces at supports are magnified through the system.
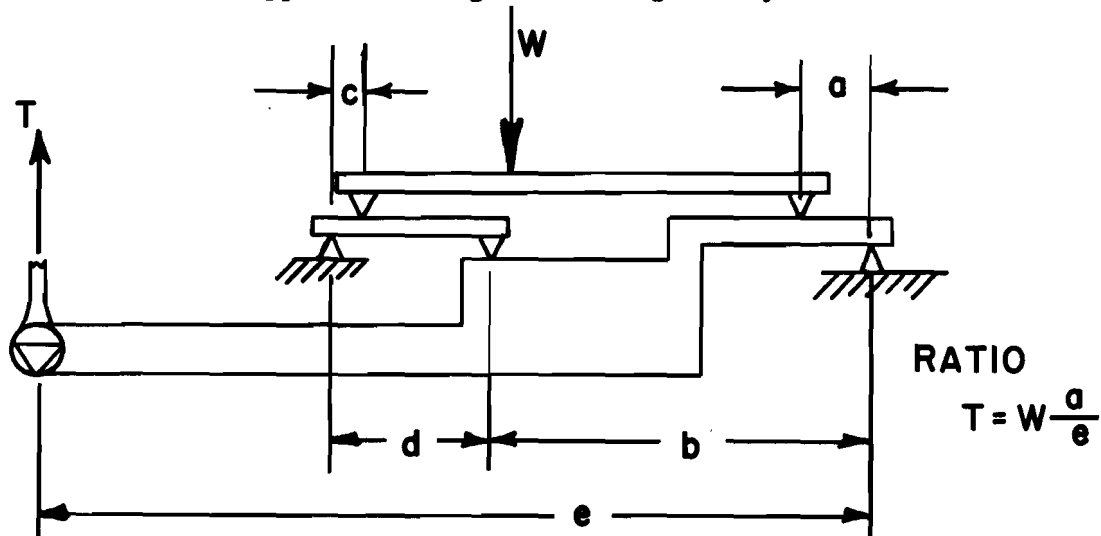

Figure 33. Schematic of Multiple Lever System

The final measurement of force T is accomplished through an unequal arm balance system. The position of W on the platform is immaterial, if c/d = a/b.

1.1.4 Pendulum balance

Indicating weighing devices are often operated on a pendulum balance system. This provides an additional feature of increased sensitivity within a loading range, as determined by the pendulum counterbalance used. Such a weighing and indicating system is described in Figure 34. The design is such that dial increments represent uniform, calibrated increments of load, T, which are usually transmitted from a multiple lever weighing system.

1.2 Elastic weighing systems

The deflection or strain of an elastic member is often used as an indirect measurement of force. Calibration of such devices is accomplished by loading with a known weight. The systems are particularly adaptable to signal generation through transducer measurement of deflection or strain, and form the basis of force measurement in most modern electronically controlled testing machines.

1.2.1 Deflection measurement

The directly observed deflection of an elastic member is typified by the simplest weighing device, a coil spring. The deflection constant of a spring is given by the following equation:

127
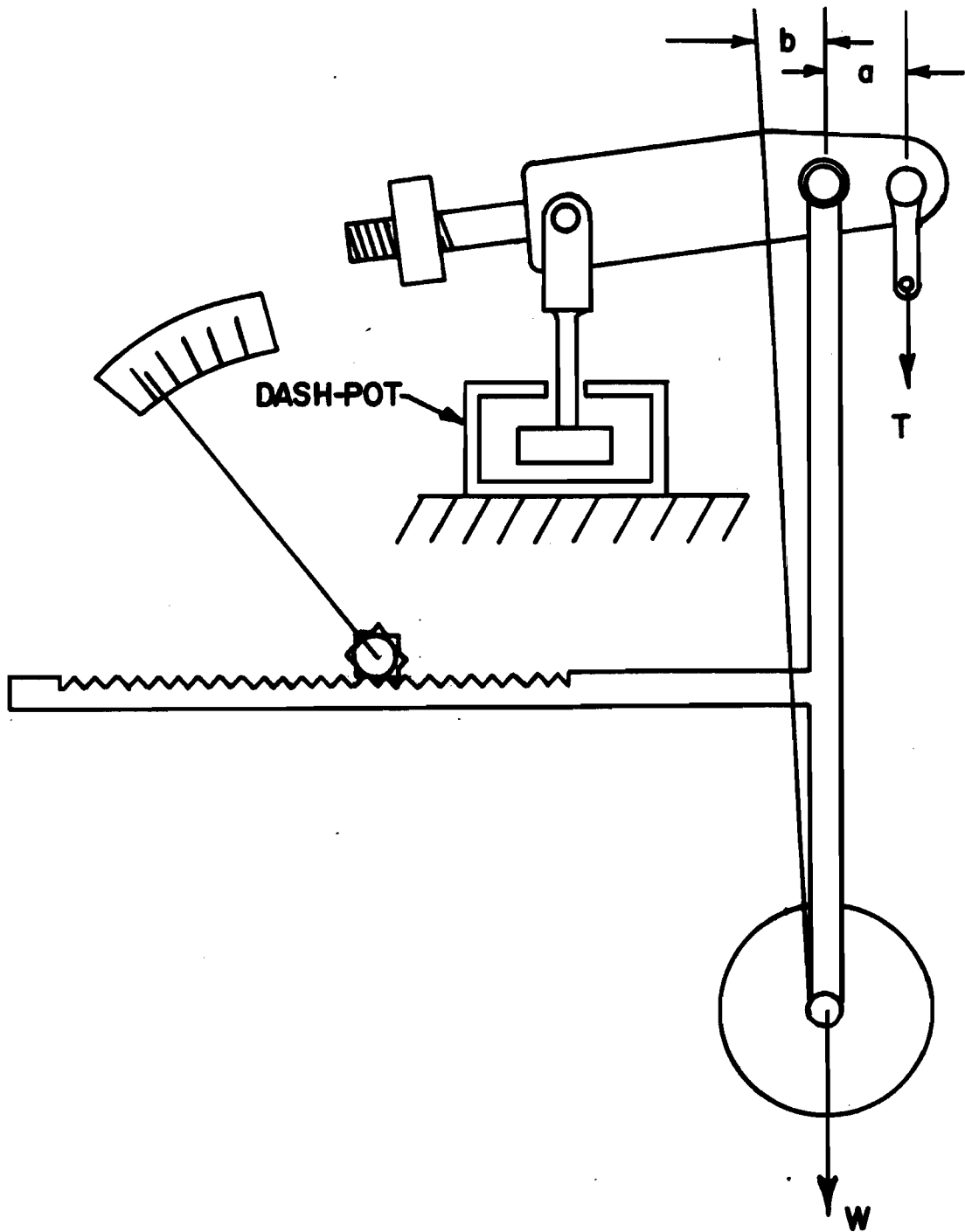
FIGURE 34 : PENDULUM BALANCE

$$K = \frac{G\,d^4}{8\,D^3\,N} \tag{69}$$

where

K = deflection constant, pounds per inch
G = shear modulus, pounds per square inch
d = wire diameter, inches
D = mean coil diameter, inches
N = number of coils

The deflection may be observed directly against a measuring scale, but is more often measured by reference to a dial gauge which magnifies the displacement.

Another type of spring which is commonly used in calibration of weighing systems is the proving ring. A carefully manufactured thin ring is diametrally loaded, the spring constant being:

$$K = 53.8 \, \frac{E\,I}{D^3} \tag{70}$$

where

K = deflection constant, pounds per inch
E = modulus of elasticity
I = moment of inertia of cross section about centroid, inches^4
D = outside diameter of ring, inches

A dial may be centrally mounted to detect the deflection, or a micrometer measurement may be used. A vibrating reed is sometimes supplied as an integral part of the micrometer mechanism, aiding significantly in establishing a consistent "contact" measurement. Electronic readout of high resolution is provided by a linear variable differential transformer (LVDT) centrally mounted in the proving ring. The deflection of other elastic members such as cantilever or torsion bars, may also be used to measure load.

1.2.2 Strain measurement

Strain gages mounted on an elastic member will permit indirect measurement of load with a high degree of precision. If the loads to be measured are large, a direct tensile or compressive loading is usually employed. For smaller loads the strain in an elastic bending member is used. The direct proportionality between load and strain, within the elastic range, permits calibration with small weights for operation at larger loads. The arrangement of strain gages on the surface of the elastic member is usually made for maximum sensitivity of that particular member. Temperature compensation is commonly provided by judicious placement of the gages.

Accuracy of ± 1/2% is commonly provided by commercial load cells of the strain gage type. The load limit is strictly a matter of design, so that very large loads may be measured with a properly designed cell.

129

1.3 Hydraulic and pneumatic weighing systems

Hydraulic and pneumatic cells operate on a force balance principle. The load applied against one side of a diaphragm or piston is exactly counterbalanced by the hydraulic or pneumatic pressure on the reverse side. The pressure is measured by a dial gauge, or by the elastic deflection of a member affected by the pressure. The simple Bourdon tube is often used for this purpose.

The use of pistons in hydraulic load cells is very limited, because of the associated problems of fluid leakage and frictional forces between piston and cylinder. A floating piston is commonly employed, with a sufficiently flexible bridge-ring for liquid containment. A typical hydraulic cell is pictured in Figure 35. Such cells are available with capacities up to 5,000,000 pounds and accuracies of 1/2%.
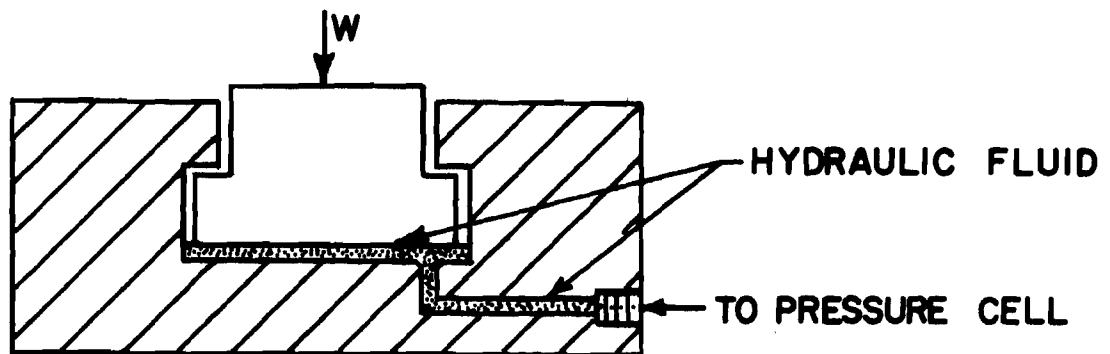
Figure 35. Typical Hydraulic Load Cell

Pneumatic cells employ a constant pressure air supply to maintain balance against the measured load. A pneumatic cell is shown in Figure 36. The diaphragm design must offer a constant horizontal area to oppose the pressure during a deflection, or a non-linear response to load would result.
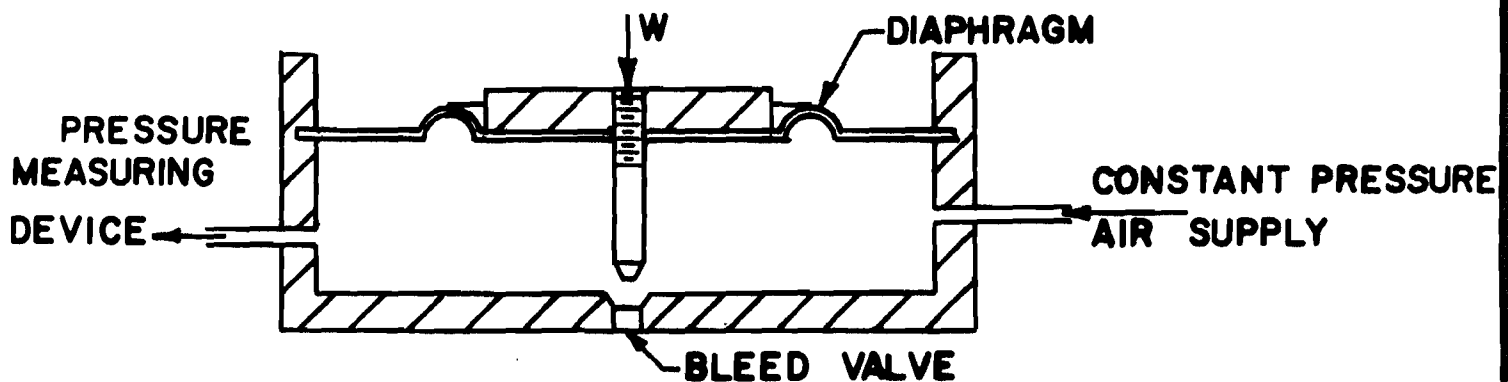

Figure 36. Typical Pneumatic Load Cell

2. Measurement of Displacement

Distances are measured by direct reference to a standard length, as a ruler, or may be amplified mechanically by suitable lever (including optical) and/or gear systems for calibrated ranges. A displacement may also be converted to a proportional electrical signal through linear variable differential transformers (LVDT) or strain gages.

2.1 Mechanical systems

The most popularly used mechanical measuring devices are dial gauges. These are available to a maximum readability of 0.0001 inches per division. Screw micrometers and vernier calipers are used extensively for the measurement of specimen dimensions. Optical lever magnification of angular displacement is used in typical torsion equipment, particularly in high temperature tests. Magnification may also be obtained through a microscope or telescope fitted with a measuring eyepiece. Movable crosshairs operated by external calibrated gearing permit measurement of extremely small displacements. Such systems are easily adapted to high temperature measurements, particularly with proper background illumination (or darkening).

2.2 Electrical systems

Transducers which convert a mechanical displacement to an electrical signal are in common use. The most desirable instruments are those which provide a linear output directly proportional to displacement.

Highly linearized multiturn potentiometers are useful for presenting a resistance change which is directly proportional to angular displacement. These are commonly driven through a mechanical gearing system which provides suitable angular amplification of the measured rotation.

The variable differential transformer is a wire wound solenoid-type device. The windings throughout one-half the length are exactly matched by opposed windings in the other half. With the core fully inserted in these opposing fields, the gross output of the system is zero. This is called the null position. Any change in position of the core with respect to the windings creates an imbalance and provides an electrical signal. The output of commercial units is linearized so that the signal amplitude is proportional to the amount of core displacement. A phase difference is created dependent upon the direction of the displacement from null position. A DC output voltage which reverses polarity on each side of null position, and which is proportional to the displacement of the core, is obtained with a simple demodulator circuit as described in Figure 37.

The resolution of a good quality LVDT is very high. Sensitivity is a function of excitation frequency and amplifier stability. At 3000 cps several commercial units will provide full-scale deflection of a recorder corresponding to 0.0002 inches, to an ultimate accuracy of one-millionth of an inch. Such systems employ much
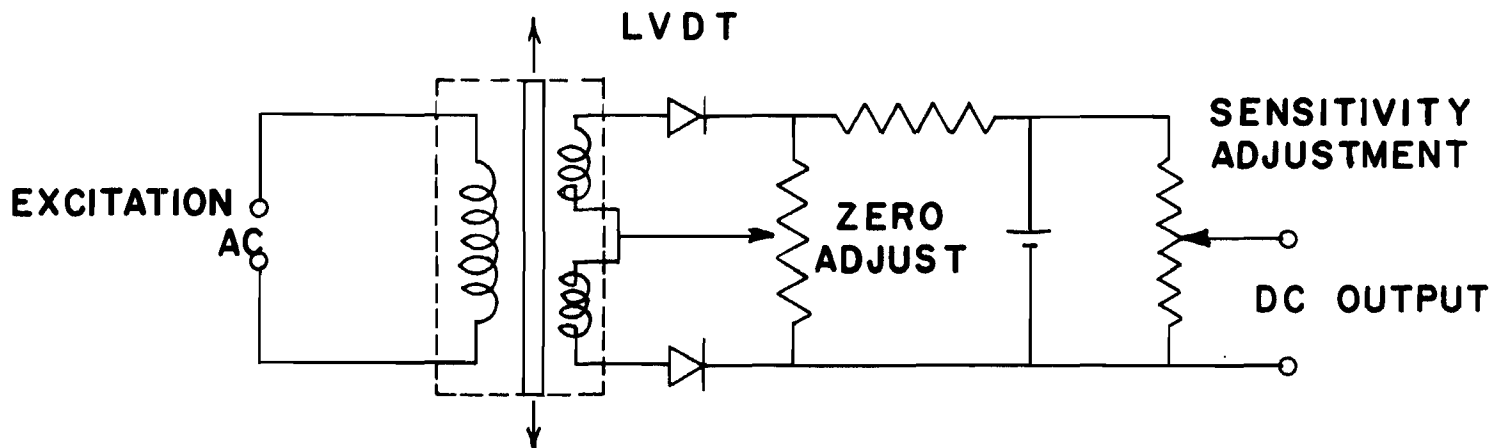
Figure 37. Simple Demodulator Circuit for
Linear Voltage Signal from LVDT

more sophisticated amplification-demodulation circuitry than portrayed in Figure 37.

Strain gages are available for operation up to temperatures of 2000°F, at sensitivities considerably reduced from lower temperature applications. Gages are supplied as wire-resistance units, semi-conductor strips, metal foil gages, and piezoelectric wafers. The high temperature usage of foil and monofilament gages is generally limited by the conductivity of the ceramic bonding cement. The temperature compensation and electrical stability of gages necessitates the use of active dummy gages, and dynamic strain measurement is usually possible at higher temperatures than corresponding static measurements.

Foil gages are generally superior to wire gages for static measurements. A higher axial strain sensitivity and lower transverse sensitivity make such gages better suited for biaxial resolution. Much larger signal output is available from semiconductor gages, but the cost is much greater than other types and temperature limits are more restrictive.

The usual circuitry in measurements with resistance gages places the active gage or gages in one arm of a bridge network. The slight changes in resistance associated with strain in the measuring gage is measured in the act of balancing the bridge. A.C. carrier frequencies are in common use to effect higher stability and less sensitivity to stray electrostatic fields. The strain measurement is in microinches per inch, with commercial equipment available which is sensitive to one microinch per inch strain. The gage factor necessary for precise measurement is usually supplied by the manufacturer to a tolerance of ± 0.2%.

3. Time or Frequency Measurement

Time measurement is based on the mean solar day, the average time for one complete revolution of the earth. Calibrated clocks, as illustrated by pendulum or balance-wheel timepieces, are used to maintain a running account of elapsed time.

The standards of particular interest to materials testing applications are subdivisions of the planetary day, such as microseconds, seconds, minutes and hours. Stopwatches and clocks of various types suffice for time measurement in periods longer than seconds. For shorter times the basis of calibration and measurement is usually an alternating signal either mechanically or electrically derived.

3.1 Time and frequency standards

Tuning-fork or piezoelectric crystal resonating systems are used as sources for frequency standards. A readily-available signal standard for calibration of frequency or time-measurement devices is the National Bureau of Standard's radio station WWV, broadcasting over 2.5, 5, 10, 15, 20, and 25 Mc. Two standard audio frequencies, 440 and 600 cycles per second, are alternately broadcast for periods of three minutes, interrupted by two minutes. The frequency accuracies as transmitted are better than 1 part in 100,000,000. Pulses exactly spaced by one second are also carried on each carrier frequency. These consist of five cycles of 1000 cycle per second frequency. One-minute intervals are marked by omitting the final pulse of each minute, and starting each minute with a double pulse.

The above national frequency and time standards are readily available to any laboratory with a short-wave radio.

3.2 Frequency and EPUT

The term "frequency" connotes a steady-state alternating condition, which exhibits a cyclic behavior. The number of cycles per second is the frequency of the occurrence.

The EPUT term, events per unit time, is generally applied to irregular or transient occurrences. A count of events by electronic means necessitates converting the event to a corresponding electrical impulse. A frequency meter and an EPUT meter measure the same quantity, except that the EPUT count is independent of the rate of occurrence. An internal time base is used to limit the count to preset intervals of time. It is this time base that requires calibration by reference to a standard signal.

Frequency is determined by reference to a standard. Multiples of a base frequency, such as 60 cycle line frequency or the 600 cycle standard of station

133

WWV, may be used to accurately calibrate ranges of measurement. Interpolation within a calibrated range is sufficient for usual accuracy. The comparison may be performed on an x-y oscillograph, the frequency standard driving one axis and the signal to be calibrated during the other axis. Even multiples are evident as stationary patterns.

Other measurement systems in popular use are electronic switches and Z-axis modulation. The electronic switch will permit dual display of signals on one screen, so that a calibrated source may be compared directly with an unknown frequency. Z-axis modulation causes brightening and darkening of the illuminated trace, each segment of the dashed line being a time standard derived from the Z-axis signal.

The principal use of frequency-measuring capabilities for property determinations is in the field of sonic determination of elastic behavior. The desired measurement is the frequency of resonance, and corresponding frequencies at known fractional amplitudes of resonance. Standard frequency meters or frequency counters are readily available for such measurements, to accuracies within 0.01%. For all but the most exacting internal friction work, such accuracy is well beyond the needs of sonic analysis.

4. Temperature Measurement

4.1 Standards

The International Temperature Scale of 1948 defines temperature according to the melting equilibrium temperatures of standard materials at standard pressure. The primary standards are as follows:

°C	°F	Reference Material
1063.0	1945.4	Gold liquid-solid
960.8	1761.4	Silver liquid-solid
444.6	832.28	Sulfur liquid-vapor
100.0	212.0	Steam liquid-vapor
0	32.0	Water-liquid-solid
-182.970	-297.346	Oxygen-liquid-vapor

Numerous secondary fixed points are accepted within the framework of this scale, the most important for ceramic reference being as follows:

°C	Reference Material
231.9	Freezing tin
327.3	Freezing lead
630.5	Freezing antimony
1453.0	Freezing nickel
1769.0	Freezing platinum
3880	Melting tungsten

A standard thermocouple, platinum versus platinum-10% rhodium, is defined as the means for interpolation between the fixed reference points, according to the equation

$$E = a + bt + ct^2 \tag{71}$$

where

E = thermocouple emf, ice-point cold junction
t = any temperature in the range 630-1063°C
a, b, c = constants determined from thermocouple measurements at antimony, silver, and gold points.

4.2 Thermocouples

Thermocouples are commonly used for temperature measurement over the entire spectrum of normal temperatures encountered in ceramic work. The high temperature regions of interest are more readily measured by the radiation techniques described below.

The junction of two dissimilar metals will generate an e.m.f. proportional to the temperature difference between the hot junction and the cold end of the metals, usually wire. That e.m.f. is measured at the cold junction, and serves to define the junction temperature through reference to a conversion table of e.m.f. versus temperature. Calibrated measuring instruments are usually direct-reading in temperature for use with specific thermocouple materials. Such instruments normally contain automatic cold-junction compensators.

The process of measuring the generated e.m.f. may be either of two general types. A null-type instrument provides a balancing e.m.f. in opposition to that being measured. At balance there is no current, so that the resistive influence of connecting circuitry is immaterial. A galvanometer-type instrument which correlates the galvanometer deflection with temperature, is sensitive to the intervening resistance between hot-junction and cold-junction. It is therefore important to maintain that resistance according to the calibration conditions.

Thermocouple types which are commonly used are Chromel vs. Alumel and Platinum vs. Platinum-Rhodium. Ten or thirteen per cent Rhodium alloy is used in the latter type, designated as types S and R, respectively. Higher temperature service may be obtained with Platinum-Rhodium alloys on each side of the thermo-couple, usually 20 vs. 5 or 20 vs. 6 per cent Rhodium. Special alloys of more refractory materials are also available for operation above 3300°F., but their use is not common.

4.3 Radiation pyrometry

Two distinct types of instruments are used for temperature measurement based on radiation. These are classified as optical and total-radiation pyrometers.

4.3.1 Optical pyrometers

The spectrum of radiation from a heated source changes in two ways with increased temperature of the radiating object. The intensity of radiation increases, and the wave-length of maximum intensity shifts to the lower end of the spectrum. The latter feature causes a color change within the visible spectrum from red through white with increasing temperature.

An optical pyrometer is a device which permits accurate color matching between a wire filament and the background color visible from a radiating surface. The filament color is changed by resistive heating from a controlled current source. The current control is calibrated in degrees. This is called a "disappearing filament" system, since a perfect color match causes the filament to blend with the background illumination.

4.3.2 Total radiation pyrometers

The heating effect of radiation on a temperature-sensitive element is used to indirectly measure the temperature of the radiating body. The optics of such systems are very important to the calibrated range of measurement since variation in focus and material between the radiating source and the collector will vary the temperature of the collector. Different materials will also indicate different temperatures, since the radiant energy depends upon the material emmittance.

Temperature-sensing collectors may be thermocouples (thermopile) or resistance thermometers. Other devices are used, but the above are most common.